Size-based insight into the structure and function of reef fish communities

by

Rowan Trebilco

M.Sc., University of Oxford, 2008

B.Sc. (Hons.), University of Tasmania, 2004

A THESIS SUBMITTED IN PARTIAL FULFILLMENT
OF THE REQUIREMENTS FOR THE DEGREE

Doctor of Philosophy

in the
Department of Biological Science
Faculty of Science

SIMON FRASER UNIVERSITY
Summer 2014

Approval

Name: **Rowan Trebilco**

Degree: **Doctor of Philosophy (Biology)**

Title of Thesis: ***Size-based insight into the structure and function of reef fish communities***

Examining Committee: **Chair:** Gordon Rintoul
Associate Professor

Nicholas K. Dulvy
Senior Supervisor
Professor

Anne K. Salomon
Supervisor
Assistant Professor
School of Resource and
Environmental Management

Isabelle M. Côté
Supervisor
Professor

Jonathan W. Moore
Internal Examiner
Assistant Professor

Simon Jennings
External Examiner
Honorary Professor
University of East Anglia, UK

Date Defended/Approved: July 15, 2014

Partial Copyright Licence

Ethics Statement

The author, whose name appears on the title page of this work, has obtained, for the research described in this work, either:

a. human research ethics approval from the Simon Fraser University Office of Research Ethics,

or

b. advance approval of the animal care protocol from the University Animal Care Committee of Simon Fraser University;

or has conducted the research

c. as a co-investigator, collaborator or research assistant in a research project approved in advance,

or

d. as a member of a course approved in advance for minimal risk human research, by the Office of Research Ethics.

A copy of the approval letter has been filed at the Theses Office of the University Library at the time of submission of this thesis or project.

The original application for approval and letter of approval are filed with the relevant offices. Inquiries may be directed to those authorities.

Simon Fraser University Library
Burnaby, British Columbia, Canada

update Spring 2010

Abstract

What would reef fish communities look like without humans? Effective ecosystem management and conservation requires a clear understanding of community structure and the processes that drive it. Relatively undisturbed reef fish communities appear to be inverted biomass pyramids (IBPs) with greater biomass of large-bodied predatory fishes compared to smaller fishes at lower trophic-levels. However, the processes that might give rise to IBPs are subject to debate. In this thesis I show that biomass pyramids and size spectra are equivalent and interchangeable representations of community structure. Key constraints on the slopes of size spectra – particularly mean community predator-to-prey-mass ratio (PPMR) – also constrain the shapes of biomass pyramids, meaning that IBPs are unlikely for closed communities. There are surprisingly few quantitative descriptions of biomass pyramids, and PPMR has not been estimated on reefs. I undertook a detailed case-study and quantify fish community size-structure using underwater visual surveys and empirically estimate PPMR using stable isotopes at a relatively undisturbed island chain in Haida Gwaii, BC. I observe an IBP, but the PPMR estimate suggests that the community should be a stack or bottom-heavy. There is 4-5 times more biomass at the largest body-sizes than would be expected given observed PPMR. I hypothesise that the most plausible explanation is energetic subsidies. Using the same fish assemblage I show how two foundational components of habitat complexity (substrate rugosity and kelp canopy characteristics) shape fish community size-structure. Higher kelp canopy cover and density leads to more biomass across all size classes, whereas higher substrate rugosity boosts the biomass of smaller-bodied fishes and leads to a more even distribution of biomass across size classes. Finally, I step back to the global scale and estimate baseline biomass spectra for the world's reef fishes, accounting for local ecological variation. Current reef fish biomass is less than half of the baseline expectation and 90% of the largest ($>$ 1 kg), most functionally-important, individuals are absent. In addition to providing the first global description of how humans have shaped reef biomass pyramids, my thesis gives new insight into how size-based processes underlie the structure and function reef fish communities.

keywords inverted biomass pyramids; ecological baselines; biomass size spectra; energetic subsidies; reef fish; kelp forests and coral reefs

To my parents.

Thanks for instilling me with a love for the ocean and other wild places.

Acknowledgments

I was looking for a challenge when I set about this PhD, and I found one. It's been an incredible opportunity to grow as a scientist and a person, and I'm immensely grateful to everyone who has helped along the way.

First, to my committee, its been a great privilege working with a trio of such exceptional ecologists and people. Nick, your creativity, breadth of knowledge, and incisive intellect have been a big inspiration, and I really valued being able to discuss science and work with you over frothy beverages. Also, you get mad respect for being the only prof in our group who commutes by bike regularly, despite breaking a collarbone in the process. Anne, thanks for always reminding me to read and cite the classics. I aspire to your example as a well-rounded ecologist (no pun intended, though I wish you, Tim and the impending offspring the best possible wishes). You've inspired me to always try to base my science on a combination of sound natural history and observation, theory, and where possible, field experiments. Isabelle, I greatly admire your insight and integrity. Thankyou for stepping up and showing support when you were needed most. Thanks also to Jonathan Moore and Simon Jennings for acting as the internal and external examiners, respectively, for my thesis. Simon — your work has been an inspiration for much of the work herein, so its an honour to have you as an external examiner.

This thesis would not have been possible without the support of my valued friends, many of whom are (or were) fellow graduate students in the Earth to Ocean group. In particular, thanks to my former house-mates in the Wall St. house — Chris Mull, Noel Swain, Jordy Thomson and Sean Anderson. Jen and Joel Harding, Chris Brown, Lynn Lee, Leandre Vigneault, Taimen Lee-Vigneault and my fellow Dulvy lab members also deserve special mention for their friendship and support.

I feel very luck for the I time spent on and under the waters of Haida Gwaii over the course of my fieldwork. The field seasons based on the Victoria Rose in 2009 and 2010 were fantastic. Lynn Lee, Leandre Vigneault, Taimen Lee-Vigneault and Alejandro Frid were a big part of what made these trips so enjoyable and memorable. Thanks to Lynn, Leandre and Taimen also for their hospitality in Tlell.

The data from Haida Gwaii presented in this thesis represent one component of broader research efforts led by Anne Salomon and Hannah Stewart. Both Anne and Hannah invested considerable time and effort securing financial and logistical support for this field program, for which and I am very grateful. In addition to Anne and Hannah, many people contributed directly and indirectly to the success of the field seasons, including Ryan Cloutier, Matt Drake, Jim Hayward, Sharon Jeffery, Joanne Lessard, Beth Piercey, Eric White, Mark Wunsch, Dominique Bureau, Seaton Taylor, and the captains (Kent Reid and Simon Dockerill) and crew of the CCGS Vector. I'm also grateful to Norm Sloan at Parks Canada, the Gwaii Haanas Archipelago Management Board and the Council of the Haida Nations Fisheries Committee for supporting the research program. I was very fortunate to have the help of several work-study and undergraduate students in the lab; Angeleen Olson and Brooke Davis, in particular, were exceptional helpers — thanks to both of you.

Although no work from Kiritimati Atoll appears in my thesis, the planning and execution of fieldwork there, and associated labwork back in BC, was a major part of my time as a PhD student. Special thanks Scott Clark for being someone to rely on on Kiritmati, and a good friend.

Thanks to Graham Edgar for inviting me to participate in the analysis workshop for the incredible Reef Life Survey (RLS) dataset, which ultimately led to my fifth chapter. I am also very grateful to Rick Stuart-Smith for all his hard work making the RLS program a success, to all the volunteer divers who helped collect the RLS dataset, and to the Australian Government for funding my attendance at the RLS analysis workshop.

I was fortunate to receive financial support from scholarships including the NSERC Vanier Canada Graduate Scholarship, a fellowship from the International Society for Reef Studies (ISRS), the J. Abbott / M. Fretwell Graduate Fellowship in Fisheries Biology, and an SFU President's Research Scholarship. I also appreciated other financial support from the Biology and department, AKS and NKD.

Finally, thanks to my family. To my parents; thanks for always fostering my inquisitiveness, enthusiasm, and individuality. I couldn't have asked for a better up-bringing, and the best parts about who I am are down to you. To my sister, Jess Melbourne-Thomas; you've always been and continue to be an inspiration and a valued friend, confidant and advisor, and I look forward to adding colleague to the list. And to my amazing wife Laurel, thanks for your unwavering love, support and encouragement.

Contents

List of Tables

List of Figures

List of Acronyms

CRMR	Consumer-to-resource mass ratio
IBP	Inverted biomass pyramid
ISD	Individual size distribution
PPMR	Predator-to-prey mass ratio
RLS	Reef Life Survey
SFU	Simon Fraser University
TE	Transfer efficiency
TLA	Three-letter acronym

Glossary

Community — The biotic component of an ecosystem; organisms inhabiting a given geographic area and sharing a common resource base.

Community size-structure — The distribution of biomass or abundance among body-sizes in a community, regardless of species.

CRMR — Consumer-to-resource mass ratio. Equivalent to predator-to-prey mass ratio (PPMR, see below), but more appropriately used in cases where consumers are smaller than their resources as may occur for detritivores, filter feeders and scavengers.

Ecological pyramids — Graphs of relative abundance or biomass among body-size classes or trophic-levels in ecological communities. Charles Elton originally described pyramids of abundance and body-size in his book '*Animal Ecology*' in 1927, but pyramids of biomass and trophic-levels have been more prevalent since Lindeman introduced the trophic-level concept in 1942 in his landmark paper '*The trophic–dynamic aspect of ecology*' (which, incidentally, was rejected when he first submitted it for publication).

PPMR — Predator-to-prey mass ratio, with both predator and prey mass measured at the individual level. At the community level PPMR is the average mass of predators at trophic-level *n* divided by the average mass of their prey at trophic-level *n-1*.

Rugosity A measure of substrate structural (or architectural) complexity. Typically quantified by closely contouring a length of fine-link chain to the substrate along a straight line then calculating the ratio between total length of the chain and the linear (straight line) distance spanned between its start and end point.

Size spectra Linear regressions of body mass class against either total abundance in each size class (abundance spectra) or total biomass in each size class (biomass spectra) of individuals, irrespective of species identity, typically on log axes. Hence, indeterminate-growing species, such as fishes, enter and grow through multiple mass classes throughout their life. Size spectra are one form of Individual Size Distribution.

Subsidy Energy from non-local production sources, external to the community being considered, that enters the community at trophic-level at or above primary consumers.

TE (trophic) Transfer efficiency, defined as the production at trophic-level *n* divided by the production at trophic-level *n-1*.

Turnover The rate at which biomass is replaced (turns over) in a community or part thereof (i.e. within a trophic-level or body-size class); typically expressed as the ratio of production:biomass (P:B) or the average lifespan in the assemblage of interest. Turnover *time*, the time required for biomass to be replaced in an assemblage is the inverse of turnover rate.

Chapter 1

General Introduction

Human activities over the last several hundred years have fundamentally changed the structure and function of marine ecosystems (Jackson, 1997; Estes et al., 2011; Pandolfi et al., 2003; Dayton et al., 1998). Fishing, in particular, has dramatically reduced the abundance of large fishes, with ecosystem-wide consequences (Dayton et al., 1995; Myers and Worm, 2005; Jennings and Blanchard, 2004). The loss of large fishes has been a result of both the highly size-selective nature of most fisheries, and the intrinsic vulnerability of large species with slow life histories to exploitation (Reynolds et al., 2001). This loss of large predatory fishes has resulted in widespread increases in the abundance of their smaller-bodied prey, often with cascading indirect effects that propagate over several trophic-levels (Dulvy et al., 2004; Estes et al., 2011; Salomon et al., 2010). The pervasive nature of these changes is widely appreciated (Jennings and Kaiser, 1998; Estes and Terborgh, 2010). However, in most areas, ecosystem change has gradually accrued since long before scientific monitoring commenced. This makes it very difficult to quantify the overall magnitude of change and to envision marine ecosystems prior to their exploitation by humans, i.e. ecological baselines are unclear (Jackson and Sala, 2001; Pauly, 1995).

Most of the worlds human population is concentrated in coastal areas, and coastal reefs harbour a large proportion of the planet's marine biodiversity (Roberts et al., 2002; Stuart-Smith et al., 2013; Reaka-Kulda, 1997). Reefs also support fisheries that feed some of the fastest growing and poorest human populations (Newton et al., 2007), as well as a diversity of other important ecosystem services and social and cultural values (Beaumont et al., 2008; Balmford et al., 2002; Oh et al., 2008). These values have stimulated the rapid growth of reef ecology into a vibrant and productive field of research over the past several decades. A Web of Science search in mid-2014 yielded a total of over 92,000 publications focused on reef ecology, with over 5,000 new publications each year over the past 3 years, as compared to only 418 new

publications in 1984, and 116 new publications in 1964[1]. However, despite more than 40 years of intensive study, there is no clear consensus about what we would expect "pristine" reef fish communities to look like in the coarsest terms (Jackson, 1997; Sandin et al., 2008; Ward-Paige et al., 2010).

One of the most long-standing and easily understood models of community structure is the biomass pyramid (Elton, 1927; Lindeman, 1942). In the absence of humans, would we expect "inverted biomass pyramids" (IBPs) on reefs, with large-bodied fishes at high trophic-levels accounting for more standing biomass than smaller fishes at lower trophic-levels? Or, are IBPs energetically unfeasible? These questions have been debated in the literature in recent years. Apparent IBPs have been documented at some of the worlds most remote, and presumably pristine, reefs (Sandin et al., 2008; Friedlander and DeMartini, 2002). But, concerns have been raised over whether this may be a result of flawed survey methodologies that over-count large mobile fishes (Ward-Paige et al., 2010; Nadon et al., 2012). If IBPs do occur, and are not simply a result of over-counting large fishes, then it is important to understand what ecological processes could give rise to them.

Ecological pyramids were originally presented by Elton in size-based terms (Elton, 1927). More recently, another size-based model of community structure – the size spectrum – has become popular among aquatic ecologists (Sheldon et al., 1972; Jennings, 2005). Size spectra describe the relationship between body-size and abundance (abundance spectra) or biomass (biomass spectra), typically with abundance or body mass summed within logarithmic body-size bins (Kerr and Dickie, 2001). The slopes of size spectra arise from inefficient transfer of energy from smaller-bodied prey to larger-bodied predators (Borgmann, 1987). As such, the "steepness" of the slope depends on how large, on average, predators are relative to their prey (summarised by the mean community predator-to-prey mass ratio, PPMR), and how much energy is lost as it is transferred from prey to predators (trophic transfer efficiency, TE; Borgmann, 1987; Brown and Gillooly, 2003; Jennings and Mackinson, 2003). The slopes of spectra respond predictably to exploitation, becoming steeper as large-bodied individuals and species are preferentially removed and smaller fishes are released from predation pressure (Dulvy et al., 2004; Gislason and Rice, 1998).

Size spectra have great utility for both estimating quantitative ecosystem baselines (Jennings and Blanchard, 2004) and for measuring change in the state of fish communities driven by fishing, habitat degradation, and climate (Merino et al., 2012; Blanchard et al., 2012; Wilson et al.,

[1]Date accessed: May 28th 2014; search term: reef; subject areas included in search: environmental sciences ecology, marine freshwater biology, zoology, biodiversity conservation, fisheries.

2010). Size spectra models and theory were developed in the context of phytoplankton-fuelled communities, and most applications to date have focused on pelagic and soft-sediment communities in temperate shelf seas. Despite the utility of size spectra for addressing environmental and management issues, only a few studies have considered size spectra on coral reefs, and none have examined the size spectra in temperate reef fish communities. The few studies that have considered size spectra on coral reefs have demonstrated that they respond to fishing in a similar fashion to what has been observed elsewhere - becoming steeper in response to the loss of large fishes and increases in the abundance of smaller fishes (Dulvy et al., 2004; Graham, 2004; DeMartini et al., 2008). A key way that reef ecosystems differ from the pelagic and soft-sediment shelf ecosystems is in the presence of foundation species (corals and kelps) that greatly increase the structural complexity of the habitat. On coral reefs, the habitat structure provided by corals has profound effects on fish community size-structure, with higher structural complexity being associated with relatively more small fishes, and more biomass overall (Alvarez-Filip et al., 2011; Wilson et al., 2010). It is not clear whether this response to habitat structural complexity also holds on temperate reefs.

The overarching objective of this thesis was to translate insights size spectra have offered into the structure and function of other marine ecosystems to temperate and tropical reefs. Specifically, I sought to explore the insights that size spectra analyses could give into how size-based processes shape reef fish communities, and into ecosystem baselines.

I first considered the relationship between size spectra and ecological pyramids in order to understand how IBPs might arise (Chapter 2). Next I considered how size-based processes shape community size-structure at regional and local scales in a temperate rocky reef kelp forest case study system (Chapters 3 and 4). Finally I expanded my focus to ask how local processes combine with human influence to shape community size-structure globally, and what insight this global perspective gives into ecological baselines.

Debate surrounding the existence of IBPs in reef fish communities was a major motivation for the first chapter of the main body of this thesis (Chapter 2). The similarity of biomass pyramids and size spectra has been noted several times (e.g. Marquet, 2005; Yvon-Durocher et al., 2011; Brown et al., 2004) but the nature of the link had not been made explicit, nor had its implications for understanding biomass pyramids been appreciated. By demonstrating that biomass pyramids and biomass spectra are equivalent and interchangeable, I show that IBPs are unlikely in closed communities given our current knowledge of how size-based energy flow constrains community structure. I go on to hypothesise that, if survey methodologies are sound, then energetic subsidies could be a plausible mechanism for IBPs. I also highlight that whether

or not a community should be considered subsidies depend on the scale of observation, with a subsided system being one for which the scale of observation does not encompass the scale at which production enters and moves through the community.

I also note in Chapter 2 that there are few empirical estimates of PPMR, and hence necessary knowledge of the underlying process of size-based energy transfer is lacking for most ecosystems and communities - including reef fishes. Further, size spectra have not been characterised on temperate rocky reefs. Hence, in Chapters 3 and 4 I seek to address both these knowledge gaps by undertaking detailed case study on the temperate rocky reef kelp forests of southern Haida Gwaii, BC. In Chapter 3, I simultaneously quantify community size-structure and estimate PPMR across a study area spanning approximately 100 km of coastline. In doing so, I confront the pattern of observed community structure with the underlying process of size-based energy flow. I observe an IBP, but the PPMR estimate suggests that the community should be a stack or bottom-heavy. There is 4-5 times more biomass at the largest body-sizes than would be expected given observed PPMR. This mismatch is unlikely to be due to our survey methodologies, hence I return to the hypothesis posed in the previous chapter and suggest that the most plausible explanation is energetic subsidies.

In Chapter 4 I go on to explore how two foundational components of habitat complexity — substrate rugosity and kelp canopy characteristics — shape fish community size-structure at the site-scale (tens of metres). I find that higher kelp canopy cover and density leads to more biomass across all size classes, whereas higher substrate rugosity boosts the biomass of smaller-bodied fishes and leads to a more even distribution of biomass across size classes. Hence it appears that the rugosity of the underlying rocky substrate has similar effects on fish community size-structure to coral on tropical reefs, while kelp appears to directly or indirectly enhance the resource base for the whole community.

In the final chapter of the main body of the thesis, Chapter 5, I expand my focus to the global scale. I measure biomass spectra in the worlds reef fish communities using a global dataset of visual surveys of unprecedented size and geographic representation. The dataset, collected by the Reef Life Survey program (RLS), includes standardized visual censuses along 50 m belt transects from 1,844 sites in 74 of the worlds marine ecoregions, and my analysis includes 1,498,952 individual fishes. Recognising and accounting for the importance of local ecological variation, I model how anthropogenic pressure has shaped community size-structure on the worlds reefs. I then use this model to predict the community size-structure that would be expected without the effects of anthropogenic pressures. This analysis suggests that current reef fish biomass is

less than half of the baseline expectation and 90% of the largest ($>$ 1 kg), most functionally-important, individuals have been lost. Considering that large-bodied community members often play key roles in regulating the structure and function of ecosystems, this has potentially profound implications for the resilience of reef ecosystems in a changing world. Fortunately, I also find that effective MPAs can restore and protect large bodied fish, providing the best available present-day analogue of reefs without humans.

Finally, Chapter 6 concludes the thesis by synthesising key findings from the previous four chapters in a broader context and considering promising directions for future research.

Chapter 2

Ecosystem ecology: size-based constraints on the pyramids of life[2]

2.1 Abstract

Biomass distribution and energy flow in ecosystems are traditionally described with trophic pyramids, and increasingly with size spectra, particularly in aquatic ecosystems. Here, we show that these methods are equivalent and interchangeable representations of the same information. Although pyramids are visually intuitive, explicitly linking them to size spectra connects pyramids to metabolic and size-based theory, and illuminates size-based constraints on pyramid shape. We show that bottom–heavy pyramids should predominate in the real world, whereas top–heavy pyramids likely indicate overestimation of predator abundance or energy subsidies. Making the link to ecological pyramids establishes size spectra as a central concept in ecosystem ecology, and provides a powerful framework both for understanding baseline expectations of community structure and for evaluating future scenarios under climate change and exploitation.

[2]A version of this chapter has been published as:
Trebilco R., Baum J.K., Salomon A.K., & Dulvy N.K., (2013). Ecosystem ecology: size-based constraints on the pyramids of Life. *Trends in Ecology and Evolution*, 28, 423–431.

2.2 Ecological pyramids and size spectra: size-centric views of community structure

Understanding the processes that structure communities in ecosystems is a fundamental goal in ecology. Elton laid the conceptual foundation for our understanding of these processes with two key observations: (i) interactions among organisms strongly shape the structure and function of communities; and (ii) the nature of these interactions is governed both by the identities and the sizes of the organisms involved (Elton, 1927). Elton further noted the strong link between organisms positions in food chains and their body-sizes, and that larger organisms higher in food chains are less abundant than smaller ones lower down. To capture both phenomena, he introduced ecological pyramids as a way to represent the distribution of abundance and biomass among body-sizes (Figure 2.1).

These first ecological pyramids were pyramids of numbers, where the layers represented bins of body-size, and the width of the layers represented the abundance of all organisms within each size class (Figure 2.1). The pyramid representation of communities quickly took hold in ecology and pyramids were re-expressed in terms of biomass (Lindeman, 1942), production, and eventually trophic-level (Hutchinson, unpublished, in Lindeman 1942). Subsequently, there was a rapidly-adopted and persistent reframing of ecological pyramids to have the layers defined by trophic-level rather than body-size class. This trophic representation of the ecological pyramid is now by far the most common form presented in ecological texts (e.g. Odum 1959; Chapman and Reiss 1999; Krebs 2009; Begon et al. 2006; Levin and Carpenter 2009).

The shape of ecological pyramids qualitatively conveys rich information about the underlying ecological processes that drive ecosystem structure. Communities within ecosystems are comprised of individuals deriving their energy from a common basal pool. Therefore, the combination of the first and second laws of thermodynamics (conservation of energy and increasing entropy) with inefficient energy transfer from predators to prey, dictates that pyramids of production (integrated over time) must always be bottom-heavy (Hutchinson, unpublished, in Lindeman 1942). In other words, there is always greater production of primary producers compared to herbivores, and greater production of herbivores than primary carnivores, and so on. Elton suggested that pyramids of numbers and biomass should be bottom-heavy (Elton, 1927), but this might not always be the case, as the shape of numbers and biomass pyramids depends on the relative rates at which biomass and energy move between size classes (DelGiorgio and Gasol, 1995; Brown et al., 2004; Sandin et al., 2008). For example, biomass pyramids may have a narrower base than apex, a form known as an inverted biomass pyramid (IBP, Lindeman 1942).

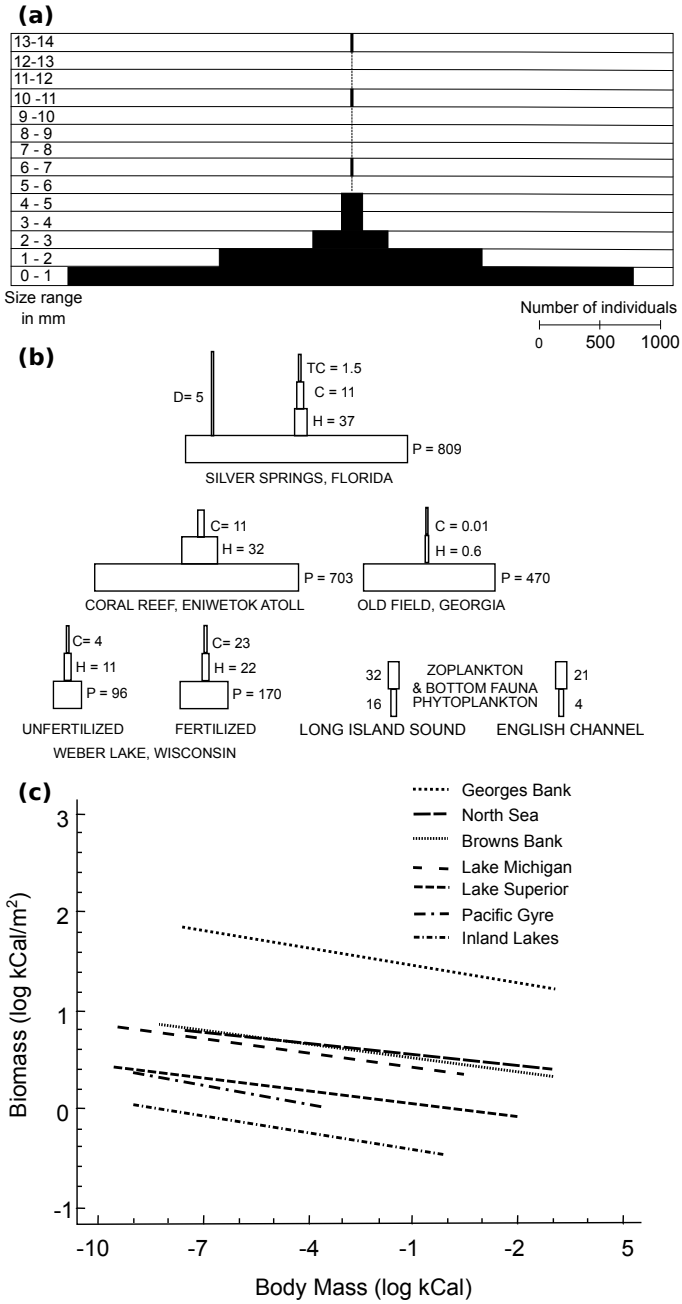

Figure 2.1: Classic examples of ecological pyramids and size spectra (a) an Eltonian pyramid of numbers for the forest-floor fauna of the Panama rain forest, redrawn from Williams (1941) (also reproduced in Lindeman 1942; Cousins 1985); (b) biomass pyramids for several ecosystems, arranged by trophic-level (g/m^2; P= producers, H = herbivores, C = carnivores, TC = top carnivores, D = decomposers), redrawn from Odum and Odum (1955); (c) biomass spectra for pelagic ecosystems, based on summary mean points for phytoplankton, zooplankton, benthos and fish, redrawn from Boudreau and Dickie (1992).

The size spectrum is an alternative representation of the distribution of abundance and biomass among body-sizes that has been popular among aquatic ecologists for several decades (Sheldon et al., 1972; Kerr and Dickie, 2001). Size spectra describe the relationship between body-size and abundance (abundance spectra) or biomass (biomass spectra), typically with abundance or body mass summed within logarithmic body-size bins (Kerr and Dickie, 2001). Thus, like ecological pyramids, size spectra involve converting a continuous variable (body-size, trophic position) into a category for ease of analysis. Also like ecological pyramids, size spectra represent a simple, powerful, and yet apparently distinct, way of understanding and predicting community structure.

It is interesting to consider why the trophic-level version of ecological pyramids has been most popular among terrestrial ecologists while size spectra, which are more closely allied to Eltons original pyramids of body-size, have been more widely adopted among aquatic ecologists. This difference may be due, in part, to differing views of the relative importance of body-size versus taxonomic identity among terrestrial vs. aquatic ecologists. The species niche concept has historically dominated in terrestrial ecology, probably because of the dominance of determinate growth among study organisms whereby function changes little with size. Conversely, in aquatic systems, where indeterminate growth dominates and ontogenetic changes in diet are common, the concept of species belonging to a single niche or trophic-level is less plausible and the size-based view has been more widely appreciated. However, the prevalence of omnivory in foodwebs compels us to now explicitly consider the functional role of individual body-size in ecosystem ecology (e.g. Cohen et al. 2003).

The slopes of size spectra describe the rate at which abundance (abundance spectra) or biomass (biomass spectra) change with increasing body-size. These slopes are remarkably consistent in aquatic ecosystems; typically ~ -1 and zero for abundance and biomass spectra respectively (Sheldon et al., 1972; Dickie and Kerr, 1987; Boudreau and Dickie, 1992). Several models have been developed to explain these slopes, ranging from null stochastic models (Law et al., 2009; Blanchard et al., 2009) to detailed process-based models of predator-prey interactions (e.g. Kerr and Dickie 2001; Benoît and Rochet 2004; Andersen and Beyer 2006; Maury et al. 2007; Silvert and Platt 1978), to simpler bulk property models based on energy transfer (Jennings and Mackinson, 2003; Brown and Gillooly, 2003; Borgmann, 1987). These models share a common basis in recognising that two key community characteristics determine size spectrum slopes: (i) the relationship between predator and prey body-sizes; and (ii) the efficiency of energy transfer from prey to predators. Drawing from terrestrial macroecology (Nee et al., 1991), recent theoretical and empirical work combined this knowledge with predictions from the

energetic equivalence hypothesis and metabolic scaling theory (Brown et al., 2004; Brown and Gillooly, 2003; Jennings and Blanchard, 2004) to provide a way to estimate baseline size spectra: the size spectrum slopes that would be expected in the absence of human disturbance (Box 1).

Box 1: From single trophic-level energetic equivalence to size spectra

If all individuals in a community share a common resource base (i.e., feed at the same trophic-level), energetic equivalence (Nee et al., 1991) predicts that energy use (E) of different body-size classes is independent of body-size (M), meaning that $E \propto M^0$ (Damuth, 1981). Given that total organism metabolic rate (MR), which determines energy use, is known to scale as $MR \propto M^{0.75}$ (Kleiber, 1932), the implications for the scalings of abundance (N) and biomass (B) with M are as follows: N should scale with M as $N \propto M^{-0.75}$,because $E \propto M^0$ and $E = MR \times N$. B should scale with M as $B \propto M^{0.25}$, because $B = M \times N$, such that $B \propto M^1 \times M^{-0.75} = M^{0.25}$ (Figure 2.2; Brown and Gillooly 2003). In size-structured ecosystems, however, only the lowest trophic-level exploits the basal resource pool directly, whereas larger consumers obtain energy indirectly from this basal resource pool by eating smaller prey. Given that the transfer of energy between predators and prey is inefficient, total energy use must decrease with body-size class and trophic-level (Lindeman, 1942). This rate of energy depreciation between trophic-levels depends on TE and PPMR for the community (Borgmann, 1987; Cyr, 2000). These two parameters can therefore be used to estimate the scaling of biomass with abundance across trophic-levels (Brown and Gillooly, 2003), or trophic continua (Jennings and Mackinson, 2003), which are often more representative than are discrete trophic-levels in real communities (Thompson et al., 2007). The expected scalings of E, N, and B with M across trophic-levels are then, respectively (and Figure 2.2):

i. $E \propto M^{log(TE)/log(PPMR)}$

ii. $N \propto M^{-0.75} \times M^{log(TE)/log(PPMR)}$

iii. $B \propto M^{0.25} \times M^{log(TE)/log(PPMR)}$

Empirical testing of this model using well-sampled fish and invertebrate communities in the North Sea demonstrated a close fit between predicted and observed size spectrum slopes (Jennings and Mackinson, 2003; Jennings and Blanchard, 2004). Furthermore, incorporating the metabolic effect of temperature on abundance, biomass, and production using the Boltzmann constant, popularized by the metabolic theory of ecology (Brown et al., 2004), enabled prediction of potential global fisheries production under a range of climate change scenarios (Merino et al., 2012). If consumers at higher trophic-levels and larger body-sizes have access to subsidies, then scaling exponents may be more positive than the size-structured expectations.

Although the conceptual similarity between ecological pyramids and size spectra has been noted in passing (e.g. Yvon-Durocher et al. 2011; Brown et al. 2004), neither the quantitative

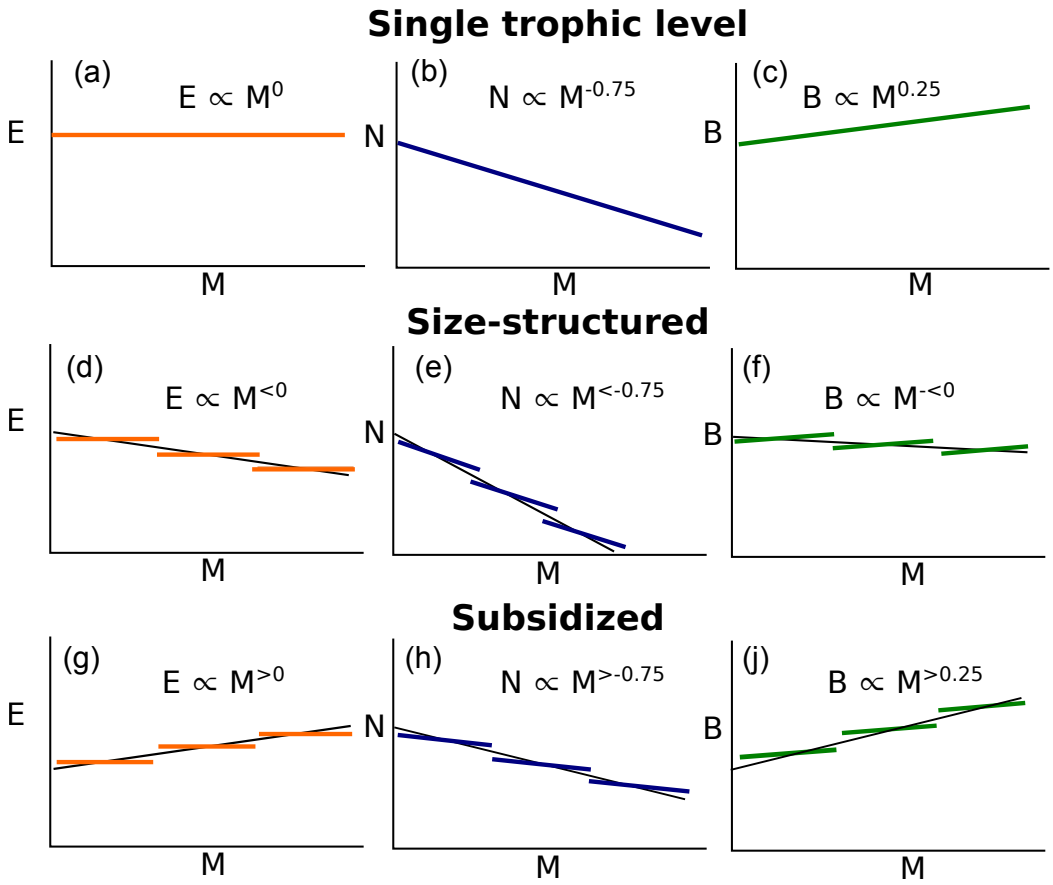

Figure 2.2: The scalings of energy use (E), abundance (N), and biomass (B), with body-mass class (M). Scalings of E, N, and B with M for multiple species within a trophic-level (a), and across multiple trophic-levels (b,c). Loss of energy between trophic-levels (or across trophic continua) with size-structured energy flow results in steeper scalings than the single-trophic-level expectations (d–f), whereas subsidies may result in shallower scalings (g–i). All axes are logarithmic. (a–f adapted from Brown and Gillooly 2003).

link nor the implications were fully appreciated. Here, we reveal the quantitative link between ecological pyramids and size spectra, and in doing so show how pyramid shape is constrained by the same characteristics that control size spectra slopes – transfer efficiency (TE) and the community-wide predator-to-prey mass ratio (PPMR, Box 2). We show how pyramid shape varies with TE and PPMR, and review available empirical estimates of TE and PPMR. Our review indicates that biomass pyramids are almost always expected to be bottom-heavy for communities that share a common resource-base. We hypothesize that inverted biomass pyramids arise from census artifacts or energetic subsidies at larger body sizes (see glossary). Most estimates of community PPMR and TE, as well as the individual-level data required for size spectra, currently come from marine ecosystems, and these are our focus here. However, making the link between ecological pyramids and size spectra demonstrates that size spectra are not an oddity of aquatic ecology, but may be of central importance in ecosystem ecology, providing a size-based lens through which to understand metabolic constraints on pyramids.

2.3 Translating between ecological pyramids and size spectra

Ecological pyramids and size spectra are alternative graphical and mathematical portrayals of the same information (Figure 2.3). The steps for converting both pyramids of numbers and biomass to the corresponding abundance or biomass spectra are identical (Figure 2.3), provided the pyramids are expressed in terms of body-size (rather than trophic-level). Conversion of a trophic-level pyramid to the corresponding size spectrum requires the additional step of converting trophic-level to body-size class (Figure 2.3). This conversion can made if the relationship between body-size and trophic-level is known (described by PPMR, Box 2).

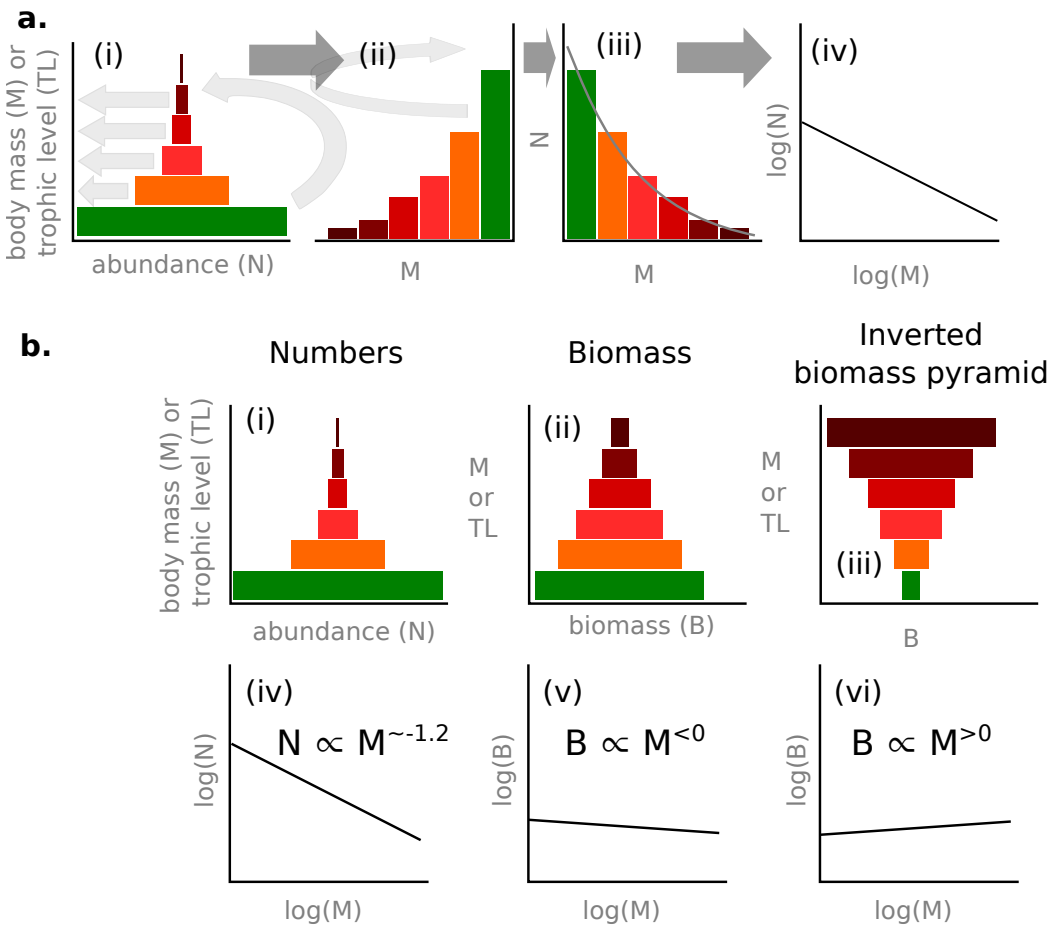

Figure 2.3: (A) When beginning with a trophic-level (TL) pyramid, first convert TL to body mass (M) to give an M pyramid. From the M pyramid, left-align M class layers and rotate 90 degrees counter-clockwise (i to ii); flip the plot onto its vertical axis (ii to iii); express both axes on the log scale, to linearize (iii to iv). (B) Typical bottom-heavy pyramids of numbers (N) (i) and biomass (B) (ii), as well as an inverted biomass pyramid (IBP) (iii), along with the corresponding size spectrum representation for each configuration (iv–vi, respectively).

Box 2: The benefits of individual-level data

Several approaches have been used for examining relations between body mass and abundance in communities (reviewed in White et al. 2007). We have focused here on size spectra, which convey the same information as individual size distributions (ISDs). An important distinction that separates both size spectra and ISDs from other analyses of body mass-abundance relations is that, for size spectra and ISDs, body-sizes are measured at the level of individuals rather than as species-level averages. Species-aggregated data can introduce bias into body mass-abundance relations (Gilljam et al., 2011; Jennings et al., 2007) and are less appropriate for testing predictions from metabolic theory (Brown et al., 2004). Similarly, use of species-level data can prevent clear and significant relations between body-size and trophic-level from being detected (Gilljam et al., 2011), and to spurious estimates of scaling coefficients based on PPMR (Gilljam et al., 2011; Jennings et al., 2007). These problems are most prominent when species have indeterminate growth, and when body mass and trophic-level are strongly related (as in marine communities), but can be important even when indeterminate growth and size-based energy flow are less prominent (as for terrestrial food-webs; Reuman et al. 2008; Gilljam et al. 2011; Jennings et al. 2007). As such, we strongly advocate for the collection of individual-level body-size and trophic-level data wherever possible. To facilitate retrospective analyses of existing species-average data, we pragmatically suggest the consideration of whether species ontogenetic size change lies within one log unit. If so, the use of species-level mean sizes has been a useful way of yielding insightful results (e.g., Hocking et al. 2013; Webb et al. 2011). Alternatively, a statistical sampling approach, based on empirical or estimated mean-variance relations of body-size within species may be used (e.g., Thibault et al. 2010). Empirical estimates of community PPMR can be obtained from stomach content or stable isotope data (Jennings, 2005). In the crudest sense, samples of whole size classes are blended and the trophic-level of a sample of the homogenate is estimated using stable isotope ratios (Jennings et al., 2008). Mean PPMR can then be calculated from the slope (β) of the community relation between trophic-level and body-mass class as: PPMR $= e^{1/\beta}$ (when body mass classes are on a log_e scale or PPMR $= 10^{1/\beta}$ when on a log_{10} scale; Jennings et al. 2002). An important future direction would be to propagate uncertainty in β, using, for example, the delta method, bootstrapping, or Bayesian methods.

The translation of ecological pyramids to size spectra illustrates how the slope of a given biomass (or abundance) spectrum directly reflects the overall shape of the corresponding biomass (or numbers) pyramid, with layers defined by body mass, and that the link for trophic pyramids depends on the community relationship between trophic-level and body-size (PPMR; Figure 2.3, Box 2). Converting from ecological pyramids to size spectra illuminates size-based constraints on the shapes expected for ecological pyramids (as explained below). Conversely, converting from size spectra to ecological pyramids is a powerful method for visualizing the abstract concept of the size spectrum, and the underlying parameter combinations (Box 3).

2.4 A size-based theory of pyramid shape

The shape of a biomass pyramid depends on the scaling of biomass (B) with body mass (M) (the biomass spectrum, $B \propto M^x$), and, in particular, whether this relationship has a positive or negative exponent x (i.e whether the slope of the biomass spectrum is positive or negative). Biomass pyramids have broad bases and narrow apices when the scaling exponent x of the biomass spectrum is less than zero, and are inverted with narrower bases than apices when $x>0$ (Figures 2.3 and 2.4, Box 1). In turn pyramid shape depends on the parameters that control the size spectrum slope – TE and PPMR. Varying TE and PPMR demonstrates how biomass (B) will scale with body mass class (M) and thus indicates the corresponding shapes of biomass pyramids (Figure 2.4). When predators are larger than their prey (i.e. PPMRs greater than 1), extreme combinations of TE and PPMR are required to invert the biomass pyramid (red domain in Figure 2.4). Conversely, bottom-heavy pyramids prevail (scaling exponents of <0) for more realistic TE values (<0.125) across a wide range of PPMR values (blue domain of Figure 2.4). Intermediate to these two situations, a scaling exponent of zero (dashed line in Figure 2.4), implies that biomass is invariant across body-sizes and trophic-levels, resulting in a biomass stack rather than a pyramid.

Pyramid shape has been previously explained by differences in turnover rates — usually expressed as production to biomass ratios (P:B) or generation lengths — between trophic-levels (Buck et al., 1996; O'Neill and DeAngelis, 1981). However, this turnover-based explanation has led to some confusion regarding what pyramid configurations are realistic (e.g. Sandin et al. 2008; Sala et al. 2012; Box 3) and it is not necessary to invoke turnover as an explanation. While there is a pattern of varying turnover rates with trophic-levels and body-sizes, turnover is the proximate rather than the ultimate explanation for pyramid shape. Turnover rate is ultimately dictated by organismal metabolic rate, which is in turn determined by body-size (Lindeman,

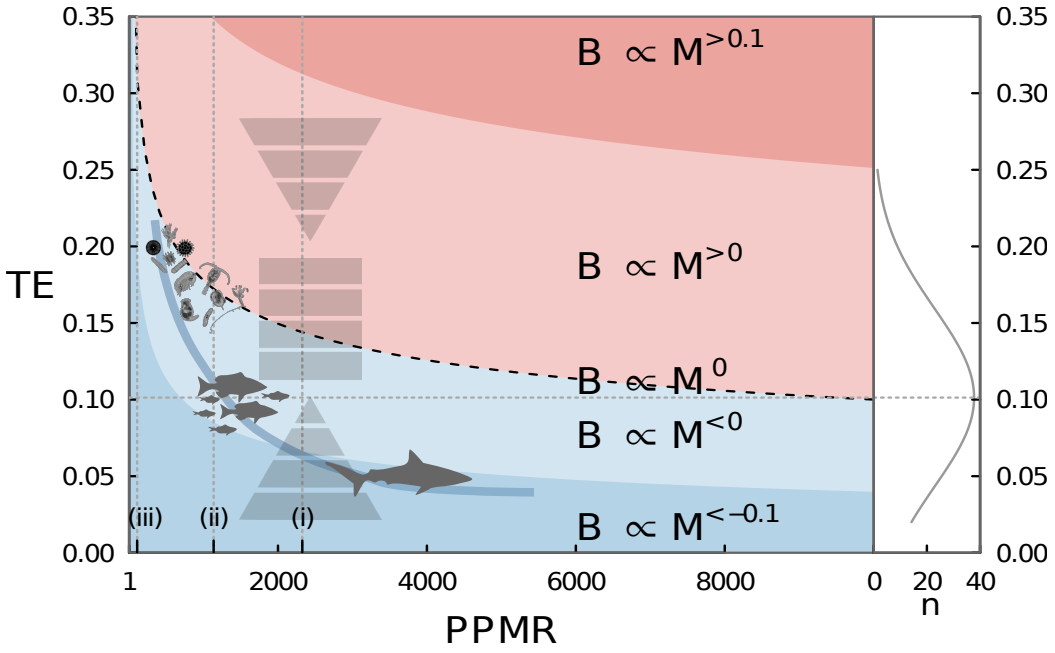

Figure 2.4: The shape of ecological pyramids depends upon the predator:prey mass ratio (PPMR) and transfer efficiency (TE). Biomass pyramids are bottom heavy when $B \propto M^{<0}$ (blue shading) and inverted when $B \propto M^{>0}$ (pink shading). Biomass stacks occur when $B \propto M^{0}$ (black broken line), with biomass invariant across body masses. The right vertical axis shows the distribution of TEs from marine food web models (mean = 0.101, s.d. = 0.058, Pauly and Christensen 1995) with the horizontal dotted gray line indicating the mean. The vertical dotted gray lines represent the only available estimates of community-wide PPMR (i, demersal fishes in the Western Arabian Sea, Al-Habsi et al. 2008; ii, North Sea fishes, Jennings and Blanchard 2004; iii, entire North Sea food web, Jennings and Mackinson 2003). Organism silhouettes illustrate TE and PPMR combinations observed or suggested for subsets of food-webs (fishes and sharks Barnes et al. 2010, both bottom heavy, and plankton, Greenstreet et al. 1997; Ware 2000, spanning from bottom heavy to inverted).

1942; Banse and Mosher, 1980; Borgmann, 1983). Fortunately, because P:B ratios (turnover rate) arise from metabolic rates, their scaling with body-size, as $P : B \propto M^{0.25}$, is both predicted by metabolic theory (Brown et al., 2004) and supported empirically (Banse and Mosher, 1980; Ernest et al., 2003; Greenstreet et al., 1997). Hence, varying turnover rate (P:B ratio) with size and trophic-levels is implicitly and automatically accounted for in size spectrum theory (Borgmann, 1983).

Box 3. The world before humans: measuring impacts and estimating baselines

The loss of large-bodied predators, rise of mesopredators, and trophic cascades are a pervasive legacy of human activities in both terrestrial and marine ecosystems, recently termed trophic downgrading (Estes et al., 2011). Management objectives are hard to define without an understanding of what once was, and what has been lost. However, because hunting and overexploitation began long before scientific data collection, appropriate baselines against which to compare modern community structure are often unavailable (Dayton et al., 1998; Pauly, 1995). Fortunately, size spectrum theory provides a unique method of predicting the structure of ecosystems before the impact of humans. Previous attempts to estimate how ecosystems looked before humans led to surveys of animal biomass at remote locations. These studies recorded high biomasses of large-bodied predators on relatively pristine reefs in the Pacific Ocean (Sandin et al., 2008) and Mediterranean Sea (Sala et al., 2012). The authors concluded that inverted biomass pyramids (where large predators account for the majority of the standing biomass) may represent the baseline ecosystem state for nearshore marine ecosystems, and suggested that differences in turnover rate between small and large fishes account for this pattern. Although it is certain that humans have caused a significant depletion of large-bodied predators across the oceans of the world, size-based constraints on trophic pyramids (see Figure 2.4) show that inverted pyramids are unlikely. Instead, these apparently inverted pyramids likely result from inflated abundance estimates (Ward-Paige et al., 2010; McCauley et al., 2012; Nadon et al., 2012) and/or from the aggregation of highly mobile predators that feed and assimilate energy from pelagic sources beyond the local reef ecosystem (subsidies).

Ecosystem baselines, under current climate conditions, have been estimated for the heavily exploited North Sea, and for the oceans of the world using the size spectrum approach. In the North Sea, the ecosystem baseline size spectra were markedly less steep than the observed biomass-at-size, suggesting the largest size classes had been reduced by up to and over 99% (Jennings and Blanchard, 2004). The power of ecological pyramids for communicating ecosystem structure can be shown by presenting the North Sea size spectra as pyramids (Figure 2.5). This shows that, although the exploited community was characterized by a very bottom-heavy biomass pyramid, the baseline expectation approached a biomass column with relatively high biomass expected in large size classes. Extrapolating beyond the range of body-sizes sampled also illustrates how the pyramid representation can be useful for visualising release in smaller size-classes (Figure 2.5).

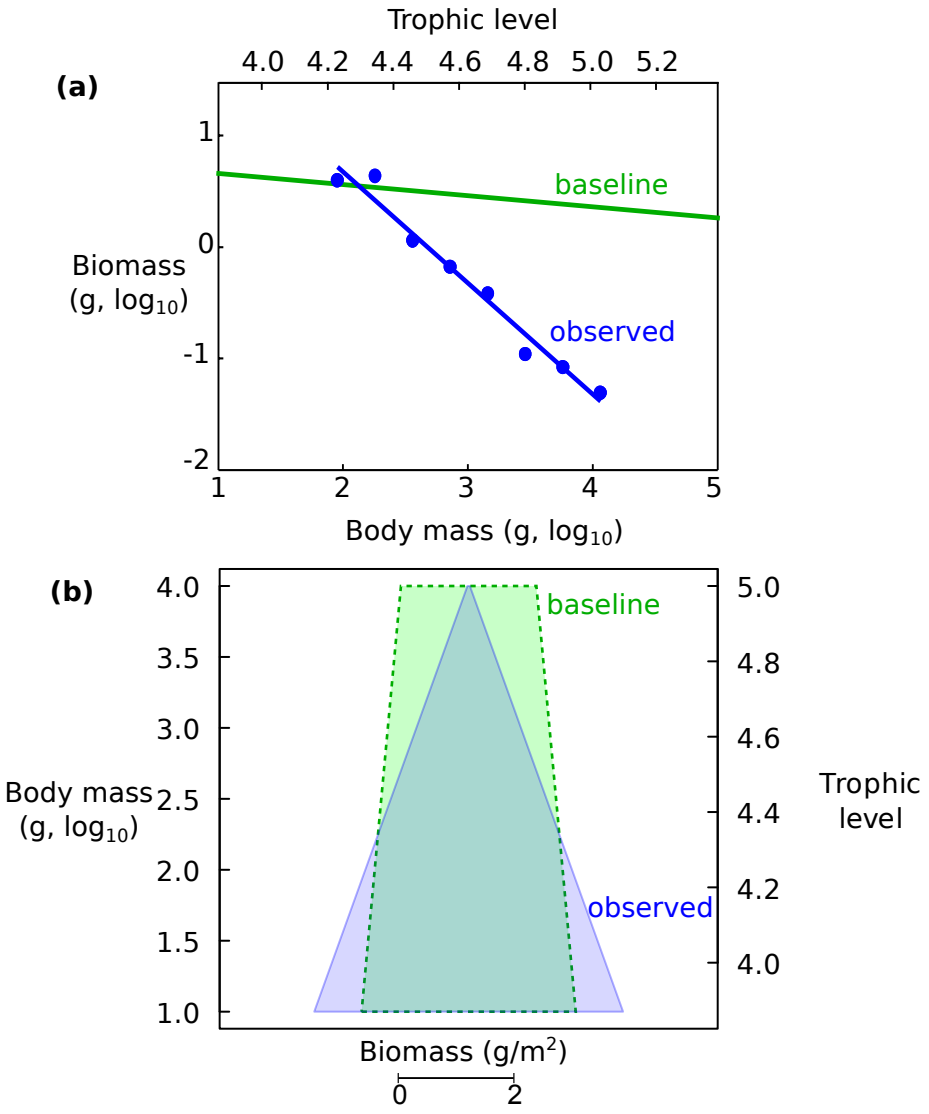

Figure 2.5: Re-expressing size spectra as biomass pyramids to understand baselines and community-scale impacts.(a) The observed (blue line and points) versus predicted baseline (green line) size spectra for the North Sea pelagic fish community can be re-expressed as biomass pyramids (b), highlighting the depletion of large-bodied community members. Extrapolating past the sampled range of body-sizes (striped blue region) also illustrates how pyramids can convey release in small body-sizes. (Panel a adapted from Jennings and Blanchard 2004).

2.5 How can we parameterize size-based pyramids?

PPMR can be estimated empirically from stomach content and/or stable isotope data (Box 2). TE has previously been empirically estimated using size-based stable isotope data (Jennings et al., 2002). However, this method depends on an assumed P:B scaling (P:B $= k * \mathrm{M}^{0.25}$, where k is a normalising constant) and there is considerable uncertainty regarding the constant in this scaling relationship (Jennings and Blanchard, 2004). More robust TEs can be estimated using mass-balance models (e.g. Pauly and Christensen 1995; Ware 2000), and models that account for energy transfer at the individual level including the probability of encountering prey, the probability of prey capture and the gross growth efficiency (Benoît and Rochet, 2004; Andersen and Beyer, 2006). It is important to emphasise here that in the context of size spectra PPMR must be estimated at the individual rather than species level (Box 2) and to date most estimates for both this version of PPMR and TE come from marine food-webs in the four-order-of-magnitude body-size range encompassed by the majority of fishes (10 g to 100 kg).

Community mean PPMRs and TEs appear to consistently fall within surprisingly narrow ranges (Figure 2.4). On average predators are 2-3 orders of magnitude heavier than their prey — mean PPMRs typically range between 100 and 3000 (Jennings et al., 2002; Scharf et al., 2000; Cushing, 1975; Jennings et al., 2001). Energy transfer is inefficient with 10-13% of prey converted into predator production — mean TEs typically fall between 0.1 and 0.13 (Pauly and Christensen 1995; Ware 2000; Jennings 2005; RHS panel of Figure 2.4). Within this TE–PPMR range, biomass pyramids are not inverted (blue zone, Figure 2.4). Inverted biomass pyramids may occur under extreme ecological conditions, when mean PPMRs are close to 3000 (the upper end of the typical range) and transfer is efficient (mean TEs of 0.15 or more). Available evidence suggests that these extremes do not occur in whole communities but may sometimes occur for low trophic-level subsets of communities, such as in planktonic size-classes. Indeed, inverted biomass pyramids often characterise planktonic assemblages, with the biomass of larger heterotrophic zooplankton outweighing that of smaller autotrophic phytoplankton (Buck et al., 1996; Gasol et al., 1997). However, such high TEs are unlikely to be representative of the whole-community mean, or of the mean for assemblages comprising larger body-sizes and higher trophic-levels (Ware, 2000; Barnes et al., 2010). Similarly, for more moderate TEs closer to the typical empirically observed range, extremely large PPMRs ($>$4000) are required for inverted biomass pyramids, which again may occur for subsets of the community with large body-sizes, but do not appear to be representative of the whole-community mean.

The general linearity of empirical size spectra (Box 4) and the strong agreement between

predictions from size spectrum theory and empirical data supports the assumption of community-wide average values for transfer efficiency and predator-to-prey mass ratio (Jennings and Mackinson, 2003; Blanchard et al., 2009; Jennings and Blanchard, 2004; Dinmore and Jennings, 2004). However, recent work suggests that individual-level PPMR in fact increases with body-size (Barnes et al., 2010). The authors point out that, as linear size spectra are empirically supported, this implies that TE must have a compensatory relationship with PPMR such that it decreases with increasing body-size (Barnes et al., 2010). This recent empirical finding is supported by a review of TE in marine food-webs (Ware, 2000), which indicated that TE generally declines with increasing trophic-level, with a mean of 0.13 from phytoplankton to zooplankton or benthic invertebrates, and 0.10 from zooplankton or benthic invertebrates to fish. Barnes et al. (2010) calculated the corresponding TE values that would result, across the range of observed PPMRs, if a linear abundance spectrum with a typical slope (β) of -1.05 was assumed (as TE $=$ PPMR$^{\beta+0.75}$). This approach for estimating TE could be used in future studies for which linear size spectra are observed, and PPMR has been quantified.

Box 4. Assumptions and limitations of the size spectrum approach

The general assumptions of size-based analyses have been described in detail elsewhere (e.g. Kerr and Dickie 2001; Jennings 2005), but specific assumptions involved with estimating community PPMR and with estimating baseline size spectra slopes deserve attention here (also see Jennings et al. 2002; Brown and Gillooly 2003). Estimating PPMR from stable isotope data assumes that fractionation of δ^{15}N is consistent across trophic-levels. Available evidence suggests that this assumption is generally valid (Brown et al., 2004; Dinmore and Jennings, 2004), but future studies that seek to estimate empirically PPMR should include sensitivity analyses for the effect of varying fractionation rates on PPMR estimates or explicitly account for uncertainty in PPMR (Box 2). Similarly, the effect of variation in TE about the estimated value used in models should be made explicit.

A key assumption in using the size spectrum approach to generate baseline estimates of community structure using empirical estimates of PPMR is that it is insensitive to the anthropogenic processes that have driven communities away from their baseline structure. This assumption is likely valid and is supported by available evidence from the North Sea (Jennings et al., 2001; Jennings and Blanchard, 2004), but should be tested in future studies in other systems. It is also important to note that the TE—PPMR model for estimating size spectrum slopes provides an estimate of the equilibrium expectation that would be realized under steady-state conditions. Natural environmental fluctuations and human disturbance will lead to deviations from equilibrium. So, although the time-averaged view of the size spectrum should conform to equilibrium expectations, the 'snapshot' view is a sample that can be nonlinear and have unexpected slope and intercept parameters. For example, in real marine food-webs, production is pulsed rather than constant, resulting in a seasonal wave of production that travels through the size spectrum (Pope et al., 1994). Similarly, human impacts such as fishing also disturb the equilibrium state, and simulation models indicate that this will result in 'waves' that propagate through the size spectrum and nonlinearities (Rochet and Benoît, 2011). However, the simplified expectations of linear spectra and steepened slopes following fishing are supported empirically (Jennings and Blanchard, 2004; Jennings and Dulvy, 2005).

2.6 Base over apex: inverted biomass pyramids in subsidised parts of ecosystems

Inverted pyramids appear to occur in sub-communities where larger body sizes are subsidised with additional energy and materials, such as in detritivorous communities and with aggregations of wide-ranging predators. This pattern has also been noted among plankton in lakes, with

inverted biomass pyramids generally indicative of zooplankton benefiting from allochthonous input from terrestrial vegetation (DelGiorgio and Gasol, 1995). Although there are few empirical estimates of TE and PPMR for communities and ecosystems other than aquatic pelagic, one study estimated PPMR for a marine benthic detritivore and filter-feeder community (Dinmore and Jennings, 2004), and body-mass-abundance relationships in soil detritivore communities have been extensively documented (Reuman et al., 2009, 2008; Meehan, 2006). These sources of information suggest that in both aquatic and terrestrial ecosystems, detritivorous and filter feeding communities are characterised by PPMRs of less than one, indicating that larger-bodied individuals feed at lower trophic-levels than do smaller members of the community. PPMRs of less than one result in inverted biomass pyramids; in the North Sea this yields a biomass spectrum slope of 0.48 (Dinmore and Jennings, 2004) for benthic invertivores (consumers of benthic invertebrates), while in soil food-webs abundance spectrum slopes are consistently shallower than -0.75 (implying biomass spectrum slopes of $>$0.25)(Reuman et al., 2009). Although one could infer from the latter that the predictions of size spectrum theory are not supported by the data for soil foodwebs if assuming PPMRs of $>$1, PPMRs in detritivorous soil food-webs are likely to be fractional (less than 1 and greater than zero), in which case observed scalings are compatible with theoretical predictions. From these observations we hypothesise that subsidised ecosystem compartments, where larger consumers have access to more production than do smaller members of the community, exhibit inverted biomass pyramid slices.

2.7 Escaping the constraints of size-based energy flow

A related mechanism may operate at much broader scales, whereby large highly-mobile consumers essentially self-subsidize, by accessing production from multiple local biomass pyramids, hence escaping the constraints of energy availability at local scales. Indeed, limited energy availability at local scales may have driven the evolution of increasing space use and increasing PPMR among larger-bodied species and size classes; many of the largest animals are wide-ranging herbivores (elephants) or filter-feeders (baleen whales, and whale sharks). Size spectra clearly illustrate that escaping local size-based energy flow is necessitated by decreasing energy availability with increasing body-size and trophic-level such that there is insufficient energy left to support minimum viable local populations of large-bodied predators at the thin end of the size spectrum wedge. Hence, we hypothesize that at some point size-based predation must become energetically unfeasible, driving the largest consumers to escape the constraints of local size-based energy flow. Such escapes will be necessary in order to access sufficient energy to support minimum

viable populations at low widely-dispersed densities (due to large body-size). Jennings (2005) suggested that such escapes may happen at system-dependent body-size thresholds. The more recent finding of Barnes et al. (2010) instead suggests that the relationship between trophic-level and body-size is in fact continuous and probabilistic, but non-linear, such that marine organisms in the largest body-size classes (100 kg to 1000 kg) have a greater likelihood of feeding with much higher PPMR than the rest of the community (PPMR = 14000 at 1000 kg vs. 1500 at 100 g). There are two ways to escape the tyranny of low energy availability at the largest size classes. (i) The largest predators must be able to feed at sufficiently expansive spatial scales with strategies that may be viewed as skimming the tops of multiple spatially-discrete local biomass pyramids, as typified by sharks, tunas, and wolves. (ii) The alternate solution is to evolve extreme PPMR and sieve the bottom of widely-dispersed and seasonally-variable pyramid bases, as typified by elephants, baleen whales, basking and whale sharks, and mobulid rays. Even though wide-ranging predators may be present locally within the census frame and appear to be part of an inverted biomass pyramid, in this situation they in fact represent the spatially-constrained tip of a biomass pyramid with a larger-than-censused base (or multiple smaller spatially discrete pyramids).

This emphasises the importance of being mindful of the spatial and temporal scales at which production occurs when seeking to understand the processes that shape assemblages (Levin, 1992; Chave, 2013). In the context of classical communities that share a common resource base, the scales of censusing should align with and lie within the community and ecosystem boundaries of local energy production. If members of an assemblage obtain production at different scales (e.g. predator aggregations) and one tries to interpret the structure of the assemblage with models that assume a common resource base, this may lead to a misleading picture of the processes responsible for observed community structure (e.g. differences in turnover time between trophic-levels being invoked to explain apparent inverted biomass pyramids in the case of predator aggregations, Box 3). One possible solution is to sample hierarchically with progressively larger sample frames for wider ranging animals (Chave, 2013; McCauley et al., 2012).

2.8 Implications and future directions

By revealing the link between ecological pyramids and size spectra, we show that they are two sides of the same ecological coin. By demonstrating their interchangeability, we are compelled to suggest that size spectrum theory be viewed as a mainstream approach to understanding ecosystem ecology alongside ecological pyramids. Ecological pyramids have not yet outlived

their usefulness because, once scaled with appropriate quantitative axes (which have often been lacking), and parameterised using size spectrum theory, they provide a powerful way of visualizing the structure of ecological communities and the impact of human activities upon them (Box 3). Importantly, reverting to Eltons original size-based view of pyramids resolves uncertainty over how and when inverted biomass pyramids may occur in real single- and multi-trophic-level communities and sheds light on the types of ecological pyramids that likely existed prior to historical depletions of large predators (Box 3, Figure 2.5, McClenachan et al. 2012).

Within a trophic-level, greater biomass occurs at increasing body-size classes. Biomass may also increase with body-size for highly efficient low-trophic-level sub-communities (i.e. plankton). But across multiple trophic-levels and for increasingly large-bodied communities, our review of current knowledge of realistic ranges for PPMRs and TEs indicates that inverted biomass pyramids are unlikely. Instead, we hypothesize that inverted biomass pyramids may occur in two situations. First, in subsidised community subsets, such as detritivorous sediment and soil communities. Second, in island communities where there may be spatial mismatch between the scale of sampling (around islands, haul-out beaches, waterholes) and the scale of production (wider ocean or entire savannah), resulting in some members of the community being subsidised by sources of energy produced elsewhere that would ordinarily be unavailable to the rest of the local community. This provides another avenue for questioning and understanding the important role that subsidies play in structuring foodwebs (Polis et al., 1997; Talley, 2008), and the role that large-mobile consumers play in linking production pools (Hocking et al., 2013; McCann et al., 2005) — a role that may have been disrupted by historical reductions of predators (McClenachan et al., 2012). Empirical tests of these mechanisms using stable isotopes, microchemistry and other tools to elucidate production sources and trophic positions in real communities will be a fruitful avenue for future research (e.g. McCann et al. 2005). While size spectra and ecological pyramids provide a useful tool for diagnosing subsidies at assemblage scales, ecologists need to be cautious in applying foodweb and community concepts to parts of foodwebs that may not satisfy the underlying assumptions of the conceptual models being employed.

Given the increasing understanding of the importance of size-based processes in terrestrial as well as aquatic ecosystems, and accompanying calls to collect data that are suitable for a wide variety of analyses (i.e. size-based, trophic, taxonomic; for example see McCauley et al. 2012; Petchey and Belgrano 2010), exploring the nexus and unification of size-based, trophic and taxonomic perspectives seems to be an important goal. Linking size spectra with trophic pyramids is an important step in this direction, and illustrates that size spectra are widely applicable for understanding constraints on community structure across ecosystems.

Size spectrum theory represents a powerful framework for understanding constraints on community structure that can be used to understand both historic baselines and future scenarios under climate change (Box 3, Yvon-Durocher et al. 2011). Size spectra are also useful for generating null hypotheses against which empirical data can be compared to identify departures that are worth investigating further (Marquet, 2005). The full potential of the approach can be evaluated as data are collected from a wider range of communities on land and in the sea, and as key assumptions are tested (Box 4). Two types of data are needed: body-mass–abundance data, ideally with body mass measured at the individual level (as opposed to species-level averages), and community-wide size-based stable isotope estimates of predator-to-prey mass ratio (Box 2). Such data are available for relatively few ecosystems at present but collecting these data should be a priority (Petchey and Belgrano, 2010; Marquet, 2005). Even in the absence of such data, approximate conversions from species-averaged to size-based representations can be made (e.g. Ings et al. 2008; Webb et al. 2011; Thibault et al. 2010; Box 2).

By linking ecological pyramids with size spectrum theory we reconcile two foundational and previously divergent ecological theories to reveal the size-based constraints to the pyramids of life. This provides a fruitful, visually-intuitive and pragmatic approach both for measuring and communicating the ecosystem consequences of global change, as well as for guiding conservation management goals and targets.

2.9 Chapter-specific aknowledgements

The manuscript upon which this chapter is based was greatly strengthened by comments and suggestions from Paul Craze, the editor of *Trends in Ecology and Evolution* two anonymous reviewers. J. Melbourne-Thomas, M. Hocking, L. Davidson, C. Mull, S. Pardo, and J. Sunday also provided valuable feedback on earlier drafts.

Chapter 3

The paradox of inverted biomass pyramids in kelp forest fish communities[3]

3.1 Abstract

Size spectra theory predicts that bottom-heavy biomass pyramids or 'stacks' should predominate in real world communities if trophic-level increases with body-size (mean predator-to-prey mass ratio, PPMR, >1). However, recent research suggests that inverted biomass pyramids characterize relatively pristine reef fish communities. Here, we estimated the slope of a temperate reef fish community biomass spectrum from underwater visual surveys at a remote island chain off the north-western coast of British Columbia, Canada. Counter to theory, the observed biomass spectrum slope we detected is strongly positive, reflecting an inverted biomass pyramid. This is at odds with theory because this slope would only be expected if trophic-level decreased with increasing body-size (consumer-to-resource mass ratio, CRMR, < 1). We then used δ^{15}N signatures of muscle tissue to estimate PPMR and instead detected strong evidence for the opposite, with PPMR $\approx$ 5500. The natural history of kelp forests suggests that this paradox could arise from energetic subsidies in the form of movement of mobile consumers across habitats, and from strongly seasonal inputs of production (pulsed production) at small body-sizes. In this case there was four to five times more biomass at large body sizes (1–2 kg) than would be expected in a closed steady-state community.

[3]N.K. Dulvy, S. Anderson and A.K. Salomon are coauthors on this chapter, which is currently in preparation for journal submission

3.2 Introduction

Half a century of temperate and tropical reef science has yielded a wealth of knowledge regarding how species interactions shape community ecology (for recent reviews see Steneck et al. 2002; Mora 2014; Steneck and Johnson 2014), yet our ability to predict community size-structure remains constrained by a lack of empirical data and theoretical treatment of them (Sandin et al., 2008; Ward-Paige et al., 2010; Trebilco et al., 2013). Inverted biomass pyramids (IBPs), where the biomass of large predatory fishes far outweighs biomass at smaller body-sizes and lower trophic-levels, have been reported on pristine reefs in the remote tropical Pacific (Friedlander and DeMartini, 2002; Sandin et al., 2008). Such IBPs may be the baseline ecosystem state for reef fish communities in the absence of human exploitation (Sandin et al., 2008). However, the plausibility of such top-heavy configurations has been debated (Ward-Paige et al., 2010; Nadon et al., 2012; Trebilco et al., 2013). Recent work demonstrating the equivalence of biomass pyramids and biomass spectra highlights that, in size-structured assemblages, where trophic-level increases with body-size, biomass distributions should be "stacks" or bottom-heavy pyramids, and not strongly inverted (Trebilco et al., 2013). Available evidence and natural history suggests that fish communities tend to be strongly size-structured because indeterminate growth and gape-limited size-selective predation predominate among fishes (Sheldon et al., 1972; Cushing, 1975; Jennings et al., 2001; Barnes et al., 2010). Hence, the empirical evidence of IBPs on reefs presents an interesting paradox.

Biomass spectra (and other forms of individual body-size distributions) provide a powerful means for understanding how size-based energy flow combines with physical and biotic conditions to shape ecological communities (Jennings and Blanchard, 2004; Petchey and Belgrano, 2010). Individual metabolic rates (and thus energy requirements) scale predictably with body-mass (M) as $M^{0.75}$ (Kleiber, 1932), and the energetic equivalence rule constrains energy use to be similar across body-sizes within a single trophic-level (Damuth, 1981; Peters, 1983). Hence, the distribution of abundance and biomass across body-sizes in multi-trophic-level communities is fundamentally constrained by how efficiently energy is transferred between trophic-levels, and by how trophic-level is related to body-size (Brown and Gillooly, 2003). The first constraint — usually referred to as trophic transfer efficiency (TE) does not vary widely — and typically ranges between 10–12 % (Pauly and Christensen, 1995; Ware, 2000). The second constraint — the relationship between trophic-level and body-size — is determined by how large, on average, predators are relative to their prey, or the average community predator-to-prey mass ratio

(PPMR). These processes are summarised in the following equation, which predicts the equilibrium biomass spectrum slope β that results from a given combination of TE and PPMR: $\beta = 0.25 + \log(\text{TE})/\log(\text{PPMR})$. Because TE cannot exceed 1, $\log(\text{TE})/\log(\text{PPMR})$ will always be negative if PPMR is > 1, and biomass spectrum slopes are therefore constrained to be less than 0.25 if trophic-level increases with body-size. This framework is also applicable for predicting community size-structure in situations where trophic level *decreases* rather than increases with increasing body size (e.g. Dinmore and Jennings, 2004), although in such situations the relationship between trophic-level and body-size is more appropriately expressed as a consumer-to-resource mass ratio (CRMR) rather than PPMR.

Biomass pyramids and biomass spectra are equivalent and interchangeable; negative biomass spectrum slopes correspond to bottom-heavy pyramids, positive slopes correspond to inverted pyramids, and slopes of zero ('flat' spectra) represent biomass stacks or columns (Trebilco et al., 2013). Hence the ecological processes, summarised by TE and PPMR, that determine the slopes of biomass spectra also determine ecological pattern — the shapes of biomass pyramids. A wide body of literature has demonstrated that, across body-sizes from plankton to fish, biomass spectra tend to be flat in pelagic marine ecosystems in the absence of exploitation, indicating biomass stacks or columns (Sheldon et al., 1972; Kerr and Dickie, 2001; Jennings, 2005). Slopes become steeper as anthropogenic impacts selectively remove large-bodied individuals and species, and often indirectly benefit smaller-bodied ones — leading to increasingly bottom-heavy pyramids (Dulvy et al., 2004; Jennings and Blanchard, 2004).

Fish predators tend to be two to four orders of magnitude larger than their prey (Cushing 1975), but there are few empirical estimates of community PPMR. To our knowledge, PPMR has never been estimated for a reef fish community. The available community-wide PPMR estimates predominantly come from fishes and invertebrates in pelagic and soft-sediment demersal systems, where values have fallen within the expected range of hundreds to thousands (Jennings et al., 2001; Jennings and Blanchard, 2004; Al-Habsi et al., 2008). These PPMRs, combined with TEs of $\sim$10%, lead to flat biomass spectra and biomass columns. Because there are no empirical estimates of PPMR for reef fish communities, it difficult to infer how the process of size-based energy flows underlies observed patterns of community structure on reefs.

Here we seek to understand whether the pattern of observed fish community structure is consistent with the predation process represented by PPMR for reef fishes in the kelp forests of Haida Gwaii, a remote archipelago located off British Columbia, Canada's northwest coast (Figure 3.1). Owing to their remote location and spatial protections (Fisheries and Oceans Canada, 2008; BCMCA, 2011), the fish communities on these reefs should be relatively pristine.

Kelp forests and coral reefs differ from pelagic systems in that energy is derived from multiple sources of external secondary production and local primary production, and in the presence of habitat-forming foundation species. Temperate kelp forests specifically provide a highly contrasting ecosystem relative to pelagic and soft-sediment systems that have been studied to date in which to explore biomass spectra and PPMR.

Knowledge of PPMR will illuminate how size-based energy flows underlie community structure in rocky reef kelp forests. A near-zero or weakly negative biomass spectrum slope (stack or pyramid) combined with an estimated community PPMR in the order of hundreds to thousands would be concurrent with theory, and with previous observations in pelagic ecosystems. Alternatively, a high positive biomass spectrum slope (inverted pyramid), in combination with a negative relationship between trophic level and body size (CRMR between 0 and 1), would be more consistent with what has been observed in detritivorous benthic infauna communities (Dinmore and Jennings, 2004). If neither of these scenarios are supported (i.e. high positive biomass spectrum slope combined with positive PPMR) this implies that the scale of observation does not match the scale at which production enters and moves through the community. Hence, knowledge of how PPMR corresponds to biomass spectrum slope will provide fundamental new insights into the processes underlying patterns of fish community structure on reefs.

3.3 Methods

This study was undertaken within and around the Gwaii Haanas National Marine Conservation Area Reserve and Haida Heritage Site, on Haida Gwaii (Figure 3.1). In order to estimate the slope of the community biomass spectrum (and hence the shape of the biomass pyramid), we conducted visual surveys of reef fish communities (3.3.1 below) and fit a hierarchical linear model of summed biomass within body mass bins (3.3.2 below).

To estimate PPMR, we first conducted community-scale sampling via hook-and-line and spear fishing to collect reef-associated fish for δ^{13}C and δ^{15}N stable isotope analysis (3.3.3 below). δ^{15}N measurements were used as a proxy for the trophic position of individual fish. We then constructed a Bayesian hierarchical model of the community relationship between trophic position and body size, from which we calculated community PPMR (3.3.4 below).

3.3.1 Underwater visual census of kelp forest fish size and abundance

Fish communities were visually surveyed using belt-transects at twelve sites; 3 sites nested within 4 areas (Louise, Lyell and Kunghit East and Kunghit west; Figure 3.1). Surveys were undertaken

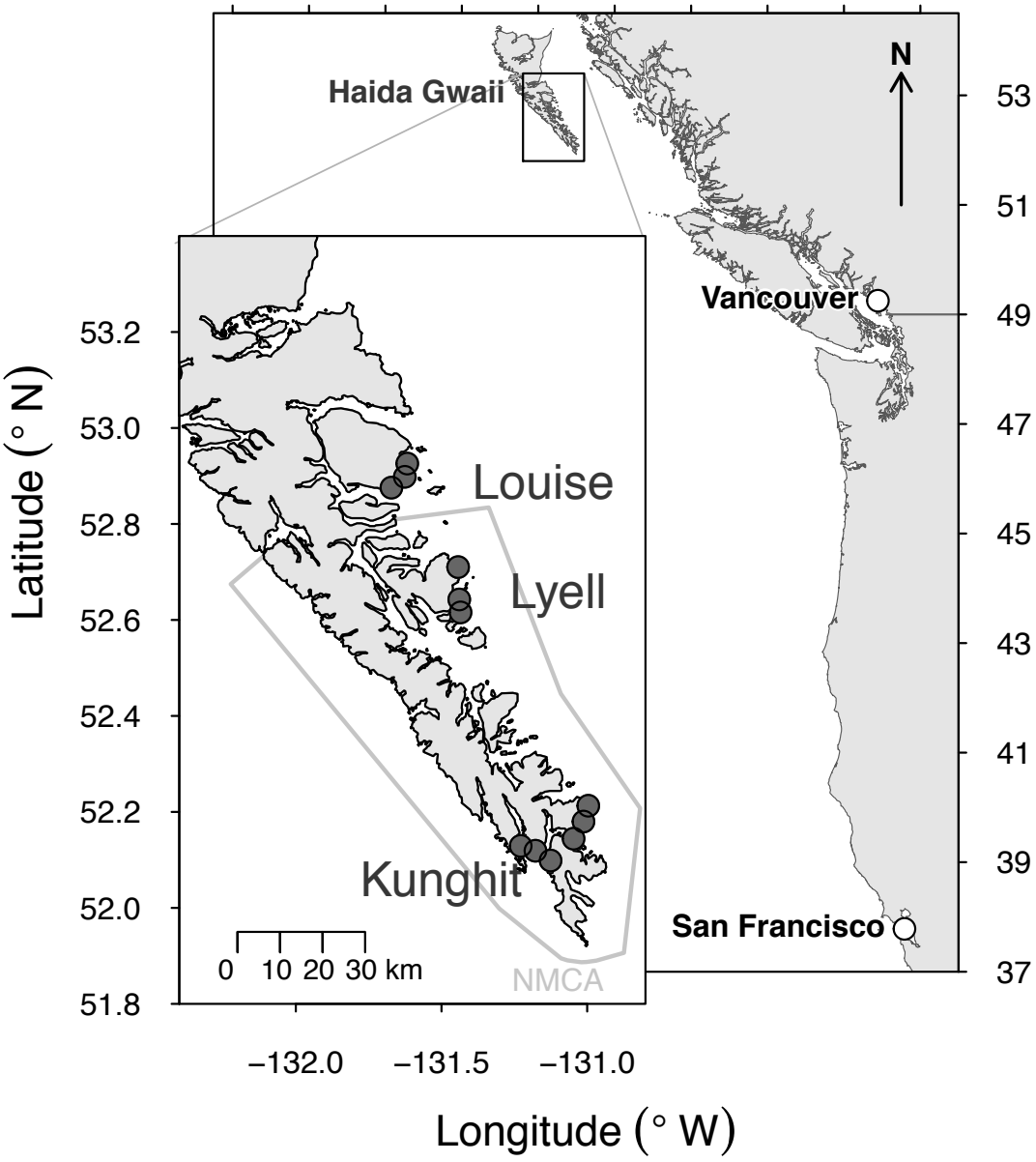

Figure 3.1: Study sites (points) were located on the southern shores of Haida Gwaii (formely the Queen Charlotte Islands) off the northwest coast of British Columbia, Canada. The boundaries of the Gwaii Haanas National Marine Conservation Area Reserve (NMCAR) and Haida Heritage Site are shown in light gray.

in the summer (between late June and early August) each year from 2009 to 2012, with the majority of sites surveyed every year (a full summary of survey protocol is provided in Trebilco et al., 2014). Four to six belt transects were surveyed at each site in each year (four at each site in 2009, six at each site in 2010, 2011 and 2012), split evenly between 'deep' and 'shallow' strata (tide-corrected depth of 12.0 $\pm$ 1.3 m and 7.7 $\pm$ 1.1 m below chart datum respectively). Transects were 30 m long by 4 m wide, and deployed parallel to shore, with the ends of each transect separated by a minimum of 5 m. For each transect an individual diver deployed a plastic transect meter tape while swimming forward at an approximately constant speed (Watson et al., 1995), recording conspicuous fishes (all fishes other than blennies, gobies, gunnels and other small cryptic species) present in the sampling 'frame'. Count time was not standardized as it was dependent on fish abundance and habitat characteristics. Individual fish lengths were visually estimated to the nearest cm. To ensure accuracy of length estimates, observers were trained by estimating the size of known-length objects underwater (following Bell et al., 1985; Polunin and Roberts, 1993). Additionally, observers carried a 'measuring pole' (an 80 cm length of PVC, labeled with cm increments, and mounted at the end of a 1.5 m pole, as per Frid et al., 2013) which was used to both directly measure fishes where possible, and to self-check visual estimates. Individual weights were then calculated using species-specific length-weight conversions from FishBase (`www.fishbase.org`).

3.3.2 Biomass spectra

We fit biomass spectra as hierarchical linear models (linear mixed effects models), to account for the spatially and temporally nested structure of the survey data, using the R package `lme4` (Bates et al., 2013). Before the model-fitting process we narrowed the size fraction used for analysis. Small fishes ($<\sim$ 15 cm) are subject to poor detectability in visual surveys (Ackerman, 2000), hence we used the corresponding mass of 32 g as the lower size cutoff for inclusion in analyses. This size class represented the median for the dataset, supporting our assumption that it was the minimum size that was surveyed effectively (Ackerman et al., 2004). Only 3 fish larger than 2048 g were observed across all surveys, hence we dropped them and set this mass as our upper cutoff. Between our mass limits of 32 — 2048 g, we calculated biomass-per log_2 size class-unit-area (B) as follows. All biomass within each of the six log_2 body-mass bins (32 — 64 g, 64 — 128 g, 128 — 256 g, 256 — 512 g, 512 — 1024 g, 1024 — 2048 g) was summed to the mid-point (M) of each body-mass bin for each area-year combination, and divided by the total area surveyed to give biomass g^{-1} m^{-2} in each mass class. We then modeled biomass spectra as hierarchical linear regressions with $\log_2(\mathrm{M})$ as the predictor and $\log_2(\mathrm{B})$ as the response.

We centred body mass class (M) about zero by subtracting the mean prior to model fitting in order to remove correlations between the slope and intercept (Daan et al., 2005). The spatially and temporally nested structure of the data was accounted for by including both area and year as crossed random effects.

3.3.3 Stable isotope estimates of individual trophic allometry

We sampled fishes for stable isotope analysis using hook-and line and spear fishing and collected a total of 234 individuals of 17 species, spanning a range of 5.6 g to 31 kg mass and 5.8 cm to 1.6 m total length (Table S1). A recent review of studies that have evaluated within-species relationships between body-size and trophic-level for inshore coastal fishes found that most studies did not sample an adequate range of body-sizes to have the power to detect significant relationships (Galván et al., 2010). To ensure we had an adequate range of body-sizes we adopted a targeted collection approach. We used both hook-and-line and spear fishing, with standard commercially-available pole spears and custom "micro" spears (Pinnegar and Polunin 2000), to maximise the range of body-sizes sampled for the species which dominated the community .

Fishes were weighed, measured and dissected in the field and a sample of white muscle was excised from each fish from the dorsal musculature behind the head. Muscle samples were immediately frozen for transportation and storage. In the laboratory, samples were thawed, rinsed with 10% HCl followed by de-ionized water, and oven dried for 48 hours at 60°C. Samples were then manually ground to a fine powder and 1 $\pm$ 0.2 mg portions were packaged into 5 x 3.5 mm tin capsules. δ^{13}C and δ^{15}N values for packaged samples were measured using a PDZ Europa ANCA-GSL elemental analyzer interfaced to a PDZ Europa 20–20 isotope ratio mass spectrometer. δ^{13}C and δ^{15}N were calculated as:

$$\delta^{15}X = \left(\frac{R_{\text{sample}}}{R_{\text{standard}}} - 1 \right) \times 1000$$

where R_{sample} and R_{standard} are the ratio of heavy:light isotopes (^{13}C:^{12}C and ^{15}N:^{14}N) in the sample and the international standard (V-PBD for C and air for N) respectively. δ units are parts per thousand (‰). Stable isotope analyses were conducted by the UC Davis Stable Isotope Facility (SIF).

3.3.4 Scaling from individual trophic allometries to the community-wide predator-to-prey mass ratio

We explored two approaches to model the community relationship between trophic position and body-size, and to estimate the community mean PPMR from the slope of this relationship.

First we use a Bayesian hierarchical approach (section 3.3.5 below), which allowed us to account for the nested nature of the data (species sampled within areas) and to explicitly incorporate important sources of uncertainty, including instrument error in measurements of δ^{15}N and uncertainty in the assumed rate of δ^{15}N fractionation (Δ^{15}N) with increasing trophic position.

Sampling for isotope samples was not random, and the relative number of samples for each species in each bin did not necessarily reflect the proportional contributions of species to biomass in each size class in the community. Further, some species caught via hook-and-line fishing were not observed on transects. To test whether this biased our results, we conducted a jackknife analysis, excluding one species at a time from the analysis and re-estimating PPMR. For each jackknife we ran 10,000 model iterations with 3 chains, discarding the first 5000 as burn-in and keeping every 5th iteration value thereafter for a total of 3000 saved samples per jackknife. This allowed us to evaluate sensitivity of estimated PPMR to the individual species included in the analysis.

It was not possible to include weightings in the Bayesian model, so as a second approach to estimating community mean PPMR we evaluated a hierarchical linear model where individual data points were weighted by the proportional contribution of each species to total biomass in each size-bin for each area (see 3.3.6 below).

3.3.5 Bayesian hierarchical linear model for the estimation of community predator-to-prey mass ratio

Preliminary exploratory analyses fitting models with the R package `lme4`, and not accounting for measurement error, indicated that a random-effect structure allowing slope to vary randomly with species and an intercept to vary randomly with species and area was best supported by the data (lowest AIC). We retained this random-effect structure in the Bayesian model that we describe below. These preliminary analyses also indicated minimal correlation between random effects. Therefore, for simplicity, we proceeded with a Bayesian hierarchical model that did not model correlation between random effects.

To build our model, we first assigned each individual fish for which δ^{15}N was measured into $\log_2$ body mass classes ($\log_2$ M). We then modeled δ^{15}N as (with α and β denoting the global slope and intercept paramaters, α_j, α_k and β_j denoting the group-level slope and intercept

deviations, $\mathcal{N}$ denoting normal distributions, σ and τ denoting standard deviations about the means):

$$\delta^{15}\mathsf{N}_i^{\mathsf{true}} = \alpha + \alpha_j + \alpha_k + (\beta + \beta_j) \cdot \log_2 \mathsf{M}_i + \epsilon_i,$$
$$\text{For } i = 1, \ldots, N \text{ observations}, \quad j = 1, \ldots, J \text{ species}, \quad k = 1, \ldots, K \text{ areas},$$
$$\alpha_j \sim \mathcal{N}(0, \sigma_\alpha^2), \quad \beta_j \sim \mathcal{N}(0, \sigma_\beta^2), \quad \alpha_k \sim \mathcal{N}(0, \tau_\alpha^2), \quad \epsilon_i \sim \mathcal{N}(0, \sigma^2).$$

We incorporated measurement error around $\delta^{15}\mathsf{N}_i^{\mathsf{true}}$ as:

$$\delta^{15}\mathsf{N}_i^{\mathsf{measured}} \sim \mathcal{N}(\delta^{15}\mathsf{N}_i^{\mathsf{true}}, 0.04),$$

where $\delta^{15}\mathsf{N}_i^{\mathsf{measured}}$ represents a measured value of δ^{15}N and 0.04 represents the assumed measurement variance (based on personal communication from the UC Davis SIF).

We chose non-informative normal priors on $\{\alpha, \alpha_j, \alpha_k, \beta, \beta_j\} \sim \mathcal{N}(0, 10^6)$, a uniform prior U(0, 100) on the residual standard deviation σ, and weakly informative half-Cauchy priors with scale parameters of 10 on the standard deviation parameters $\sigma_\alpha, \sigma_\beta$ and τ_α to constrain the parameter to reasonable values and aid computation (Gelman, 2006). The priors are unlikely to drive the posterior distributions of the standard deviation hyperparameters as they allow for far greater values than the data suggest, while somewhat limiting extreme values and thereby aiding computation.

We then estimated PPMR incorporating uncertainty in fractionation rate (Δ^{15}N) as:

$$\mathsf{PPMR} = 2^{\Delta^{15}\mathsf{N}/\beta}, \quad \Delta^{15}\mathsf{N} \sim \mathcal{N}(\mu_{\Delta^{15}\mathsf{N}}, \sigma^2_{\Delta^{15}\mathsf{N}}).^4$$

We assumed a mean fractionation ($\mu_{\Delta^{15}\mathsf{N}}$) of 3.2 ‰ with a standard deviation ($\sigma^2_{\Delta^{15}\mathsf{N}}$) of 1. 3.2 ‰ has been recommended as an assumed value for fish white muscle tissue (Sweeting et al., 2007), and adding a wide standard deviation around this assumed mean encompasses the other widely recommended value of 3.4 ‰ (Minagawa and Wada, 1984; Post, 2002) as well as making our PPMR estimate robust to emerging evidence that fractionation rate may vary with body-size and species (although such variation is likely to be small within the range of body-sizes considered here Wyatt et al., 2010; Hussey et al., 2014).

We drew samples from the posterior distribution of all parameters using `JAGS` (Plummer,

[4] with the base of 2 in $2^{\Delta^{15}\mathsf{N}/\beta}$ reflecting the log_2 binning for body mass, M.

2003). We ran 100,000 iterations with three chains, discarded the first 50,000 iterations as burn in, and recorded every 10^{th} iteration value thereafter for a total of 15,000 posterior samples. We assessed chain convergence with the Gelman-Rubin diagnostic (all were below 1.1) and visual inspection of the chains and performed graphical posterior predictive checks to ensure our probability model could recreate similar data (Gelman et al., 2014).

3.3.6 Biomass-weighted hierarchical linear model for the estimation of community predator-to-prey mass ratio

Using visual survey data, we calculated the proportion of the total observed biomass in each size bin contributed by each species in each area (with biomass from all survey observations summed within areas). These proportions were then matched to isotope samples based on the species from which each sample was obtained, the body mass bin into which each sampled fish fell, and the area in which each fish was caught, and included as weightings in a hierarchical linear model for the relationship between trophic position and individual body mass, fit using the R package `lme4` (Bates et al., 2013). Not all species for which isotope samples were obtained were observed on visual surveys. Further, not all species that were observed on surveys were observed at all sizes in all areas. Therefore, we used the following decision rules to assign missing weightings:

1. If a species was not observed on visual surveys for a given $\log_2$ mass-class in one area, but was observed in that mass-class in other areas, isotope samples for the mass-class/area combinations where it was not observed were assigned the mean weighting for that mass-class from those areas where it was observed.

2. If a species was not observed in a given $\log_2$ mass-class in any area, isotope samples for that species/mass-class were assigned a weighting of half of the lowest weighting from all other species observed in that mass-class and area.

3. If no fish of any species were observed in a $\log_2$ mass-class in any area, samples were assigned a weighting of 0.5

Using these weightings, we modeled biomass spectra as hierarchical linear regression with $\log_2(\text{M})$ as the predictor and $\log_2 \delta^{15}\text{N}$ as the response. The spatially nested sampling design was accounted for by allowing intercept to vary randomly with area. Slope was allowed to vary randomly by species. PPMR was calculated from the global regression slope (β) as $\text{PPMR} = 2^{\Delta^{15}\text{N}/\beta}$ assuming a fractionation rate ($\Delta^{15}\text{N}$) of 3.2 ‰.

3.4 Results

We surveyed a total of 203 transects and observed 4537 fishes between 32 and 2048 g. This included 19 species, predominantly rockfishes (family Sebastidae) and greenlings (family Hexagrammidae; table S1). The estimated biomass spectrum slope was 0.45 (Figure 3.2). The bootstrapped 95 % confidence intervals around the slope estimate were 0.15–0.75, and the marginal and conditional R^2 values were 0.17 and 0.37 respectively (Nakagawa and Schielzeth, 2012). This positive size spectrum slope implies an inverted biomass pyramid.

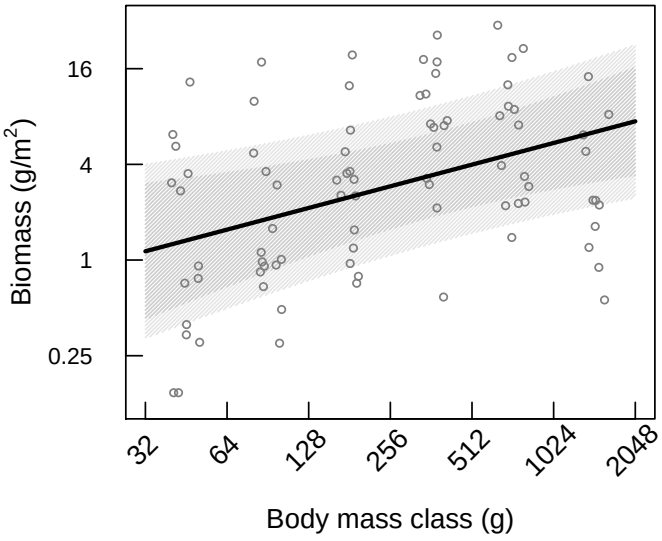

Figure 3.2: The biomass spectrum for the kelp forest fish community of of Haida Gwaii, British Columbia, Canada. Gray bands indicate 95% confidence intervals incorporating uncertainty in fixed (inner band) and random effects (outer band). Marginal $R^2 = 0.17$; conditional $R^2 = 0.37$

Both modelling approaches indicated that trophic position, as described by δ^{15}N signatures, increased strongly with body-size at the community scale (Figure 3.3 and Figure A.1). The hierarchical Bayesian modelling approach yielded a probability distribution for community PPMR with a median of $\sim$ 5500 (95 % credible intervals $\sim$ 50 – 1×10^6, Figure 3.4). The jackknife analysis indicated that no single species had a disproportionate effect on the estimated community relationship, as the probability distribution for estimated PPMR did not change substantially when individual species were excluded from the model (Figure A.2). The PPMR estimate from the biomass-weighted hierarchical linear model was 5861 — almost identical to the median estimate from the Bayesian model, indicating that, although the Bayesian approach did not weight species by their proportional contribution to total biomass, it provides an unbiased estimate of

the true community PPMR.

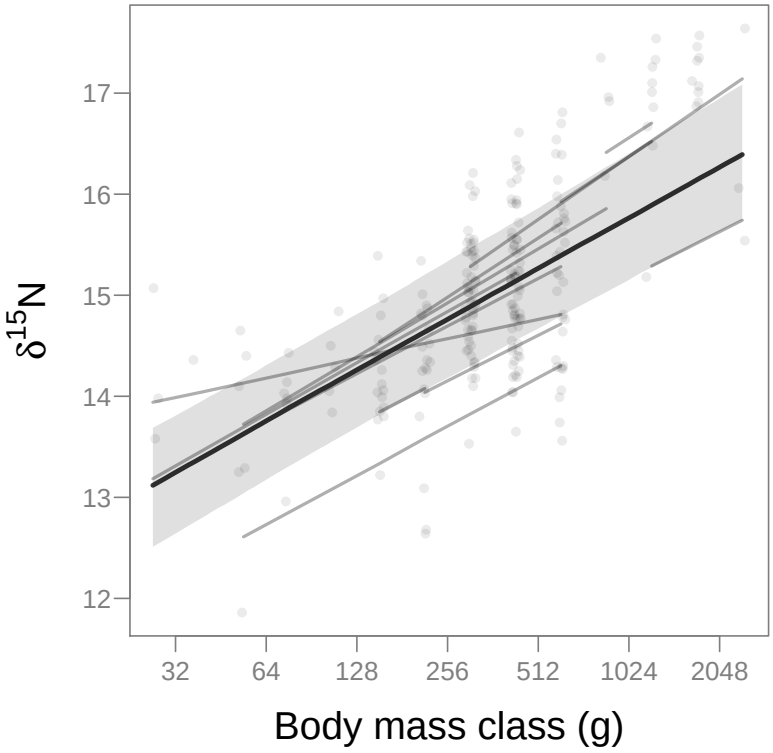

Figure 3.3: The relationship between δ^{15}N, a proxy for trophic position, and body-size for the kelp forest reef fishes on Haida Gwaii, British Columbia, Canada. Black line and gray shaded band indicate the global fit and 95% confidence intervals. Gray lines indicate the mean fits for individual fish species.

The strongly inverted biomass distribution we observed is energetically unfeasible given the underlying predation process (PPMR), unless subsidized from outside the sampling frame. Such a strongly inverted biomass pyramid (yellow line in Figure 3.4) would only be expected within the TE/PPMR space that corresponds to the 95 % confidence bounds of our estimated biomass spectrum (shown by the yellow hatched area in Figure 3.4). This would require one or other of two conditions, either very efficient energy transfer (TE $>$0.2, pyramid *i* in righthand panel of Figure 3.4) or situations where consumers are smaller than their resources (CRMR, $<$1, lefthand panel of Figure 3.4). Neither combination of transfer efficiency or PPMR/CRMR is likely. Instead the observed predation-based transfer of energy suggests that only a stacked distribution of biomass is possible (rectangle *s* in Figure 3.4). The observed range of PPMR estimated here is shown by the bottom panel in Figure 3.4. The intersection this PPMR distribution with the likely range for TE (as derived from foodweb models; Pauly and Christensen 1995) is shown by the crosshair

in Figure 3.4, which is consistent with a flat biomass spectrum and a stacked biomass pyramid with similar biomass across all size classes. Instead we observed four to five times more biomass in the largest size class (1024—2048 g) than in the smallest (32—64 g).

A biomass spectrum slope of more positive than 0.25 is only possible if CRMR is less than one (consumers smaller than their resources), and there was only a 1 % probability of PPMR being less than 10 given our posterior distribution on PPMR. Even the lower 95 % confidence interval limit on the estimated biomass spectrum slope of 0.15 could only be realised in a closed size-structured community if PPMR was outside the 95 % credible intervals of the empirical estimate ($>10^5$), in combination with a TE of $>$0.2 (Figure 3.4), which also falls outside the 95 % quantiles for estimated TEs from foodweb models (reported by Pauly and Christensen 1995).

3.5 Discussion

Here, for the first time, we report that a temperate reef fish community is structured as an inverted biomass pyramid while, paradoxically, the estimated predator-to-prey mass ratio (PPMR) corresponds to expectations for bottom-heavy pyramids. The inverted biomass pyramid configuration we observe is similar to what has been reported for other relatively pristine reef fish communities (e.g. Sandin et al., 2008; Sala et al., 2012). However, the natural history of fishes (Cushing, 1975; Scharf et al., 2000), our findings here (Figure 3.4), and evidence from other studies that have empirically estimated PPMR for fish communities in other ecosystems (e.g. Jennings and Blanchard, 2004; Al-Habsi et al., 2008; Barnes et al., 2010) all suggest that fishes tend to be characterised by positive PPMRs (reflecting size-based energy flow), that should result in bottom-heavy pyramids or trophic stacks (biomass spectra with slope $\leq$ 0). This suggests that other processes overwrite size-based energy flows in these systems. Two key hypotheses that could explain observed inverted biomass pyramids are census error (Ward-Paige et al., 2010) and subsidies (Trebilco et al., 2013). We consider these in the context of our study system below.

Two types of census error that might lead to the erroneous description of inverted biomass pyramids (positive biomass spectrum slopes) are systematic errors in abundance estimates (over-counting large fishes and/or under-counting small fishes) and systematic errors in body-size estimation (overestimating the size of large fishes and/or underestimating the size of small fishes). In this study, if the community was truly represented by a trophic stack, biomass in the largest or smallest size class would have had to have been over- or under-estimated respectively

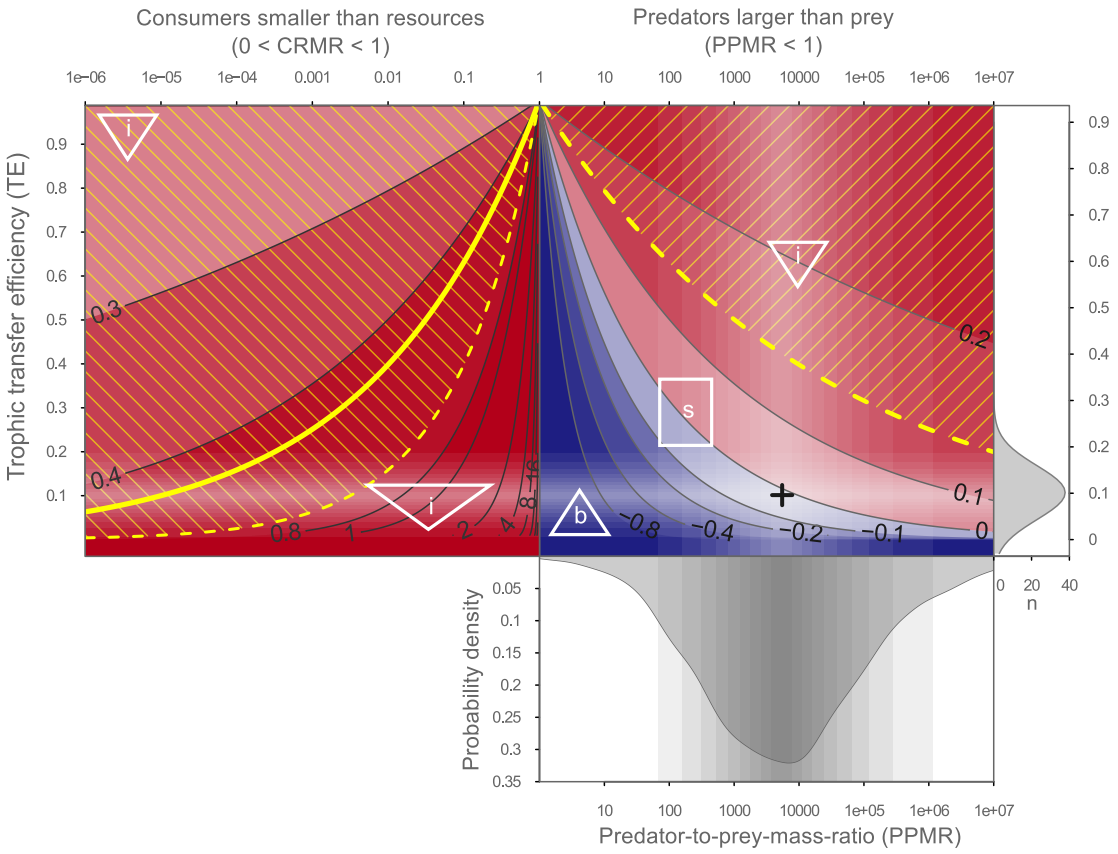

Figure 3.4: Expected biomass spectrum slopes (top panels) resulting from varying combinations of mean community predator-to-prey mass ratio (PPMR) and transfer efficiency (TE), shown with reference to the probability distribution of estimated PPMR for the reef fish community of Haida Gwaii (bottom panel). The top right panel shows scenarios with predators larger than prey (PPMR >1); top left panel shows scenarios with predators smaller than prey (0< PPMR <1). Positive slopes (red area) correspond to inverted biomass pyramids (represented by triangles labeled *i*), while negative slopes (blue area) correspond to bottom-heavy pyramids (triangles labeled *b*) and zero slopes imply stacks/columns (rectangle labeled *s*). x Yellow shading lines indicate the range of slopes corresponding to to the 95 % confidence bounds around the empirically estimated biomass spectrum slope of 0.45 (solid yellow line). Right vertical axis shows TEs derived from from marine food web models (n = 48, mean = 0.101, s.d. = 0.058; Pauly and Christensen (1995)). Shaded bands represent 5 % quantile increments between 5 % and 95 % for TE and PPMR, and the black cross hair indicates the highest probability for both distributions (PPMR = 5500, TE = 0.101)

by four-to-five fold to give rise to the observed configuration. We next consider the likelihood of each of these forms of census error being responsible for such over- or under-estimation.

Evidence from simulation models suggests that over-counting of large fishes arises when they are highly mobile (e.g. large sharks and jacks in the tropics; Ward-Paige et al. 2010), and if they are attracted to divers or exhibit net movement toward divers (Watson et al., 1995; Watson and Quinn, 1997; Ward-Paige et al., 2010). However, the fishes in our study system are both smaller and less mobile than the sharks and jacks that have been suggested to be over-counted in other studies. Further, they do not exhibit strong attraction to divers and are typically observed 'hovering' rather than swimming actively. Hence it is unlikely that over-counting of large fishes was responsible for the disparity in our results. The abundance of small cryptic fishes is well recognised to be dramatically under-estimated in visual surveys. To avoid this problem, we deliberately restricted the range of body sizes included in our analysis to a size range that can be censused effectively using visual surveys (Ackerman et al., 2004). Therefore it is also unlikely that under-counting of small-bodied fish was responsible for our results.

Untrained observers have a tendency to underestimate the size of fishes smaller than 30 cm and to overestimate the size of fishes larger than 30 cm, with a mean estimation error of approximately 10 % (Edgar et al., 2004). Trained observers are able to estimate sizes far more accurately, and without bias (e.g. Dulvy et al., 2004). To to ensure the accuracy of our size estimates, observers were well-trained and also carried 'reference poles' to benchmark visual estimates. Hence, we can also rule out systematic errors in size-estimation driving our results.

While census error is unlikely to be responsible for the inverted biomass pyramids we observed, the natural history of temperate reefs suggests that energetic subsidies are highly likely. Two processes are likely to subsidise the fish communities in this study system and facilitate inverted biomass pyramids: the movement and foraging of mobile consumers across habitats; and seasonally pulsed inputs of production at small body-sizes. We expand on these mechanisms below, but first it is important to emphasise that the extent and magnitude of energy subsidies are relative to the scale of observation (Trebilco et al., 2013).

Energetic subsidies have traditionally been defined in terms of the movement of energy across ecosystem boundaries (Polis et al., 1997; Talley, 2008). However, in systems that lack clearly-defined ecosystem boundaries (such as reefs) and where the assemblage is defined by the scale of observation, it is informative to consider observed assemblages may be subsidies by production from outside of the scale of observation. In this context, a subsidised assemblage is one for which the sampling scale does not encompass the spatial and temporal scale of the production that supports it (Polis et al., 1997; Trebilco et al., 2013). To illustrate this concept with a

well-known example, consider streams where anadromous salmon provide nutrient subsidies to local stream and riparian plant and animal communities (Naiman et al., 2002; Hocking et al., 2013; Harding et al., 2014). In this case, when the scale of observation is the stream, the system is subsidised because the production-base for the nutrients that salmon bring to streams spans the ocean-basin scale at which salmon forage. But, if the scale of observation is expanded to encompass both the ocean basins where salmon forage at sea, and the streams where they spawn, the system is no longer subsidised.

A similar (though smaller) mismatch between the spatial scale of observation and the scale of the production-base is likely for the kelp forest fish assemblage of Haida Gwaii. Temperate reef-associated fishes typically have ranges with small "core areas" (tens of metres in diameter; Tolimieri et al. 2009) but may undertake brief longer-range excursions (hundreds of metres) to forage (Tolimieri et al., 2009; Galván et al., 2009). The 'snapshot' temporal scale of our surveys means that such foraging excursions are unlikely to be captured and hence observed communities may be 'subsidised' by prey production that occurs at a broader spatial scale than is represented by the distribution of fishes on transects. Observations that off-reef production is often important for sustaining on-reef fish biomass lend support to this mechanism (e.g. Bray et al., 1981; Galván et al., 2009; McCauley et al., 2012; Wyatt et al., 2012).

A mismatch in the temporal scale of production vs. observation is also likely in this highly seasonal system. Importantly, small-bodied schooling forage fishes, notably Pacific herring (*Clupea pallasii*), are an important resource base for temperate reef fishes (Murie, 1995; Smith et al., 2011) but as they are only ephemerally present for several weeks each year, they are not captured in surveys outside this narrow window of time. During the time that they are present, juvenile Pacific herring have been observed to dominate rockfish diets (particularly for larger rockfish; Murie 1995), and both rockfishes (Keeling, 2013) and greenling (Rooper and Haldorson, 2000) have been observed to also prey on herring eggs, which are deposited on macro-algae and rocky substrates in the inter-tidal and shallow sub-tidal zone during seasonal spring-spawning events. Due to the high calorific content of herring and their eggs, these resources may contribute a substantial proportion of the annual energy budget of reef fish in this study system (Murie, 1995). Similarly, newly recruited juveniles of reef associated species are likely to be important prey for larger fishes. Empirical evidence from other systems also supports this hypothesis, with significant intra-annual variation in abundance having been shown for other temperate reef fish communities (Irigoyen et al., 2013).

The way in which energetic subsidies affect community size-structure depends upon the body-size at which the extra production enters local communities, and on whether the production input

is constant or pulsed over time (Yang et al., 2008; Anderson et al., 2008). Subsidies that enter the community at large body-sizes will lead to less bottom-heavy/more-inverted pyramids (less-negative/more-positive biomass spectrum slope; Trebilco et al. 2013). We hypothesise that the seasonal pulses of forage fish such as Pacific herring and reef fish recruits described above have this effect in our study system. Subsidies that enter communities at small body-sizes (e.g. zooplankton associated with upwelling) will have the effect of increasing the total amount of energy and biomass available to be propagated to larger body sizes. If such subsidies are constant over time, this will have the effect of broadening the base of biomass pyramids, but may not affect the overall distribution of body-sizes (i.e. increase biomass spectrum intercept, with no effect on slope). However, if production is pulsed, there will be a tendency for production and biomass to be transient at small size classes and to accumulate at larger sizes (Pope et al., 1994). Hence, snapshot censuses will be more likely to capture less bottom-heavy configurations (less-negative/more-positive biomass spectrum slopes). Given the highly seasonal nature of our high-latitude study system, we suggest that this process is also likely to contribute to the observed IBPs. Explicit tests of these hypothetical mechanisms will be an important goal for future work.

Resource pulses and subsidies have previously been recognized to be closely related (often being one and the same) and to overlap in the way that they influence communities (Anderson et al., 2008; Yang et al., 2008). Although they span a continuum, subsides have been distinguished from pulses on the basis of spatial transport (with subsidies involving the transport of engergy across ecosystem boundaries) and the degree of pulsedness. The need to integrate understanding of subsidies and resource pulses has been highlighted previously (Anderson et al., 2008). We suggest that this is especially true when ecosystem boundaries are not clear as the distinction between subsidies and resource pulses then becomes blurred.

Our study represents an important methodological advance in estimating PPMR in that we explicitly account for multiple sources of uncertainty to arrive at a probability distribution rather than a point estimate. The probability distribution for PPMR was centred around predators being approximately 5500 times heavier than their prey, reflecting a strong positive relationship between trophic-level and body-size both within species and across the whole fish community. Even while accounting for multiple sources of uncertainty, this PPMR estimate is similar to estimates from other size-structured marine communities — as might be expected given that gape-size allometry is highly conserved across fishes. In the North Sea, several point estimates of PPMR for the fish community range from several hundred to several thousand (Jennings et al., 2001; Jennings and Warr, 2003; Jennings and Blanchard, 2004). Part of this variability

stems from the assumptions made in different studies, and the Bayesian approach we adopted here explicitly deals with these assumptions and associated uncertainty in a more transparent and quantitative manner. The only other marine fish community of which we are aware for which PPMR has been estimated is the Western Arabian Sea, where the estimate was 2327. Interestingly, this assemblage included herbivorous parrotfishes, and when these were excluded from the analysis, the PPMR estimate increased to 7792, which is closer to our estimate.

We recognise that our Bayesian methodology is potentially susceptible to bias since the data were not weighted by their proportional contribution to total community biomass. However, the fact that we obtained an almost identical PPMR estimate (5861) using a biomass weighted hierarchical linear model gives confidence that the PPMR estimate we obtained from the Bayesian model accurately reflects the true community PPMR. The insensitivity of the PPMR estimate to species weightings is a result of the fact that species-level slopes for the relationship between trophic position and body size are all similar (and positive) in this system (Figure A.3). Weighting by biomass would be more important if slopes varied widely among species, and developing methods that both account for uncertainty and allow for species biomass weightings will be an important goal for future studies.

Community predator-to-prey mass ratios are thought to covary negatively with foodchain length, with larger PPMRs being characteristic of shorter food chains (Jennings and Warr, 2003). Thus, the relatively high PPMR estimate for the kelp forest fish assemblage of Haida Gwaii suggests that the foodchain is relatively short. This is also reflected in the narrow span of δ^{15}N values across the range of body-sizes sampled. For the smallest body-size class sampled of 4–8 g, the mean δ^{15}N was 13.1‰, and the minimum observation was 11.9‰, while for the largest size class of 16–32 kg the mean was 16.4‰, and the maximum observation was 17.2‰. Thus, assuming a trophic fractionation rate of 3.2 ‰ per trophic-level, mean trophic position spanned only 1.1 trophic-levels, and the span from the lowest trophic-level individual observed to the highest was only 1.8 trophic-levels. This is similar to the range of trophic-levels observed for the fish community of the Western Mediterranean Sea of 1—1.3 trophic-levels (Al-Habsi et al., 2008). The types of predator-prey interactions present in communities and variability/frequency of disturbance are thought to be the most important predictors of food-chain length, with short food chains expected in size-structured communities subject to high variability and/or frequent disturbance (Post, 2002; Jennings and Warr, 2003). Communities dominated by organisms that are long-lived, slow-growing, relatively sedentary and well-defended from predation are also expected to have short foodchains (Post, 2002). Thus, both high seasonality and the dominance of long-lived slow growing rockfishes may contribute to the short foodchains observed in the kelp

forests of Haida Gwaii. We have only considered readily observable reef associated fishes here, so this is not necessarily reflective of a short foodchain for the whole community. However, we also sampled rock scallops at the same sites at which fishes were collected and observed a mean δ^{15}N of 10.4 (Trebilco, unpublished data). Large long-lived bivalve molluscs such as scallops have previously been used as isotopic baseline in calculating absolute trophic-levels for fishes, assuming that such long-lived filter feeders occupy trophic-level 2. Assuming a fractionation rate of 3.2, this would indicate that fishes span trophic-levels 3—4 in this study.

In this study we implicitly assumed that a shared isotopic baseline for δ^{15}N was representative of all fish sampled. Isotope estimates for dominant prey species (forage fish, crabs and other benthic invertebrates, and zooplankton; see Table A.1) would be required to explicitly test this assumption, but were not available for this study. However, this assumption was supported by the observation of a mean δ^{15}N of 10.4 for rock scallops (placing them one trophic level below the smallest fish sampled). As the longest-lived filter feeding invertebrates present on the reefs of Haida Gwaii, rock scallops provide the best available time-integrated baseline estimate for δ^{15}N for this system.

3.5.1 Conclusion

By making the first estimate of community PPMR for a reef ecosystem, this study fundamentally advances our understanding of the processes underlying patterns of reef fish community structure. Several authors have explained the phenomenon of inverted biomass pyramids on reefs using closed-community models (e.g. Sandin et al., 2008; Wang et al., 2009), but our results highlight the importance of recognising the energetically open nature of reef fish assemblages. In this system this results in four-five times more biomass of large fish (1–2 kg). Subsidies are ubiquitous; in fact, it has been argued that most systems are subsidised, or energetically open (Polis et al., 1997). Several authors have noted that resource subsidies may lead to patterns of community structure that are inconsistent with models that assume assemblages are energetically 'closed' — and based solely on in-situ productivity (Polis et al., 1997; Hocking et al., 2013). Other research has highlighted the importance of the heterogeneity of production in space and time, coupled with sampling scale, when describing the structure of marine communities (Barry and Dayton, 1991). We suggest that focusing on how reef communities are shaped by spatial subsidies and temporal subsidies in the form of resource pulses, and on how the scale of observation affects estimates of community structure, will be fruitful lines for future inquiry.

Chapter 4

Habitat complexity shapes size-structure in a kelp forest reef fish community[5]

4.1 Abstract

Understanding how habitat complexity shapes fish communities is necessary for informing marine spatial zoning and reserve selection and to predict the impacts of future habitat change. In kelp forests, the presence and characteristics of canopy-forming kelps and the architectural complexity, or rugosity, of the underlying rocky substrate are known to influence reef fish recruitment, abundance, biomass and species composition. However, it is not yet clear how these foundational elements of habitat complexity shape the distribution of biomass across body-size classes. Here, we use biomass spectrum models to evaluate how fish community size-structure in high latitude kelp forests is shaped by substrate rugosity and the degree of closure and density of the kelp canopy. We find that the presence of a closed kelp canopy increases overall fish biomass, on average, by 75% across all size classes compared to open-canopy reefs. Furthermore, on the highest-rugosity rocky reefs the biomass of small fishes (32–64g) is 800% higher than on the lowest rugosity reefs, while large fish (1-2kg) biomass is 60% lower than on the lowest rugosity reefs. Consequently, biomass is more evenly distributed across body-size classes on high rugosity reefs. By decomposing the biomass spectrum into total biomass and mean individual body-mass, we find that the most complex sites with both closed kelp canopies and high stipe densities have greater fish biomass. Higher kelp stipe densities also tend to be associated with larger fishes, but this effect is outweighed by the tendency for more small-bodied fishes with increasing rugosity. This study demonstrates how size-based analyses can shed new light on the ecology of kelp forest communities and will be useful for tracking important changes in kelp forest communities in coming decades – for example as fish communities change with the maturation of marine protected areas, and as habitats change with the expansion of sea otter populations throughout their former range.

[5]N.K. Dulvy and A.K. Salomon are coauthors on this chapter, which is currently in preparation for journal submission

4.2 Introduction

Habitat structural complexity is profoundly important to ecological communities, as a key influence on the abundance and richness of species. Species abundance and richness are magnified in complex habitats through the provision of niches and environmental resources (MacArthur and MacArthur, 1961; Tews et al., 2004), and increased habitat complexity can also lead to reduced predation and density-dependent competition (Willis and Anderson, 2003; Hixon and Beets, 1993; Shulman, 1984). For many ecosystems, the presence and characteristics of foundation species is a key determinant of habitat structure (Ellison et al., 2005). Many such foundation species, however, are in decline due to human exploitation and changing climate (Steneck et al., 2002; Ellison et al., 2005; Alvarez-Filip et al., 2009).

Kelps — large brown macroalgae of the order Laminariales — are the primary foundation species on temperate rocky reefs (Dayton, 1985). The ecological and economic importance of kelp forests is comparable to that of coral reefs in tropical waters (Steneck and Johnson, 2014; Smale et al., 2013; Beaumont et al., 2008). Broadly, kelp forests 'fuel' coastal foodwebs by capturing inorganic carbon and making it available it to higher trophic-levels, thereby increasing secondary production and consumer biomass both locally and across neighboring and distant habitats (Dayton, 1985; Krumhansl and Scheibling, 2012; Salomon et al., 2008; Duggins et al., 1989; Dunton and Schell, 1987). Thus, kelp cover can provide structural habitat (additional to the underlying substrate) and food (directly or indirectly), and typically gives rise to higher levels of biodiversity than are found in simple, unstructured habitats (Dayton, 1985; Steneck et al., 2002).

Associations with kelp habitat vary widely among fish species and life stages (Jones, 1988). Kelp facilitates the recruitment of larval fishes and provides key habitat for juveniles of many reef associated species (e.g. Connell and Jones, 1991; and reviewed by Carr and Syms, 2006). Hence, numerous observational and experimental studies have found that the abundance and biomass of early life stages (recruits and young-of-the-year) of a wide range of reef-associated fish species are increased by the presence and extent of kelp canopy (e.g. Levin and Hay, 1996; Choat and Ayling, 1987; Siddon et al., 2008; Anderson et al., 1989). Associations with kelp canopy for adult life stages are more variable among both species and locations. Studies focused on individual species or groups (defined based on trophic ecology, or position in the water column) have found that the abundance of some species and groups is much greater in kelp forests than in comparable areas without a kelp canopy, while other species and groups are more abundant

outside kelp forests. For example, Holbrook et al. (1990) found that planktivores and macro-invertivores were more abundant in kelp forests while other trophic groups were more abundant in areas without kelp cover in Southern California's *Macrocystis*-dominated kelp forests. Several studies document higher abundance and biomass of large-bodied benthic invertivores in areas without kelp canopy cover (Choat and Ayling, 1987; Jones, 1988; Holbrook et al., 1990; Siddon et al., 2008), while others report the opposite for other locations and species (Cowen, 1983). Fewer studies have examined patterns for total community abundance and biomass, but results have been similarly mixed among those that have. Some report that total fish abundance and biomass are higher in the presence of a kelp canopy, and increase with increasing canopy density (Leaman, 1980; DeMartini and Roberts, 1990) while others report the opposite (Siddon et al., 2008).

In addition to kelp canopy characteristics, the structural complexity or rugosity of the underlying rocky substrate is another key component of habitat structure on temperate reefs. The effects of substrate rugosity on reef fishes appear less variable than those that have been reported for kelp canopy, with more complex or higher-relief substrates supporting more fishes than less complex lower relief substrates in terms of both abundance (Ebeling et al., 1980; Jones, 1988; Cole et al., 2012) and biomass (Anderson et al., 1989). The inconsistent effects of kelp cover on fish community structure may be in part due to interdependence between the effects of kelp cover and substrate charateristics, with kelp becoming relatively less important with increasing substrate rugosity (or relief; Larson and DeMartini, 1984; Choat and Ayling, 1987; Anderson, 1994). However, it is not clear how consistent this interdependence between the effects of kelp and substrate rugosity is. This is especially true for high northern latitude, *Nereocystis lutkeana*-dominated kelp forests, which are much less well-studied than more southern *Macrocystis pyrifera* forests (Springer et al., 2006). Understanding this interaction is particularly important in the context of predicting the implications of future changes, as key drivers of change (herbivory and climate) will affect kelp cover more strongly than substrate rugosity.

The traditional approach for understanding the importance of habitat structure for temperate reef fish communities has been to study how the abundance of species (or groups of species) varies with habitat characteristics. This approach stems naturally from the concept of species niches, as the amount of niche space may be expected to depend on habitat structure. However, as responses to habitat characteristics vary widely between species (as described above), it is difficult to establish generalities and make predictions about how future changes in habitat are likely to affect community structure and dynamics (Jones, 1988).

Despite the contingencies of species-specific responses, fish community size-structure appears

to respond predictably to both habitat characteristics and overfishing, regardless of taxonomic composition (e.g. Chapter 5; Alvarez-Filip et al., 2011; Jennings and Dulvy, 2005). Total community biomass and mean individual body mass are two simple and informative summary metrics of size-structure (Shin et al., 2005; Dulvy et al., 2004). Size spectra — linear regressions of body mass class against either total abundance in each size class (abundance spectra) or total biomass in each size class (biomass spectra) of individuals, irrespective of species identity, typically on log axes — provide a more integrated picture of size-structure (Shin et al., 2005; Graham et al., 2005). The intercept of a biomass spectrum reflects the total amount of biomass in a community while the slope represents the relative dominance of small- vs. large-bodied community members (Kerr and Dickie, 2001; Borgmann, 1987). Processes that give rise to relatively more small-bodied fishes lead to more negative/less positive biomass spectra slopes, while processes that result in relatively more large-bodied fishes generate more positive/less negative slopes. To our knowledge, the effects of habitat structure on community size-structure on temperate reefs have not yet been quantified. Although community size-structure has received very little attention on temperate reefs, it represents a promising avenue for understanding the community-scale effects of habitat characteristics as well as fishing and other drivers of change.

Here, we take a size-based approach to examine the importance of both *Nereocystis* canopy characteristics and substrate rugosity for the structure of a temperate reef fish community. Specifically, we ask how mean body-size, total biomass and the slope and intercepts of community biomass spectra vary with *Nereocystis* canopy cover and stipe density, and substrate rugosity. We quantitatively test the community-scale effects of habitat structure by simultaneously considering the importance of substrate rugosity and kelp cover.

4.3 Methods

4.3.1 Study area

We conducted this study on temperate near-shore rocky reefs off the northwest coast of British Columbia (BC), Canada, within and around the Gwaii Haanas National Marine Conservation Area Area Reserve and Haida Heritage Site, Haida Gwaii (formerly the Queen Charlotte Islands; Figure 4.1). On this part of the Pacific Coast, kelp forests dominate rocky substrates in shallow waters on all but the most exposed shores (Springer et al., 2006; Steneck and Johnson, 2014), and we restricted our surveys to areas with hard substrates. *Nereocystis luetkeana* is the dominant canopy-forming species around Haida Gwaii, and the understory comprises a variety of other species from the order Laminariales.

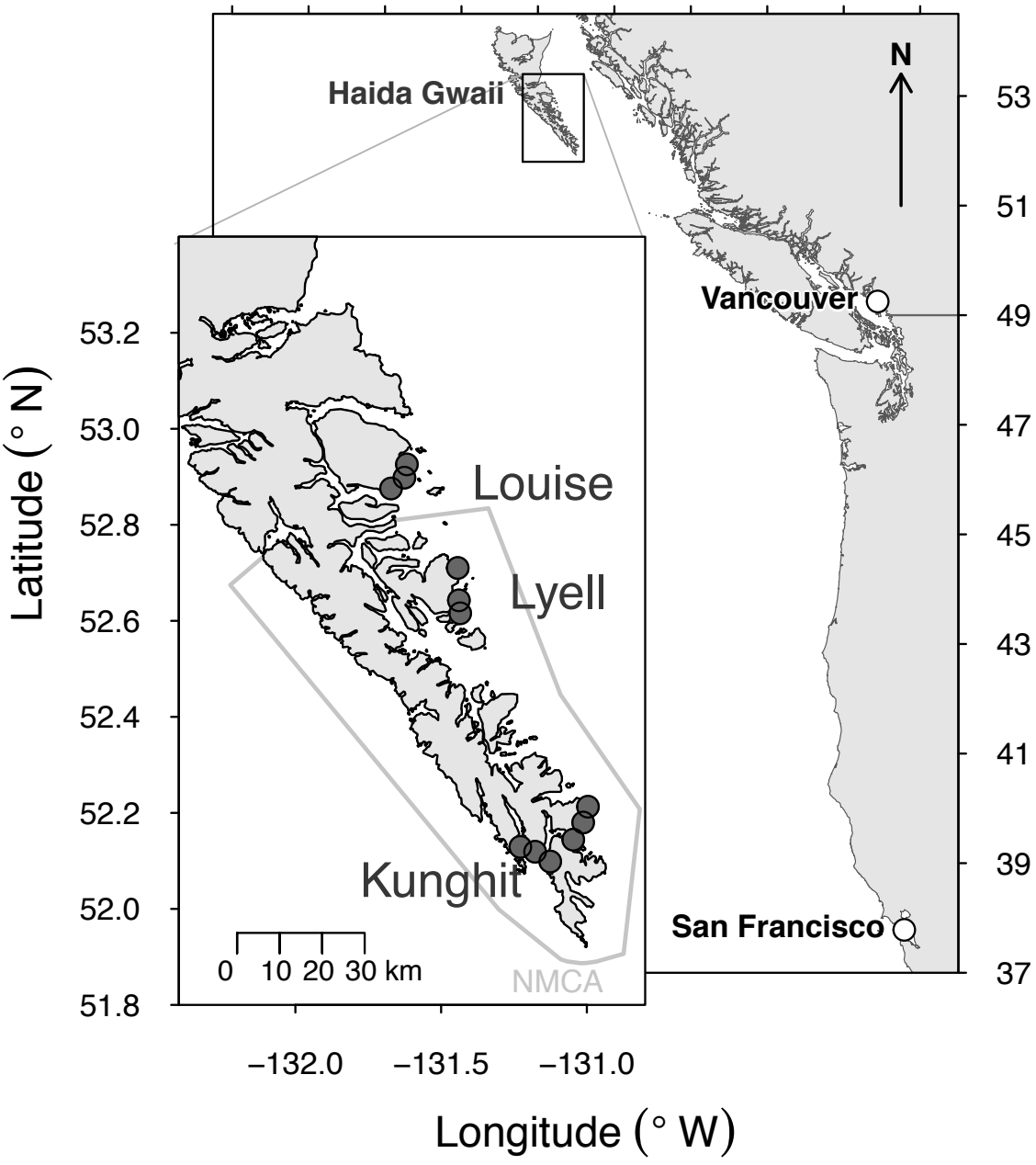

Figure 4.1: Research sites (gray points) on the northwest coast of British Columbia, Canada, within and around the Gwaii Haanas National Marine Conservation Area Reserve and Haida Heritage Site (NMCA) at the southern end of the island archipelago of Haida Gwaii. A total of 12 rocky reef sites were nested within 4 areas (n=3 sites per area).

Historically, sea otters (*Enhydra lutris*) were the dominant predator of invertebrate grazers on the BC coast, but they were extirpated from BC by the fur trade early in the 1900s (Gibson, 1988; Kenyon, 1969; Fedje and Mathewes, 2011). As for most areas on the Pacific Coast where urchin predators have been removed, in BC this led to the formation of extensive sea urchin barrens, and a kelp zone that is largely restricted to depths affected by wave turbulence (Watson and Estes, 2011). Sea otters have not yet returned to southern Haida Gwaii, hence this pattern typifies the sites we surveyed, with kelp being replaced by barrens below an average depth of 8.9 $\pm$ 0.46 m below chart datum.

4.3.2 Underwater visual census of kelp forest fish size and abundance

Fish communities were visually surveyed using belt-transects at 12 sites: 3 sites in each of 4 areas (Louise, Lyell,Kunghit East and Kunghit West) in southern Haida Gwaii (Figure 4.1). Surveys were undertaken in the summer (between late June and early August) each year from 2009 to 2012, with the majority of sites surveyed every year (a full summary of survey protocol is provided in Trebilco et al., 2014). Transects were 30 m long by 4 m wide and laid parallel to shore, with the end of each transect separated by a minimum of 5 m. Replicate transects were surveyed at each site in each year (n=4 in 2009, n=6 in 2010-2012), split evenly between 'deep' and 'shallow' strata (tide-corrected depth of 12.0 $\pm$ 1.3 m and 7.7 $\pm$ 1.1 m below chart datum, respectively).

For each transect, an individual SCUBA diver deployed a plastic transect meter tape while swimming forward at an approximately constant speed (Watson et al., 1995), recording conspicuous fishes (i.e. all fishes other than blennies, gobies, sculpins, gunnels and other small cryptic species – refer to Table B.1 for a species list) present in the sampling area. Count time was not standardized as it depended on fish abundance and habitat characteristics. The size (total length) of each individual fish counted on transects was visually estimated to the nearest cm. To ensure accuracy of length estimates, observers were trained by estimating the size of known-length objects underwater (following Bell et al., 1985; Polunin and Roberts, 1993). Additionally, observers carried a 'reference pole' (an 80 cm length of PVC, labeled with cm increments, and mounted at the end of a 1.5 m pole, as per Frid et al., 2013) which was used to both directly measure fish where possible, and to benchmark visual estimates. Individual weights were calculated from lengths using species-specific length-weight conversions from FishBase (`www.fishbase.org`).

4.3.3 Measurement of habitat covariates

We quantified key habitat characteristics including depth, substrate rugosity, and two measures of *Nereocystis* canopy cover. Depth was recorded at the start of each fish transect, and transects were deployed following a constant depth contour. Recorded depths were subsequently tide-corrected to chart datum, which in Canada is based on the lowest low water large tide (LLWLT).

We measured rugosity by contouring a 3 m length of fine-link chain (1 cm links) to the reef parallel to the transect tape, then calculating the ratio between the length of the chain (3 m) and the distance along the transect line between the start and end point (following Risk, 1972; Alvarez-Filip et al., 2011). We took three randomly stratified rugosity measurements per transect at each site in one year, and the means of these measurements were calculated for each site/depth stratum combination.

The two measures of *Nereocystis* canopy cover recorded were a visually assessed transect-scale score for canopy extent (1 = closed canopy, 0.5 = fragmented canopy, 0 = no canopy), and a site-scale measurement of *Nereocystis* stipe density. Transect-scale canopy scores were recorded during the visual surveys described above. Site-scale *Nereocystis* stipe density was estimated by counting all *Nereocystis* stipes $>$ 1 m length along a single 2 m wide transect, perpendicular to shore, running from the deepest extent of the kelp bed to the shore at a haphazardly chosen point approximately at the middle of the span of the fish transects (refer to Trebilco et al., 2014, for further detail). Stipe density was then calculated in stipes m^{-2}. These transects were completed for 25 of the 37 unique combinations of site and year in the dataset. The two measures of *Nereocystis* cover quantify different characteristics of the kelp canopy and are not strongly correlated (Figure B.2). Stipe density describes the overall density of the bed for each site, while canopy scores reflect the absolute cover on the transects surveyed within each site.

4.3.4 Data subsetting for modeling

Before model-fitting we narrowed the size fraction of reef fishes used for analysis because the sample population should be restricted to the range of body-sizes that can be surveyed effectively when estimating size spectrum slopes (Graham et al., 2005; Ackerman, 2000). Because small fishes ($< \sim$ 15 cm) are subject to poor detectability in visual surveys (Ackerman, 2000), the corresponding mass of 32 g was used as the lower size cutoff for inclusion in analyses. This size class represented the median for the dataset, supporting our assumption that it was the minimum size that was surveyed effectively (Ackerman et al., 2004). Only 3 fish larger than 2048 g were observed across all surveys; hence, we dropped them and set this mass as our upper

cutoff. We kept the range of body-sizes considered consistent for all models to maximize the comparability of results.

Only the subset of 25 site/year combinations for which *Nereocystis* density data were obtained were included in models including *Nereocystis* density as a predictor. All other models used data from all sites and years. For all models, we aggregated data across transects within depth strata. Depth and kelp canopy score were recorded for individual transects, so we took the averages across transects within each combination of site, depth stratum and year. As described above, *Nereocystis* stipe density was a site-level average, while rugosity was averaged across transects within depth strata at each site.

4.3.5 Statistical analysis

We fit three sets of linear mixed-effects models to examine how substrate rugosity, kelp canopy cover and stipe density, and depth stratum explain each of three key aspects of community size-structure – average individual body mass, total biomass, and community biomass spectra (Table B.1). All models were fit using the R package `lme4` (Bates et al., 2013), and all analyses were conducted using R version 3.0.2 (R Core Team, 2013) For each set of models, we evaluated two subsets: one using transect-level canopy score as the predictor for *Nereocystis*; and the other using site-level *Nereocystis* stipe density.

Model structure

For community biomass spectra, we assigned individual fish to six $\log_2$ mass classes (i.e. 32 — 64 g, 64 — 128 g, 128 — 256 g, 256 — 512 g, 512 — 1024 g, 1024 — 2048 g). We then summed all biomass in each bin to the bin mid-point (M) for each depth stratum within each site, and divided by total area surveyed to give biomass (B) per-unit-area (g m^{-2}) within each size class. We centred body mass class (M) about zero by subtracting the mean of the log bin midpoints prior to model fitting in order to remove correlations between the slope and intercept (Daan et al., 2005). We then modeled biomass spectra with $\log_2(\mathrm{M})$ as the predictor and $\log_2(\mathrm{B})$ as the response.

To evaluate the effects of kelp canopy and substrate rugosity on the slopes of biomass spectra we included interaction terms between each covariate and the bin mid-point M. A three way interaction term between rugosity, the kelp covariate, and M was also included in each model to assess whether the effects of rugosity and kelp on biomass spectra slopes were inter-dependent. The non-interactive effect of each covariate gives its effect on biomass spectra intercepts (or 'height', as M was centered around 0).

Total biomass and mean body-size models had total biomass ($\sum(B)$) and mean body-size ($\overline{M}$) respectively as the response variables. To assess whether the effects of kelp canopy and substrate rugosity on these aspects of size-structure are interdependent, we included interaction terms between rugosity and the kelp covariate (Table B.1).

In all models, we accounted for the spatially- and temporally-nested structure of the data by including both year, and site nested within area (Louise, Lyell, East Kunghit, West Kunghit) as crossed random effects. The random structure allowed intercept to vary randomly with year in all models. The intercept also varied randomly with site nested within area for total biomass and mean body-size models, while both slope and intercept were allowed vary randomly with site nested within area for biomass spectrum models.

While it is not of specific interest in this study, we expected that the depth stratum of transects may be important as shallow transects were generally inside or on the edge of the kelp canopy, while deep transects were generally outside the canopy. To account for this effect we included depth stratum as a fixed effect in all models.

Model and covariate comparisons

For each subset of models, we fit a saturated model with all covariates using maximum likelihood (ML; see Table B.1 for a list of saturated models). After fitting saturated models, we conducted all-combinations model selection based on Akaike's Information Criterion for small sample sizes (AICc) using the function `dredge` in the R package `MuMIn` (Bartoń, 2013; Burnham and Anderson, 2002). We retained models with delta AICc < 2, and generated model-averaged coefficient estimates and their associated confidence intervals using the natural average method (Burnham and Anderson, 2002; Grueber et al., 2011). We chose the natural average method as it is not yet well-established how best to calculate uncertainty around estimates using the alternative zero method (Grueber et al., 2011). In doing so, we recognise that parameter estimates for poorly supported parameters are biased slightly away from zero (Grueber et al., 2011). For ease of interpretation, effect sizes are presented in standardized units, where a 1 unit change in a predictor implies that a change of 1 standard deviation (SD) of that predictor would result in a change of 2SD in the response (Schielzeth, 2010; Gelman, 2008).

This approach yields three lines of evidence that we use to evaluate the effect habitat covariates on each measure of community size-structure: (i) the magnitude and direction of averaged coefficients; (ii) the 95% confidence intervals around coefficient estimates, a measure of coefficient precision; and (iii) the relative variable importance (RVI) of each predictor, which is the sum of the model weights of all the models in the model-averaged set that included the predictor.

To visualise the effects of substrate rugosity and canopy cover on community size-structure, we used averaged models to calculate biomass spectra for different combinations of substrate rugosity and canopy cover, accounting for the other covariates and random effects.

4.4 Results

We surveyed a total of 203 transects, encompassing 4537 reef fishes between 32 and 2048 g. This included 19 reef-associated species, predominantly from the families Sebastidae (rockfishes) and Hexagrammidae (greenlings; Table B.2).

4.4.1 Total biomass and mean individual fish body mass

Bivariate relationships suggest a trend for greater total fish biomass and larger mean individual body mass with higher *Nereocystis* stipe density (Figure 4.2 a and b respectively). Associations of total fish biomass and mean individual body mass with kelp canopy score are not as visually obvious as those with stipe density, though patterns are suggestive of slightly greater total fish biomass and smaller mean individual mass with higher canopy score (Figure 4.2 c and d respectively). Higher substrate rugosity tends to be associated with greater total biomass (Figure 4.2 e), but smaller mean individual body mass (Figure 4.2 f).

Model results reveal strong support for an association between higher *Nereocystis* stipe density and greater total biomass and mean body mass, (Figure 4.3 and Table B.3), but did not show support for an effect of canopy score (Figure 4.3 and Table B.3). The trends for greater total biomass and lower mean individual body mass with increasing substrate rugosity evident in bivariate plots are also supported by model selection results regardless of which *Nereocystis* covariate is used (Figure 4.3 and Table B.3).

We found evidence that the effects of stipe density and rugosity on mean fish size are compensatory, as indicated by model support for a negative interaction between these predictors (Figure 4.3 and Table B.3). This implies that the trend for larger mean body-size with increasing *Nereocystis* stipe density becomes weaker as substrate rugosity increases. We did not find evidence of compensatory relationships between *Nereocystis* density and rugosity on total fish biomass, or between between canopy score and rugosity for either total biomass or mean individual body mass (as indicated by a lack of support for these interaction terms; Figure 4.3, B.3).

We included depth stratum in models to avoid confounding with rugosity and *Nereocystis* canopy characteristics, and there was support for lower total fish biomass in the shallow depth

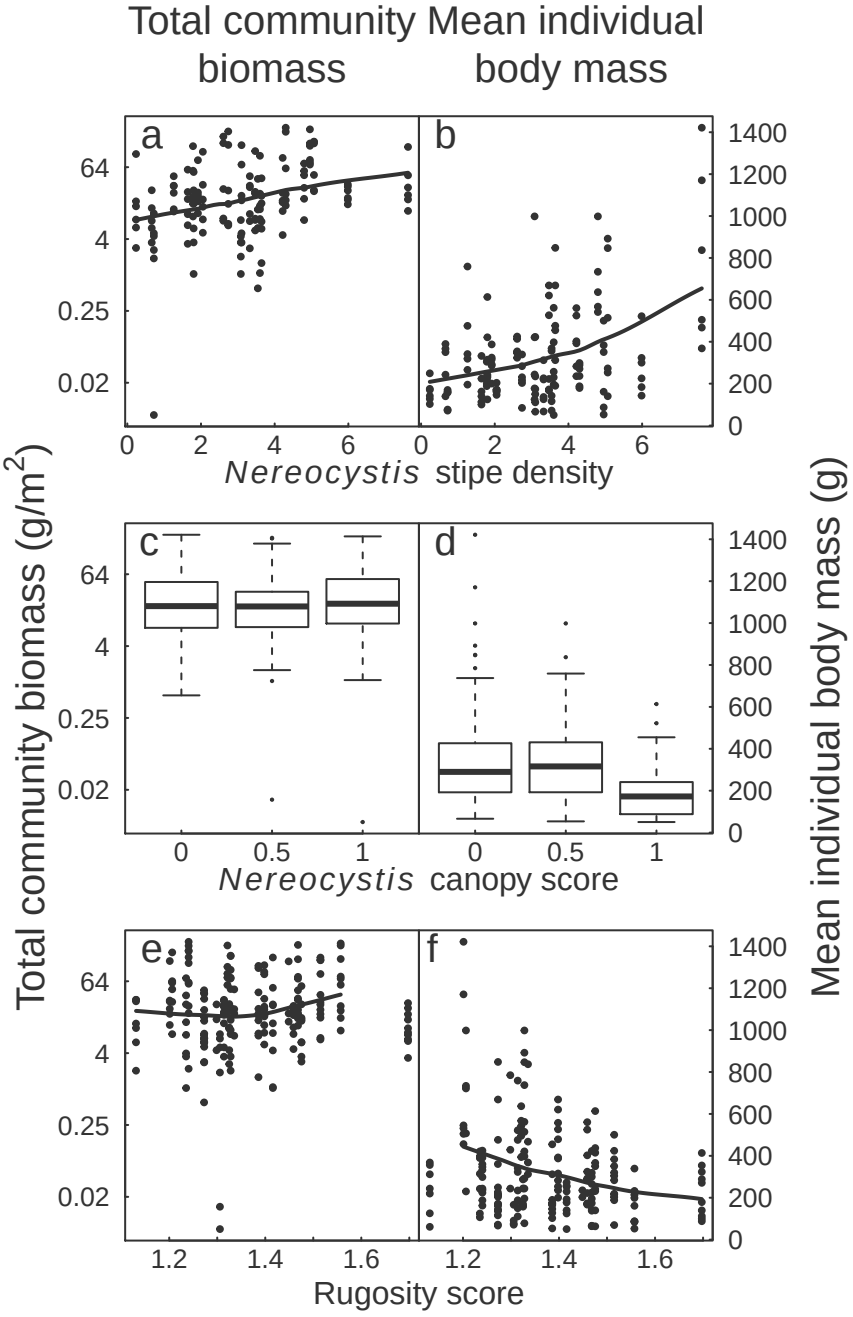

Figure 4.2: Bivariate relationships between aspects of kelp forest reef fish community size-structure (total reef fish biomass and mean individual reef fish body mass) and habitat complexity covariates. Lines are LOWESS smoothers.

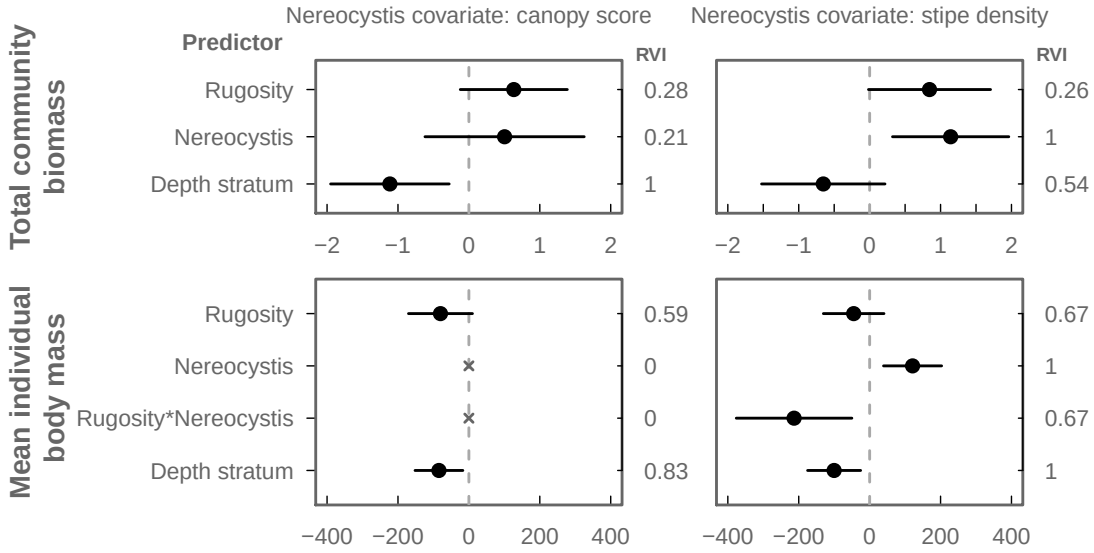

Figure 4.3: Standardised coefficients and 95% confidence intervals for therelationships of habitat covariates with total fish biomass (top) and mean individual body mass (bottom) from averaged models with a ΔAICc $<$2. Left-hand panels are for models including canopy score as the covariate for *Nereocystis*; right-hand panels are for models with stipe density as the *Nereocystis* covariate. A RVI of zero indicates variable was not in any of the best-supported models.

stratum in both model sets (the deep stratum was the reference level, hence the negative effect implies lower biomass in the shallow stratum).

4.4.2 Community biomass spectra

Across the reef fish community, total biomass tends to increase with increasing body mass class. Consequently the community biomass spectrum has a positive slope of 0.78 $\pm$ 0.08 (Figure 4.4).

Model selection results for the effects of covariates on the slope and intercept of biomass spectra (Figure 4.5, Table B.4) are largely in agreement with results from models for total biomass and mean individual body mass (Figure 4.3, Table B.3). Higher rugosity tends to be associated with relatively more small-bodied fishes and more biomass overall, as indicated by support for a negative effect on biomass spectra slopes and a positive effect on intercept, respectively (Figure 4.5, B.4). Higher kelp canopy cover and stipe density both tend to be associated with higher total biomass overall, as indicated by support for positive effects of both predictors on the biomass spectrum intercept (Figure 4.5, B.4). A notable differences between the results of the size spectrum vs. mean individual mass models is that there is not support for an effect of stipe density on body size distribution (slope) in the size spectrum models (whereas

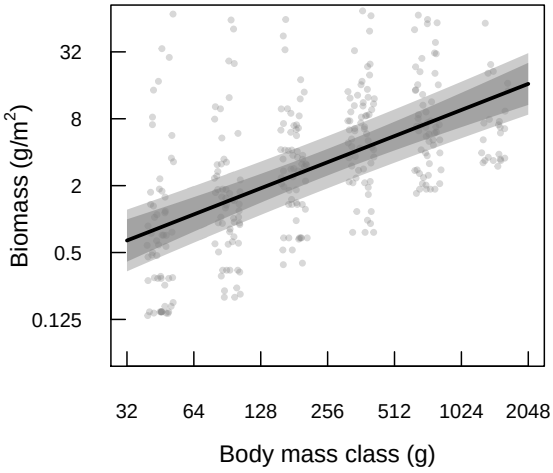

Figure 4.4: The site-scale community biomass spectrum for kelp forest fishes. Points are jittered (randomly offset) on the x axis so that individual points can be seen. Shaded bands indicate 95% confidence intervals incorporating uncertainty in the fixed (dark band) and random (light band) effects.

there is support for a trend for larger mean body-size with increasing *Nereocystis* stipe density in the mean body size models). There is some support for a negative effect of depth on biomass spectra intercepts, which is congruent with evidence from total biomass models for lower biomass at shallower depths. An effect of depth on biomass spectra slopes was also included in the best supported models (Figure 4.5; Table B.4); however, this was the most weakly supported of the covariates in both model sets, and the effect did not have a clear direction as reflected by the confidence intervals extensively overlapping zero (Figure 4.5).

The combined effects of *Nereocystis* canopy cover and substrate rugosity on fish community size-structure can be summarised in predicted biomass spectra (Figure 4.6). This shows how higher kelp canopy cover is associated with more biomass overall, but no clear difference in size-structure, while higher rugosity leads to relatively more small-bodied fishes and more biomass overall. In terms of total biomass, the effect of kelp canopy translates to 75% more biomass overall for a closed vs. open kelp canopy (at constant rugosity). For rugosity, this translates to 60% less biomass of the largest fishes (1–2 kg) and 800% more biomass of the smallest fishes (32–64 g) at high- vs. low-rugosity (at constant canopy cover).

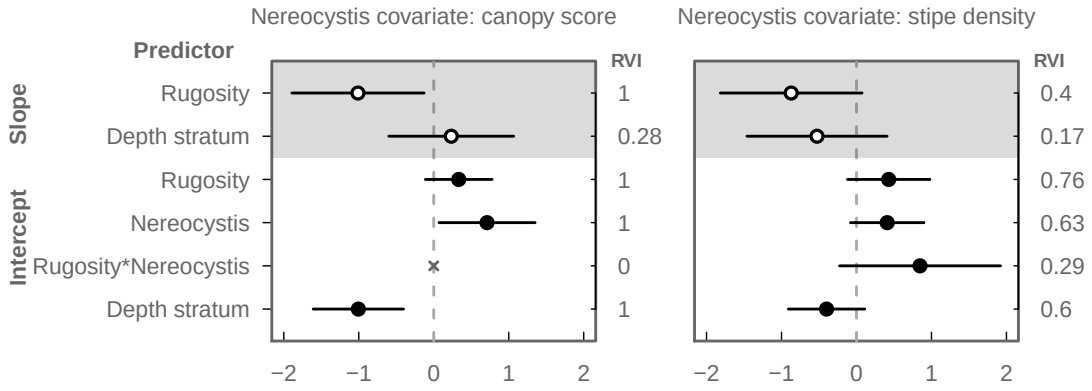

Figure 4.5: Standardised coefficients and 95% confidence intervals for the relationships of habitat covariates with the slopes (open points, gray background) and intercepts (closed points, white background) of community biomass spectra from averaged models with a ΔAICc $<$2. Left panel is for models including canopy score as the covariate for *Nereocystis*; right panel is for models with stipe density as the *Nereocystis* covariate. A RVI of zero indicates variable was not in any of the best-supported models.

4.5 Discussion

By examining how habitat complexity shapes the size-structure of a temperate reef fish community, we show that kelp canopy cover, stipe density, and substrate rugosity have important and interdependent effects on the total biomass of fishes present, and on how fish biomass is distributed across body-sizes. Higher kelp canopy cover and higher stipe density are both associated with greater fish biomass. Higher substrate rugosity is associated with both higher overall fish biomass, and relatively more small-bodied fishes. Both kelp canopy characteristics and substrate rugosity have previously been recognised as important determinants of fish abundance (Larson and DeMartini, 1984; Ebeling et al., 1980; Willis and Anderson, 2003), but our findings are novel in several important respects. By examining the effects of canopy and substrate characteristics simultaneously, we demonstrate that that the main effect of kelp is to increase total biomass, while the main effect of rugosity is to boost the biomass of small fish, resulting in a more even distribution of biomass across body-sizes and more biomass overall. This approach also shows that the effects of rugosity and kelp are interdependent; although higher kelp stipe densities tend to be associated with larger fishes, this effect is outweighed by the trend for more small-bodied fishes at high rugosity. In taking a size-based approach we also demonstrate how size-based analyses can shed new light on the ecology of kelp forest communities. This presents the opportunity for informative comparisons with studies that have used a similar approach on

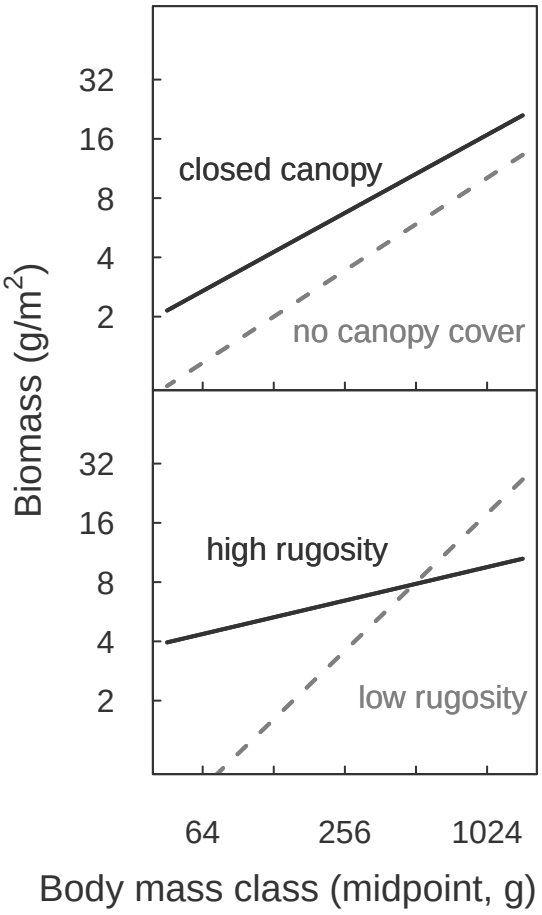

Figure 4.6: Predicted kelp forest reef fish biomass spectra for high and low kelp canopy cover at intermediate rugosity (1.35, top), and for high (1.7) and low (1.0) rugosity while holding kelp canopy cover constant (bottom).

coral reefs, and generates several exciting avenues for future research.

Previously, kelp canopy cover has mainly been observed to benefit small fishes (recruits and young of the year, Siddon et al., 2008; Springer et al., 2006; Carr and Syms, 2006), while higher substrate rugosity (or relief) has been observed to be associated with increased total abundance and biomass (Ebeling et al., 1980; Anderson et al., 1989; Cloutier, 2011). Contrastingly, we observed a positive effect of substrate rugosity on smaller fish, while higher kelp canopy cover and density tended to be associated with increased biomass across body-sizes. These differences may be partly due to the fact that the range of body-sizes we considered did not include young of the year and recruits, which are well recognized to depend strongly on kelp habitat (Siddon et al., 2008; Springer et al., 2006; Carr and Syms, 2006), but which contribute little to total biomass. While our findings for rugosity contrast with previous work in kelp forests, they are congruent with observations on coral reefs, where less complex substrates have been shown to lead to relatively fewer small-bodied fishes and more positive/less negative size spectrum slopes (Graham et al., 2005; Alvarez-Filip et al., 2011; Wilson et al., 2010; Rogers et al., 2014).

An important way in which kelp forests differ from coral reefs is that kelp contributes a vertical dimension to habitat complexity, above the benthos, which is less extensive or absent on coral reefs (Choat and Ayling, 1987; Ebeling and Hixon, 1993). An underlying mechanism by which increased substrate rugosity leads to increased biomass at small sizes is thought to be the provision of refuges from predation (Friedlander and Parrish, 1998; Rogers et al., 2014). Our findings suggest that the mechanism by which canopy-forming kelps affect community structure may be quite different. Increases in total biomass and size spectrum intercepts are generally accepted to reflect increased total production (Kerr and Dickie, 2001; Jennings, 2005). Hence, our results suggest that canopy-forming kelps affect fish community structure by directly or indirectly enhancing the resource base, rather than by providing refuge from predation for small fishes. However, it remains to be seen whether these responses are consistent for kelp forest communities with different species compositions.

Four issues that we were not able to address in this study represent key avenues for future research. First, the substrate structural complexity measurement we used (rugosity) is representative of one scale of habitat complexity, but several different scales of complexity are likely to be important in shaping fish communities (Nash et al., 2012). Examining how different scales of substrate complexity affect community structure on temperate reefs deserves further attention. Second, previous work has demonstrated that the amount of kelp edge may be more important to fishes than the absolute amount of kelp habitat (Anderson et al., 1989). The fact that the kelp effects we observed were consistent for both canopy cover and stipe density supports total

habitat being more important than edge size in this system, but this could be directly addressed in future studies via kelp removal experiments. Third, it is interesting to note that previous studies have documented higher fish abundance and biomass in *Macrocystis* forests than in *Nereocystis* forests where they co-occur elsewhere in the NE Pacific (Bodkin, 1986; Leaman, 1980). While the data we have presented here are limited to *Nereocystis* forests, there are also *Macrocystis* patches in the area we surveyed and these patches have relatively few fishes (personal observation). It would be interesting to ascertain whether this difference is driven by substrate characteristics. Finally, while linear approximations of community size spectra have proven extremely useful for understanding overall patterns of community structure, and for quantifying changes, there is emerging evidence that explicitly exploring departures from linearity can be highly informative (Rogers et al., 2014). Exploring whether and how habitat complexity is associated with non-linearities in size spectra for temperate reef fishes is an important direction for future study.

Our findings have conservation and management implications for temperate rocky reefs, particularly those at high latitudes dominated by *Nereocystis*. Along the northwest coast of North America, marine protected areas have been established with the specific goal of protecting and restoring depleted rockfish populations (Parker et al., 2000; Yamanaka and Logan, 2010; Haggarty, 2014). Our finding that increased kelp cover is associated with more fish biomass adds to the body of evidence that suggests protection and/or enhancement kelp habitat will be important to ensuring the success of existing protected areas (Airoldi et al., 2008; Graham, 2004; Dayton et al., 1998). Kelp cover should also factor into decisions on where to site new protected areas if their stated objective is to protect and sustain reef-associated fishes. Importantly, in this context of site selection for new protected areas, our findings show that substrate characteristics should also be considered. Several studies have reported that higher substrate rugosity is associated with higher abundance of rockfish and other bottom-associated fishes (Richards, 1987; Love et al., 2002; Cloutier, 2011), but the size-based nature of this association has not, to our knowledge, been previously recognised. Our results suggest that observed trends of increased fish abundance with increased substrate rugosity may be largely driven by small-bodied fishes. Hence, if the goal of management is to protect a diverse size-structure (i.e. including large fishes), then it will likely be beneficial if reserves encompass not only high-rugosity areas, but a diverse range of rugosities.

Size spectra and other forms of body-size distributions are increasingly well recognised as key indicators of community state and structure. Several recent studies on coral reefs have demonstrated their utility for quantifying the effects of both habitat characteristics and fishing

on fish communities (see Chapter 5 and Alvarez-Filip et al., 2011; Dulvy et al., 2004; Wilson et al., 2010). Our study demonstrates that size spectra can also provide new insights into the factors that shape fish communities in temperate kelp forests. Size-based analyses have been particularly useful for quantifying and tracking community-scale changes in other marine ecosystems; similarly, we expect that forecasting and tracking important changes in kelp forest communities in coming decades will be an application for which size-based analyses, like those we have presented here, will be particularly useful. Another will be quantifying the effects of habitat changes that are likely to occur as sea otter populations expand throughout their former range (Reisewitz et al., 2006; Watson and Estes, 2011). In both cases, collection of baseline and monitoring data will be critical. Lastly, quantifying the community-scale effects of fishing is an increasingly common application of these approaches (an application that is closely inter-related with assessing MPA effects). Given that fishing appears to be the greatest manageable threat to kelp forest ecosystems over the 2025 time horizon (Steneck et al., 2002) we suggest that the field of kelp forest ecology and fisheries management may benefit from more widespread applications of these approaches.

4.6 Chapter-specific acknowledgments

Dr. Hannah Stuart (Fisheries and Oceans Canada) initiated and led the kelp transects and clearings described in this chapter, and she will be offered co-authorship prior to the submission of this work to a peer-reviewed journal.

Chapter 5

Reef fish biomass without humans[6]

Abstract

The worlds reefs have undergone centuries of human-driven transformation. However, the full nature and magnitude of change remains unclear because it began long before the advent of scientific monitoring. Here we use biomass spectra to derive baselines for reef fishes in the absence of humans. The underlying size-based processes structuring fish biomass appear largely consistent across the world's reefs. Accounting for local abiotic and ecological variation, we estimate that reef fish biomass is currently less than half of the baseline expectation and 90 % of the largest, most functionally important individuals ($>$1 kg), are absent. Depletion has been greatest on reefs around the Mediterranean Sea, East Africa and Japan. Restoring and preserving the full size-structure of reef fish communities is an important goal in order to safeguard the long-term resilience of reef ecosystems. Fortunately, effective marine protected areas can be a powerful tool for achieving this goal.

[6]N.K. Dulvy and A.K. Salomon are coauthors on this chapter, which is currently in preparation for journal submission. Please refer to acknowledgments for a full list of contributers who will be included as coauthors upon submission.

Please note that the structure of this chapter reflects the fact that it has been prepared for submission to *Science*, and it has been formatted accordingly.

Reef fish biomass without humans

Reef ecosystems harbor a large fraction of global marine biodiversity (Roberts et al., 2002; Stuart-Smith et al., 2013; Reaka-Kulda, 1997) as well as supporting fisheries and other ecosystem services crucial to the well-being of the worlds fastest-growing and poorest human populations (Newton et al., 2007). While the effects of contemporary impacts such recent overfishing, habitat degradation, and pollution are readily apparent, the impacts of long-term overfishing of reef fish biomass are less clear (Cramer et al., 2012; Roff et al., 2012; Jackson, 1997). The ecological footprint of fisheries catches suggests that half of the worlds reefs may be overfished (Newton et al., 2007), but without historic baselines the magnitude of reef fish depletion has proven difficult to ascertain (Jackson, 1997; Pandolfi et al., 2003). Recent surveys of the few remaining remote, and presumably near-pristine, atolls suggest the impact of overfishing on reef function may be considerable (Sandin et al., 2008; DeMartini et al., 2008). These surveys suggest the baseline configuration of fish community structure may an inverted biomass pyramid consisting of a high standing biomass of large reef fishes and sharks (Sandin et al., 2008). Large-bodied community members often have disproportionate functional importance, and play key roles in maintaining ecosystem connectivity and resilience (Ling and Johnson, 2012; McCauley et al., 2012; Bascompte et al., 2005; Rooney et al., 2006). The key question, therefore, is whether the inverted pyramids at these few atoll ecosystems are truly globally representative of baselines for reefs without humans.

Here, we draw upon the macroecological approach of biomass spectra models to derive ecosystem baselines in the absence of humans. The ubiquity of indeterminate growth and gape-limited-size-selective predation leads to very strong size-structuring in marine ecosystems (Jennings, 2005; Barnes et al., 2010). This, combined with disproportionate effects of exploitation on large-bodied individuals and species (Reynolds et al., 2001; Jennings et al., 1999), makes size spectra a uniquely powerful method for quantifying community and ecosystem-scale anthropogenic change (Dulvy et al., 2004; Jennings and Blanchard, 2004; Shin et al., 2005). The size spectrum can be described by the slope and intercept of a log-linear model and, in the absence of external influences, the intercept reflects the form and magnitude of primary production entering a community, while the slope arises from the loss of energy at increasingly larger size classes (Borgmann, 1987; Kerr and Dickie, 2001). Size spectra are steepened by overexploitation of the largest individuals and species, and subsequent release from predation of mesopredatory size classes (Dulvy et al., 2004; Jennings and Blanchard, 2004). Size spectra are commonly described in terms of either abundance (abundance spectra) or biomass (biomass spectra). It is simple to

convert from abundance to biomass spectra (the slope of a biomass spectrum is equal to the slope of the abundance spectrum + 1; Brown and Gillooly 2003; Trebilco et al. 2013), but we focus on biomass spectra here because they are graphically interchangeable with biomass pyramids which provide easily interpreted and widely understood depictions of community structure (Figure 5.1, Trebilco et al. 2013).

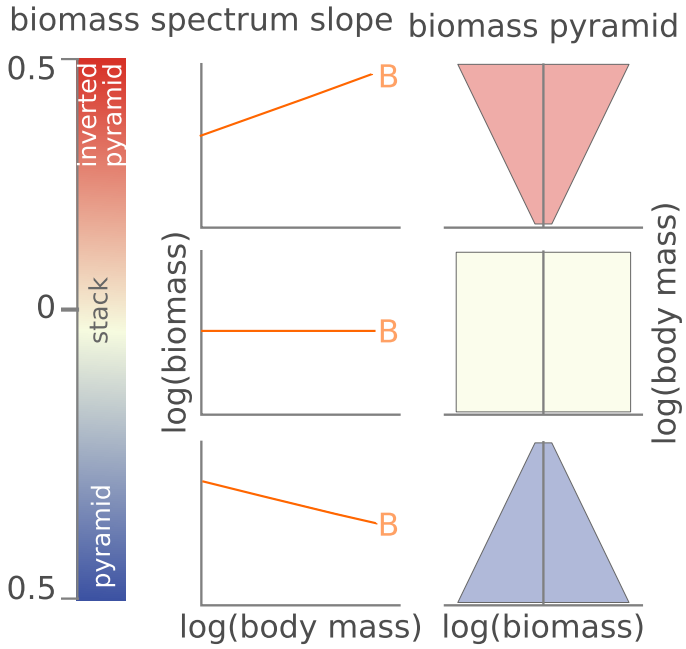

Figure 5.1: Slopes of biomass spectra (orange lines, B) indicate the shapes of biomass pyramids. Positive biomass spectra slopes correspond to inverted biomass pyramids, while negative slopes represent bottom-heavy pyramids and zero slopes represent intermediate 'biomass columns'

We measure biomass spectra of the worlds reef fish communities using a global dataset of visual surveys of unprecedented size and geographic representation. The Reef Life Survey (RLS) dataset consists of standardized visual censuses of fishes along 50 m belt transects from 1,982 sites in 74 of the worlds marine ecoregions (Figure 5.2, see Appendix C for further details). Our analysis includes 1,625,177 individual fishes between the estimated weights of 32 g and 65.5 kg. We modeled biomass spectra as a function of human coastal population density – a proxy for fishing pressure (Stewart et al., 2010) – and the presence and strength of local spatial protections, while accounting for local abiotic and ecological covariates. We used a linear mixed-effects model to account for the spatial structure of the data (see Appendix C for model specification). Following Edgar et al. (2014), spatial protection was quantified as the number of key conservation 'NEOLI' features for each site (**n**o take; well **e**nforced, **o**ld, >10 years; **l**arge,

>100km2; and **i**solated by deep water or sand) ranging from zero at sites possessing no NEOLI features to five at sites that had all five (see supplementary material and Edgar et al. 2014). By setting human coastal population to zero and maximising protection (NEOLI score of 5) while keeping other parameters at their observed values, we then use this linear model to predict reef ecosystem baselines of fish biomass, while accounting for local abiotic and ecological conditions.

At the local site scale of our analysis, the slopes of fish biomass spectra span a continuum across temperate rocky reefs and tropical coral reefs (Figure 5.2). While there is considerable overlap in the range of slopes, tropical coral reefs tend to have flatter spectra (mean slope: -0.03, 95% confidence intervals of mean: -0.16 — 0.10, range: -0.21 — 0.27) consistent with ecological stacks (Figure 5.1, Figure 5.2). By comparison temperate rocky reefs tend to have more positive slopes (mean slope: 0.24, 95% confidence intervals of mean: 0.10 – 0.37, range: -0.53 — 0.92) consistent with inverted biomass pyramids where larger-bodied fishes outweigh smaller community members. The overlap in the range of slopes across latitudes suggests the underlying ecological processes shaping the slope and intercept of size spectra on reef fish communities are remarkably similar, and that differences are due in large part to local abiotic conditions, and anthropogenic pressures.

This was supported by our models, which revealed that the effects of abiotic and ecological conditions on the slopes and intercepts size spectra are largely consistent across temperate and tropical reefs (Figure C.1). Deeper reefs tend to have more biomass and more positive spectra (less bottom heavy or more inverted pyramids), while reefs that experience more seasonal variability in temperature have more positive spectra. The remarkable continuum of size spectra slopes reflects the common importance of local abiotic factors, irrespective of species richness. Furthermore, reef spectra are consistently influenced by local human population densities and the strength of spatial protection.

By comparing observed biomass spectra to baseline predictions, we estimate that more than half (median 59%) of fish biomass has been lost from the worlds reefs, with the greatest depletions (median 92%) in the largest, most functionally important size fractions (>1 kg, Figure 5.4). Depletion of total biomass has generally been greater on temperate rocky reefs (median 70%) than on tropical coral reefs (median 44%), with the greatest depletions on temperate rocky reefs in Northeast Europe and Mediterranean Seas, Japan, Atlantic and Pacific U.S.A., and the Falkland Islands. On tropical coral reefs, the depletion of total fish biomass is greatest in East Africa, with considerable depletion also evident in many parts of the Pacific Ocean (e.g. Sunda, Vanuatu, Solomon Islands, and Hawaii) and the Caribbean Sea (Figure 5.3, Table C.2). The largest, most functionally important body-sizes ($>$ 1 kg) have been almost entirely eliminated

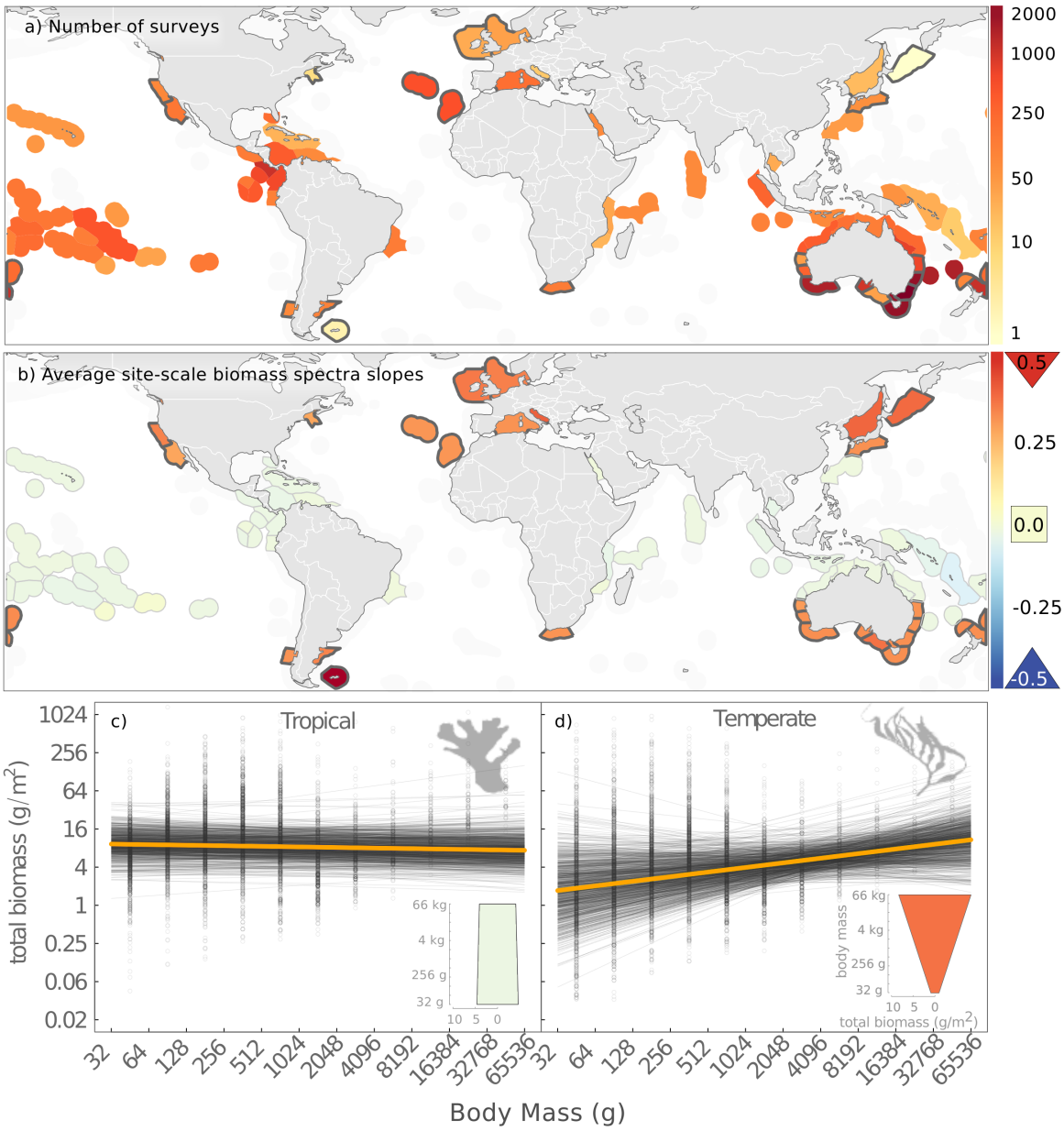

Figure 5.2: Distribution of reef fish survey effort (a) and size-structure of reef fish communities (b,c-d). Dark gray outlines in (a) and (b) indicate investigated ecoregions classified as temperate; ecoregions without dark gray outlines were classified as tropical. The colour ramp for (a) indicates the number of fish surveys per ecoregion. The colour ramp for (b) indicates average site-level biomass spectra slopes from (c and d) over ecoregions. Site-scale slopes are generally flat or slightly negative for tropical reefs, indicating biomass columns, whereas slopes are generally positive for temperate reefs - indicating inverted biomass pyramids. Axes for (c and d) are logarithmic

across temperate rocky reefs and tropical coral reefs: less than a tenth of the estimated baseline biomass remains (median losses of 93% for temperate rocky reefs and 89% for tropical coral reefs).

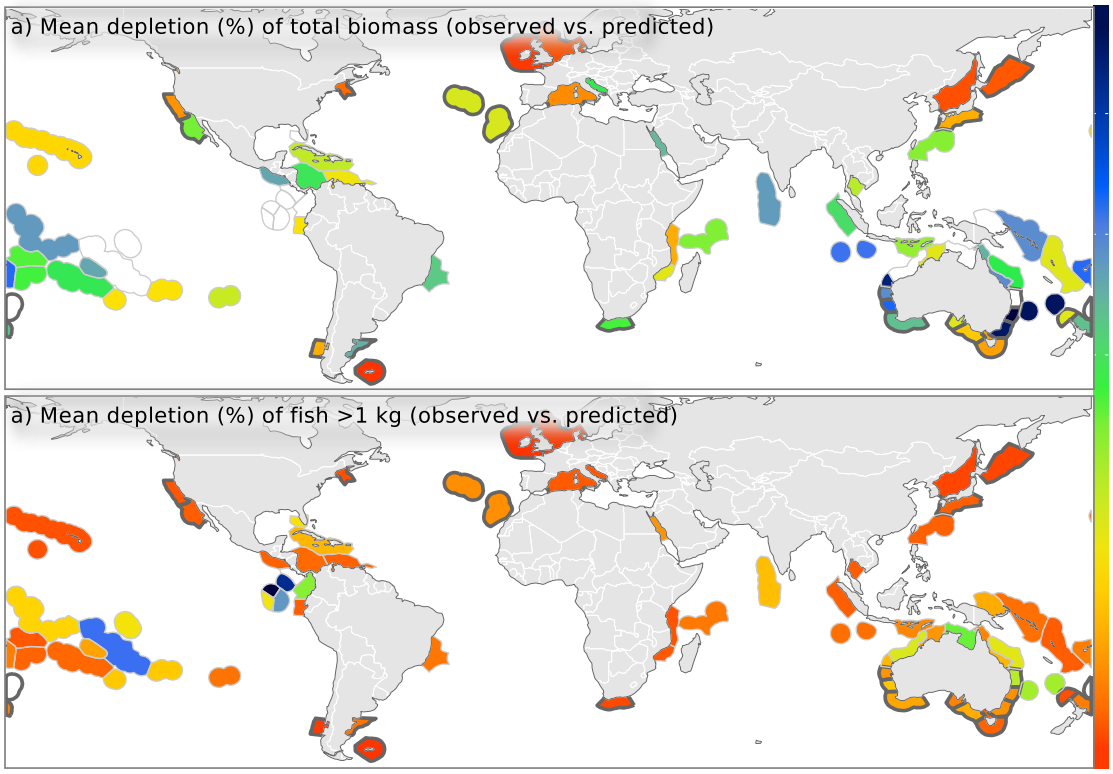

Figure 5.3: Average percent depletion of (a) total biomass and (b) biomass of large fishes (>1 kg). Depletion is calculated by comparing observed biomass with model-predicted biomass for a well-protected site with no human coastal population. Temperate ecoregions are shown with dark outline, and ecoregions with positive values are shown in white (see Figure C.4)

While depletion of total biomass dominates, there remain reefs that have as much or more biomass than the baseline expectation. The observed total biomass was greater than the modeled baseline estimate at 23% of sites. Such outliers were especially prominent in the remotest and best-protected locations, including: Galapagos, Cocos, and Kermadec Islands, as well as in the Panama Bight, the Florida Keys, and around the Nicoya Peninsula of Costa Rica (Table C.2; Figure C.4). Observed biomass of large fishes exceeded the baseline estimate at only 4% of sites, with estimated losses of more than 75% across 82% of the sites sampled (88% of temperate rocky reefs, and 74% of tropical coral reefs). Only in the Galapagos, Cocos and Kermadec Islands and Nicoya Peninsula was the biomass of large fishes consistently greater than the baseline estimate

(Table C.2; Figure C.4).

Our results indicate that, in absence of humans and under contemporary climate, the ecosystem baseline of reef fish biomass is an inverted biomass pyramid dominated by a greater standing biomass of the largest size classes of fishes (Figure 5.4). The slope of the size spectrum and corresponding pyramid shape is strongly influenced by local human population densities and the strength of spatial protections. While there is considerable uncertainty in the relationship between human coastal population and community size structure when temperate and tropical latitudes are considered separately (Figures C.2 and C.3). However, globally there is a trend for the largest size classes to be proportionally reduced at higher human coastal population densities, shifting fish community structure from an inverted pyramid (Figure 5.4, top LHS) to a more uniform ecological stack (Figure 5.4, top RHS) with approximately similar biomass in each size class or a traditional (bottom heavy) pyramid.

Even at high human coastal population densities, those marine protected areas with the greatest number of key features are effective in preserving the baseline inverted pyramid ecosystem structure. The recovery of baseline biomass pyramid shape is most likely if Marine Protected Areas have at least 4 of the 5 NEOLI features (no-take, well-enforced, old, large, and isolated; Figure 5.4). This general pattern of steepening slopes with increasing overfishing from highest human population densities, and the ameliorating effects of the most effective MPAs are apparent in both tropical coral and temperate rocky reefs (Appendix C, Figures C.2 and C.3). Our findings are conservative in that we underestimated the baseline biomass of all fishes for the most pristine reefs in our sample (Table C.2).

Our findings are consistent with other local-scale estimates of the effects of fishing on community structure for fishes (e.g. Myers and Worm, 2005; Friedlander and DeMartini, 2002; Jennings et al., 1999). However, if fish in the larges size class included in our analysis (32—64 kg) were historically the prey of extremely large wide-ranging marine predators that have now been lost, it is possible that biomass of large fish observed at some pristine sites may in fact be inflated relative to the true historical baseline. But, given that the largest size class included in this analysis is 32—64kg, and that reef fish are typified by predator-to-prey mass ratios in the orders of hundreds to thousands, this would imply that potential missing predators of the largest fish in our analysis would have been in the range of hundreds to thousands or tens of thousands of kilograms. Hence the only predators that could have filled this role historically would have been large sharks (white sharks at temperate latitudes, tiger sharks and potentially hammerheads and threshers in the tropics) and potentially marine mammals and billfish. Given that these groups of predators are not documented to feed extensively on reefs where they are

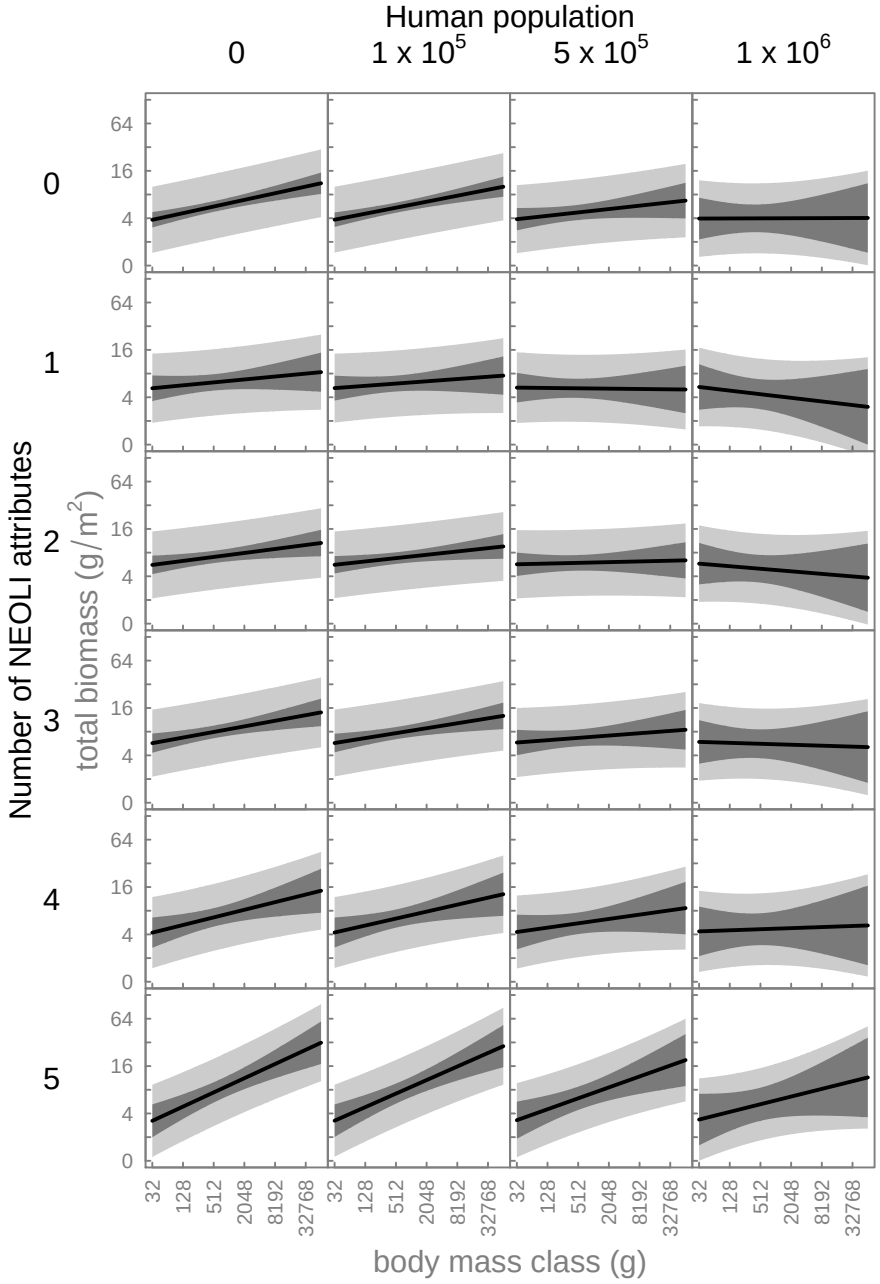

Figure 5.4: Predicted biomass spectra with varying strength of MPA protection and human coastal population density. Increased fish biomass and relatively more large fishes are predicted with both increasing effectiveness of MPAs (more NEOLI attributes) and lower human coastal population. Higher human coastal population is associated with greater uncertainty in the effect of protection. Gray bands indicate 95% confidence intervals accounting for uncertainty in fixed effects only (dark gray) and both fixed and random effects (light gray).

still present, it seems unlikely that predation release in the largest size classes at the relatively pristine sites included in our analysis has biased the baseline estimates.

Comparisons of fish community structure along fishing pressure gradients or inside versus outside well-enforced protected ares consistently reveal profound depletions of fish numbers and biomass, particularly of the largest, most functionally important, species (Dulvy et al., 2004; DeMartini et al., 2008; Edgar et al., 2014; Babcock et al., 2010). On tropical coral reefs, the largest predatory fishes play a key role regulating predation and grazing at lower trophic levels, and their removal often has profound and far-reaching effects (McCauley et al., 2012; Madin et al., 2010; Madin and Gaines, 2010). In Kenya the overfishing of predatory fishes, particularly the orange-lined triggerfishes, enabled reef-eroding abundances of grazing sea urchins (McClanahan and Muthiga, 1988; Mcclanahan, 2000). An 80% reduction in predator biomass across the most lightly-populated reef islands in the world in Fiji led to the declines in the abundance of 15 functionally important predators, unleashing outbreaks of crown-of-thorn starfishes that led to island-wide phase shifts from coral-to-algal dominance (Dulvy et al., 2004). The impact of human populations on adjacent to temperate kelp reefs is most apparent in the widespread elimination of air-breathing megafauna and invertebrates, including: the global extinction of Stellars sea cow and the region-wide extinction of sea otters, the serial depletion of abalone, lobsters, sea cucumbers and urchins (Dayton et al., 1998; Tegner and Dayton, 2000; Steneck et al., 2004). While the ecosystem-scale impacts of fishing on temperate rocky reef fishes is less well-studied than on tropical coral reefs, the ecological extinction of the largest, most functionally important, fishes such as snapper, sheephead, giant seabass, Atlantic cod and wolf fishes, is well documented (Steneck et al., 2004; Estes et al., 2010; Dayton et al., 1998). Also, the overfishing of important invertebrate predators on temperate rocky reefs in the southern hemisphere has been shown to have had similar ecosystem-level effects to the removal of vertebrate predators elsewhere (Ling and Johnson, 2012; Shears and Babcock, 2002)

Here we reveal that local overfishing and the ecological extinction of functionally important fishes are underlain by a more systematic depletion of the largest fishes size classes on reefs worldwide, akin to the loss of large-bodied animals that has been described on land (Darimont et al., 2009; Estes et al., 2011). The widespread reduction in overall reef fish biomass we describe, and in particular the loss of biomass of the largest, most functionally important, size classes, has the potential to undermine the resilience of reef ecosystems to other stressors such as warming and acidification in a rapidly changing world. Moving toward more sustainable fisheries can go a long way toward ensuring not only more stable and secure food sources for the poorest coastal people, but restoring baseline body-size distributions that are associated with greater

reef resilience. Fortunately, effective marine protected areas can recover and preserve overall fish biomass distributions, particularly in the largest, most functionally important, size classes. In doing so they provide they provide modern-day baselines for reefs without humans.

Chapter-specific acknowledgements

Early analyses for this chapter were conducted at a workshop on Maria Island, Tasmania, which was organised and facilitated by Graham Edgar, Rick Stuart-Smith and other staff of the Reef Life Survey (RLS) program - notably Antonia Cooper, Liz Oh, Just Berkhout. A huge amount of work went into making this workshop a reality and I am very grateful to all involved; not to mention all those who contributed the countless hours of survey work represented by the RLS dataset itself (see main thesis aknowledgements). The analysis workshop was highly collaborative and inclusive, and many of the participants contributed directly to building the RLS dataset. As such, several other participants (in addition to GE and RSS) will be included as authors on the manuscript arising from this chapter including: Alejo Irigoyen, David Galván, Sergio Navarrete, Stuart Kinninmonth, Neville Barrett, and Russell Thomson.

Chapter 6

Synthesis

In this thesis I draw on size-based ecological theory and models, a detailed empirical study of a kelp forest case study system, and a global-scale analysis, to give new insights into how size-based energy flows combine with energetic subsidies, local conditions and anthropogenic pressure to shape reef fish communities. This work has important implications for the field of ecology in general, for reef ecology in particular, and for conservation and management. In this discussion I synthesise these implications and identify key directions for future research.

6.1 Implications for general ecology and theory

As something that almost all budding ecologists learn about in high school or as undergraduates, ecological pyramids are perhaps the longest-standing and most widely-recognised model of the structure of ecological communities (and of how trophic energy flows underlie community structure). By linking size spectra with ecological pyramids (Chapter 2), I provide a quantitative framework for deriving expectations for the shapes of biomass pyramids, which was previously lacking. In addition to shedding light on the debate surrounding IBPs in marine ecosystems, this communicates the relevance of size spectra to terrestrial ecologists who have long appreciated biomass pyramids, but are only beginning to consider size-based perspectives.

A useful feature of size-based ecological theory is that it can provide null hypotheses for community structure against which empirical data can be compared, to identify departures that are worth investigating further (Marquet, 2005). This is the case for IBPs among reef fishes, which fall outside the range of expectations for community structure given our current knowledge of size-based energy flow in marine ecosystems. Over-counting of large-bodied mobile predators may have been a factor in the studies that sparked the original debate over IBPs on reefs (e.g. Sandin et al., 2008; Ward-Paige et al., 2010; Nadon et al., 2012). However, this thesis

(and previous work by Ackerman et al. 2004) provides strong evidence that IBPs are not solely an artifact of survey methodologies. I hypothesise that energetic subsidies are the most likely explanation, and while I was not able to test this hypothesis directly, my findings in Chapter 3, and the natural history of reef ecosystems provide strong support for the plausibility of this mechanism.

This thesis, along with recent work by Hocking et al. (2013), shows that size spectra provide a useful and general way to diagnose energetic subsidies. I highlight that a given assemblage is subsidised when the scale of sampling does not encompass the spatial and temporal scale of its resource base, which reinforces the importance of carefully considering scale when interpreting observed community structure — a message that is relevant across marine and terrestrial ecosystems. I also build on previous understanding of spatial subsidies and resource pulses (temporal subsidies) by demonstrating how knowledge of the nature of underlying size-based energy flows (i.e. is PPMR) gives insight into how size-based energy flow combines with subsidies to shape community structure.

An important goal for future research will be to move from the recognition that scale and subsidies play a key role in shaping community structure, to a clear mechanistic understanding of these processes. Several different approaches could be employed to work toward this goal. An empirical approach would be to sample hierarchically with progressively larger sample frames for wider ranging animals (Chave, 2013; McCauley et al., 2012), and in some cases this may be possible through the re-analysis of existing datasets. Recently developed, publicly-available, multi-species size spectrum modeling tools will also be very useful for gaining insight into the role of scale and subsidies. Key questions that could be addressed using these tools in the immediate term are:

(i) How does the input of external production to different body sizes (and species) affect community size structure?

(ii) How does seasonal/pulsed production affect 'snapshot' samples of community structure, and how is this affected by the frequency of pulses and the timing of sampling relative to the pulses?

As mentioned in Chapter 2, the limited availability of individual-level size-abundance data and the fact that there are very few empirical estimates of PPMR — especially outside marine ecosystems — is currently the major limiting factor in developing a general understanding of how size-based processes shape community structure across ecosystems. As such, collection of individual-level data and empirical estimation of PPMR from a wider range of systems should also

be an ongoing priority. Such data will enable us to confront the pattern of community structure with the underlying process of size-based energy flow across a wide range of ecosystems. In turn, this will give rise to a better understanding of the fundamental similarities and differences in the structure and function of different ecosystems.

6.2 Implications for reef ecology

Planktivorous fish on coral reefs form a "wall of mouths" that efficiently strips zooplankton from the oceanic waters that wash over reefs (Hamner et al., 1988). This planktonic input can account for a substantial proportion of the overall energy budget of both temperate and tropical reef fish communities (Polunin, 1996; Bray et al., 1981). The subsidy provided by such planktonic input would be expected to effectively 'broaden the base' of reef biomass pyramids, as it enters the community at a low trophic-level, through typically small-bodied planktivores. However, the prevalence of IBPs on reefs suggests that the wall of mouths concept could be usefully expanded to encompass a broader range of body sizes in order to understand how inputs of off-reef production shape reef fish communities.

Several recent studies show that non-local production can be important for sustaining on-reef fish biomass (McCauley et al., 2012; Wyatt et al., 2012; Galván et al., 2009), but elucidating the magnitude and size-based nature of these inputs will be a key direction for future research. Additionally, it will be important to investigate how off reef-production combines with multiple sources of local on-reef production (e.g. entering the community through benthic invertivores vs. herbivores and detritivores) to shape community size structure. Models of 'coupled' size spectra (Blanchard et al., 2009) present a promising approach to addressing this issue.

By making the first estimate of community PPMR for a reef ecosystem, Chapter 3 of this thesis fundamentally advances current understanding of the processes underlying patterns of community structure among reef fishes. Specifically, the high positive estimated PPMR supports the expectation that size-based predation underlies energy flow among reef fish. This greatly strengthens the inference that subsidies may be responsible for reef IBPs by demonstrating the mismatch between the pattern of community structure with the underlying process of size-based energy flow. Interestingly, the PPMR estimate I obtained for Haida Gwaii suggests that PPMRs may be higher for some reef fish communities than previously thought, and in the range that would be expected to give rise to *weakly* inverted pyramids/columns at realistic values of TE. It will be interesting to ascertain whether such high PPMRs are common among reef fish communities, or a unique feature of the Haida Gwaii ecosystem.

In this thesis I also present the first examination of size spectra, and the effects of habitat on community size-structure, for a temperate reef fish community (Chapter 4). The trend for higher biomass of small bodied-fish and more biomass overall with increasing substrate rugosity that I document is consistent with previous work on coral reefs, which suggests that the effects of substrate rugosity on size structure may be universal across reef fish communities. My results also show that the effect of canopy cover on community structure is different and distinct to that of substrate rugosity, and the effect indicates that the major role of kelp is to directly or indirectly enhance the resource-base, rather than by providing refuge from predation for small fishes (although the body size-range I included in my analysis did not include recruits and young of the year, which can have strong associations with canopy cover, though they contribute little to total community biomass). It remains to be seen whether these responses are consistent for kelp forest communities with different species compositions, but I hope that the publication stemming from this chapter will help stimulate future studies using similar analyses in kelp forests elsewhere.

Community ecology research on reefs has traditionally focused on species and their interactions. Overall, my thesis research shows that a focus on how size-based energy flows and subsidies shape community size structure provides an alternative and complimentary approach that has great potential for improving our understanding of the structure and function of both temperate and tropical reefs. As noted above, there has been some up-take of size-based methods among coral reef ecologists over the last ten years, which has led to important advances in our understanding of how fishing and habitat shape community structure. However, size based approaches have yet to 'catch on' among temperate reef ecologists. The time is ripe for temperate reef ecologists to jump on the size-based band-wagon! Evaluating whether the habitat effects I document are consistent across other locations and species assemblages would be an interesting place to start.

Linear approximations of community size spectra have proven extremely useful for understanding overall patterns of community structure and for quantifying changes, and will remain useful for these purposes. However, there is emerging evidence that explicitly exploring departures from linearity can be highly informative, particularly in the context of understanding how size-based predation and habitat structure combine to shape communities (Rogers et al., 2014). Exploring non-linearities in size spectra for both temperate and tropical reef fishes will be another important direction for future study.

6.3 Implications for conservation and management

The key implications of this thesis for conservation and management relate to 3 broad topics: (i) the scale of 'communities' and ecosystem function; (ii) the utility of size-based analyses for quantifying community structure and tracking change; and (iii) the loss of large fish from reef ecosystems, and their recovery.

If subsidies are universal on reefs, this implies that energy flow and ecosystem function take place at much broader spatial scales than the reefs themselves. Conservation and management strategies that do not encompass the scale of the production-base supporting reefs are likely to run into problems. This lends further support to arguments that management and conservation should expand in scale and scope towards a seascape and ecosystem approach with well-enforced MPAs as one key component (Hughes et al., 2005; Halpern et al., 2010; Mora, 2006). The directions for future research relating to subsidies identified above will likely generate important insights to guide this process.

Forecasting and tracking important changes in kelp forest communities in coming decades will be an application for which size-based analyses, like those I present in Chapter 4, will be particularly useful. Tracking change in fish communities with the maturation of marine protected areas, and as habitats change with the expansion of sea otter populations throughout their former range, are two examples of contexts where size-based approaches will likely be useful. My findings in Chapter 4 are also relevant in the context of managing existing protected areas and selecting new sites for future protection as high and variable rugosity and extensive kelp cover will be beneficial if the goal is to protect or restore fish.

Finally, this thesis provides a new global perspective on the magnitude of change in the structure of reef fish communities that has been bought about by human activities. I hope that this will provide a useful global context to guide local conservation activities. Losses are worrying, but the good news is that effective MPAs are a powerful tool for protecting and restoring reef fish biomass, particularly at large, functionally important, body sizes.

References

Ackerman, J. (2000). Reef fish assemblages: a re-evaluation using enclosed rotenone stations. *Marine Ecology Progress Series 206*, 227–237.

Ackerman, J. L., D. R. Bellwood, and J. H. Brown (2004). The contribution of small individuals to density-body size relationships: examination of energetic equivalence in reef fishes. *Oecologia 139*(4), 568–571.

Airoldi, L., D. Balata, and M. W. Beck (2008). jembe. *Journal of Experimental Marine Biology and Ecology 366*(1-2), 8–15.

Al-Habsi, S. H., C. J. Sweeting, N. V. C. Polunin, and N. A. J. Graham (2008). δ^{15}N and δ^{13}C elucidation of size-structured food webs in a Western Arabian Sea demersal trawl assemblage. *Marine Ecology Progress Series 353*, 55–63.

Alvarez-filip, L., N. K. Dulvy, I. M. Côté, A. R. Watkinson, and J. A. Gill (2011). Coral identity underpins architectural complexity on Caribbean reefs. *Ecological Applications 21*(6), 2223–2231.

Alvarez-Filip, L., N. K. Dulvy, J. A. Gill, I. Cote, and A. R. Watkinson (2009). Flattening of Caribbean coral reefs: region-wide declines in architectural complexity. *Proceedings of the Royal Society of London B Biological Sciences 276*(1669), 3019–3025.

Alvarez-Filip, L., J. A. Gill, and N. K. Dulvy (2011). Complex reef architecture supports more small-bodied fishes and longer food chains on Caribbean reefs. *Ecosphere 2*(10), 118.

Andersen, K. H. and J. E. Beyer (2006). Asymptotic size determines species abundance in the marine size spectrum. *American Naturalist 168*(1), 54–61.

Anderson, T. W. (1994). Role of macroalgal structure in the distribution and abundance of a temperate reef fish. *Marine Ecology Progress Series 113*(3), 279–290.

Anderson, T. W., E. E. DeMartini, and D. A. Roberts (1989). The relationship between habitat structure, body size and distribution of fishes at a temperate artificial reef. *Bulletin of Marine Science 44*(2), 681–697.

Anderson, W. B., D. A. Wait, and P. Stapp (2008). Resources from another place and time: responses to pulses in a spatially subsidized system. *Ecology 89*(3), 660–670.

Babcock, R. C., N. T. Shears, A. C. Alcala, N. S. Barrett, G. J. Edgar, K. D. Lafferty, T. R. Mcclanahan, and G. R. Russ (2010). Decadal trends in marine reserves reveal differential rates of change in direct and indirect effects. *Proceedings of the National Academy of Sciences of the United States of America 107*(43), 18256–18261.

Balmford, A., A. Bruner, P. Cooper, R. Costanza, S. Farber, R. E. Green, M. Jenkins, P. Jefferiss, V. Jessamy, J. Madden, K. Munro, N. Myers, S. Naeem, J. Paavola, M. Rayment, S. Rosendo, J. Roughgarden, K. Trumper, and R. K. Turner (2002). Economic reasons for conserving wild nature. *Science 297*(5583), 950–953.

Banse, K. and S. Mosher (1980). Adult body mass and annual production/biomass relationships of field populations. *Ecological Monographs 50*(3), 355–379.

Barnes, C., D. Maxwell, D. Reuman, and S. Jennings (2010). Global patterns in predator-prey size relationships reveal size dependency of trophic transfer efficiency. *Ecology 91*(1), 222–232.

Barry, J. P. and P. K. Dayton (1991). Physical heterogeneity and organisation of marine communities. In J. Kolasa and S. T. A. Pickett (Eds.), *Ecological heterogenity*, pp. 270–320. Springer-Verlag, New York, USA.

Bartoń, K. (2013). *MuMIn: Multi-model inference. R package version 1.9.13*.

Bascompte, J., C. J. Melián, and E. Sala (2005). Interaction strength combinations and the overfishing of a marine food web. *Proceedings of the National Academy of Sciences of the United States of America 102*(15), 5443–5447.

Bates, D., M. Maechler, B. Bolker, and S. Walker (2013). *lme4: Linear mixed-effects models using Eigen and S4. R package version 1.0-5*.

BCMCA (2011). *Marine Atlas of Pacific Canada: a product of the British Columbia Marine Conservation Analysis (BCMCA)*. British Columbia Marine Conservation Analysis, Vancouver, Canada.

Beaumont, N. J., M. C. Austen, S. C. Mangi, and M. Townsend (2008). Economic valuation for the conservation of marine biodiversity. *Marine Pollution Bulletin 56*(3), 386–396.

Begon, M., C. R. Townsend, and J. L. Harper (2006). *Ecology: From Individuals to Ecosystems*. Blackwell Science, Oxford, UK.

Bell, J. D., G. Craik, D. A. Pollard, and B. C. Russell (1985). Estimating length frequency distributions of large reef fish underwater. *Coral Reefs 4*(1), 41–44.

Benoît, E. and M.-J. Rochet (2004). A continuous model of biomass size spectra governed by predation and the effects of fishing on them. *Journal of Theoretical Biology 226*(1), 9–21.

Bertness, M., S. B. S. J. (Ed.) (2014). *Marine Community Ecology and Conservation*. Sinauer Associates, In press.

Blackwood, J. C., A. Hastings, and P. J. Mumby (2011). A model-based approach to determine the long-term effects of multiple interacting stressors on coral reefs. *Ecological Applications 21*(7), 2722–2733.

Blanchard, J. L., S. Jennings, R. Holmes, J. Harle, G. Merino, J. I. Allen, J. Holt, N. K. Dulvy, and M. Barange (2012). Potential consequences of climate change for primary production and fish production in large marine ecosystems. *Philosophical Transactions of the Royal Society of London B Biological Sciences 367*(1605), 2979–2989.

Blanchard, J. L., S. Jennings, R. Law, M. D. Castle, P. Mccloghrie, M.-J. Rochet, and E. Benoît (2009). How does abundance scale with body size in coupled size-structured food webs? *Journal of Animal Ecology 78*(1), 270–280.

Bode, A. (2003). The pelagic foodweb in the upwelling ecosystem of Galicia (NW Spain) during spring: natural abundance of stable carbon and nitrogen isotopes. *ICES Journal of Marine Science 60*(1), 11–22.

Bodkin, J. L. (1986). Fish assemblages in *Macrocystis* and *Nereocystis* kelp forests off central California. *Fishery Bulletin 84*(4), 799–808.

Borgmann, U. (1983). Effect of somatic growth and reproduction on biomass transfer up pelagic food webs as calculated from particle-size-conversion efficiency. *Canadian Journal of Fisheries and Aquatic Sciences 40*, 2010:2018.

Borgmann, U. (1987). Models on the slope of, and biomass flow up, the biomass size spectrum. *Canadian Journal of Fisheries and Aquatic Sciences 44*(S2), 136–140.

Boudreau, P. R. and L. M. Dickie (1992). Biomass spectra of aquatic ecosystems in relation to fisheries yield. *Canadian Journal of Fisheries and Aquatic Sciences 49*(8), 1528–1538.

Bray, R. N., A. C. Miller, and G. G. Geesey (1981). The fish connection: a trophic link between planktonic and rocky reef communities? *Science 214*(4517), 204–205.

Brose, U., T. Jonsson, E. L. Berlow, P. Warren, C. Banasek-Richter, L.-F. L. Bersier, J. L. Blanchard, T. Brey, S. R. Carpenter, M.-F. C. Blandenier, L. Cushing, H. A. Dawah, T. Dell, F. Edwards, S. Harper-Smith, U. Jacob, M. E. Ledger, N. D. Martinez, J. Memmott, K. Mintenbeck, J. K. Pinnegar, B. R. C. Rall, T. S. Rayner, D. C. Reuman, L. Ruess, W. Ulrich, R. J. Williams, G. Woodward, and J. E. Cohen (2006). Consumer-resource body-size relationships in natural food webs. *Ecology 87*(10), 2411–2417.

Brown, J. and J. Gillooly (2003). Ecological food webs: high-quality data facilitate theoretical unification. *Proceedings of the National Academy of Sciences of the United States of America 100*, 1467–1468.

Brown, J. H., J. F. Gillooly, A. P. Allen, V. M. Savage, and G. B. West (2004). Toward a metabolic theory of ecology. *Ecology 85*(7), 1771–1789.

Bruno, J. F., W. F. Precht, P. S. Vroom, and R. B. Aronson (2013). Coral reef baselines: how much macroalgae is natural? *PeerJ PrePrints 1*, e19v1.

Buck, K. R., F. P. Chavez, and L. Campbell (1996). Basin-wide distributions of living carbon components and the inverted trophic pyramid of the central gyre of the North Atlantic Ocean, summer 1993. *Aquatic Microbial Ecology 10*(3), 283–298.

Burnham, K. P. and D. Anderson (2002). *Model Selection and Multimodel Inference: A Practical Information-theoretic Approach*. Springer-Verlag, New York.

Carr, M. and C. Syms (2006). Recruitment. *The ecology of marine fishes: California and adjacent waters. University of California Press, Berkeley*, 411–427.

Chapman, J. and J. Reiss (1999). *Ecology: Principles and Applications*. Cambridge University Press, Cambridge, UK.

Charnov, E. (1993). *Life history invariants*. Oxford University Press, Oxford UK.

Chave, J. (2013). The problem of pattern and scale in ecology: what have we learned in 20 years? *Ecology Letters 16 Suppl 1*, 4–16.

Choat, J. H. and A. M. Ayling (1987). The relationship between habitat structure and fish faunas on New Zealand reefs. *Journal of Experimental Marine Biology and Ecology 110*(3), 257–284.

CIESIN and CIAT (2005). *Gridded Population of the World Version 3 (GPWv3)*. Technical report.

Cloutier, R. (2011). Direct and Indirect Effectsof Marine Protection: Rockfish Conservation Areas as a Case Study. Master's thesis, Simon Fraser University.

Cohen, J. E., T. Jonsson, and S. R. Carpenter (2003). Ecological community description using the food web, species abundance, and body size. *Proceedings of the National Academy of Sciences of the United States of America 100*(4), 1781–1786.

Cole, R. G., N. K. Davey, G. D. Carbines, and R. Stewart (2012). Fish-habitat associations in New Zealand: geographical contrasts. *Marine Ecology Progress Series 450*, 131–145.

Connell, S. D. and G. P. Jones (1991). The influence of habitat complexity on postrecruitment processes in a temperate reef fish population. *Journal of Experimental Marine Biology and Ecology 151*(2), 271–294.

Cousins, S. H. (1985). Ecologists build pyramids again. *New Scientist 107*, 50–54.

Cowen, R. K. (1983). The effects of sheephead (Semicossyphus pulcher) predation on red sea urchin (Strongylocentrotus franciscanus) populations: an experimental analysis. *Oecologia 58*(2), 249–255.

Cramer, K. L., J. B. C. Jackson, C. V. Angioletti, J. Leonard-Pingel, and T. P. Guilderson (2012). Anthropogenic mortality on coral reefs in Caribbean Panama predates coral disease and bleaching. *Ecology Letters*, no–no.

Cushing, D. H. (1975). *Marine Ecology and Fisheries*. Cambridge University Press, Cambridge, UK.

Cyr, H. (2000). Individual energy use and the allometry of population density. In J. H. Brown (Ed.), *Scaling in biology*, pp. 267–295. Oxford University Press, Oxford, UK.

Daan, N., H. Gislason, J. G. Pope, and J. C. Rice (2005). Changes in the North Sea fish community: evidence of indirect effects of fishing? *ICES Journal of Marine Science 62*(2), 177–188.

Damuth, J. (1981). Population density and body size in mammals. *Nature 290*(23), 699–700.

Darimont, C. T., S. M. Carlson, M. T. Kinnison, P. C. Paquet, T. E. Reimchen, and C. C. Wilmers (2009). Human predators outpace other agents of trait change in the wild. *Proceedings of the National Academy of Sciences of the United States of America 106*(3), 952–954.

Darwin, C. (1909). The voyage of the beagle. In *The Harvard Classics*, Volume 29, pp. 109. P.F. Collier and Son Company, London UK.

Dayton, P. K. (1985). Ecology of kelp communities. *Annual Review of Ecology, Evolution, & Systematics 16*, 215–245.

Dayton, P. K., M. J. Tegner, P. B. Edwards, and K. L. Riser (1998). Sliding baselines, ghosts, and reduced expectations in kelp forest communities. *Ecological Applications 8*(2), 309–322.

Dayton, P. K., S. F. Thrush, M. T. Agardy, and R. J. Hofman (1995). Environmental effects of marine fishing. *Aquatic Conservation: Marine and Freshwater Ecosystems 5*(3), 205–232.

DelGiorgio, P. A. and J. Gasol (1995). Biomass distribution in freshwater plankton communities. *American Naturalist 146*, 135–152.

DeMartini, E. E., A. Friedlander, S. A. Sandin, and E. Sala (2008). Differences in fish-assemblage structure between fished and unfished atolls in the northern Line Islands, central Pacific. *Marine Ecology Progress Series 365*, 199–215.

DeMartini, E. E. and D. A. Roberts (1990). Effects of Giant Kelp (*Macrocystis*) on the Density and Abundance of Flshes in a Cobble-Bottom Kelp Forest. *Bulletin of Marine Science 46*(2), 287–300.

Dickie, L. M. and S. R. Kerr (1987). Size-dependent processes underlying regularities in ecosystem structure. *Ecological Monographs 57*(3), 233–250.

Dinmore, T. A. and S. Jennings (2004). Predicting abundance-body mass relationships in benthic infaunal communities. *Marine Ecology Progress Series 276*, 289–292.

Duggins, D. O., C. A. Simenstad, and J. Estes (1989). Magnification of secondary production by kelp detritus in coastal marine ecosystems. *Science 245*(4914), 170–173.

Dulvy, N., R. Freckleton, and N. Polunin (2004). Coral reef cascades and the indirect effects of predator removal by exploitation. *Ecology Letters 7*(5), 410–416.

Dulvy, N. K., N. Polunin, A. C. Mill, and N. Graham (2004). Size structural change in lightly exploited coral reef fish communities: evidence for weak indirect effects. *Canadian Journal of Fisheries and Aquatic Sciences 61*(3), 466–475.

Dunton, K. H. and D. M. Schell (1987). Dependence of consumers on macroalgal (Laminaria solidungula) carbon in an arctic kelp community: δ^{13}C evidence. *Marine Biology 93*(4), 615–625.

Ebeling, A. W. and M. Hixon (1993). Tropical and Temperate Reef Fishes: Comparison of Community Structures. In P. Sale (Ed.), *The Ecology of Fishes on Coral Reefs*, pp. 509–536. Academic Press.

Ebeling, A. W., R. J. Larson, and W. S. Alevizon (1980). Habitat Groups and Island-Mainland Distribution of Kelp-bed Fishes off Santa Barbara, CA. In P. D. M (Ed.), *Multidisciplinary symposium on the California Islands*, pp. 403–431. Santa Barbara Museum of Natural History.

Ebeling, A. W., R. J. Larson, W. S. Alevizon, and R. N. Bray (1980). Annual variability of reef-fish assemblages in kelp forests off Santa Barbara, California. *Fishery Bulletin 78*(2), 361–377.

Edgar, G., R. Bustamante, J. Farina, M. Calvopina, C. Martinez, and M. Toral-Granda (2004). Bias in evaluating the effects of marine protected areas: the importance of baseline data for the Galapagos Marine Reserve. *Environmental Conservation 31*(3), 212–218.

Edgar, G. J., N. S. Barrett, and A. J. Morton (2004). Biases associated with the use of underwater visual census techniques to quantify the density and size-structure of fish populations. *Journal of Experimental Marine Biology and Ecology 308*(2), 269–290.

Edgar, G. J., N. S. Barrett, and R. D. Stuart-Smith (2009). Exploited reefs protected from fishing transform over decades into conservation features otherwise absent from seascapes. *Ecological Applications 19*(8), 1967–1974.

Edgar, G. J. and R. D. Stuart-Smith (2009). Ecological effects of marine protected areas on rocky reef communities–a continental-scale analysis. *Marine Ecology Progress Series 388*(August), 51–62.

Edgar, G. J., R. D. Stuart-Smith, T. J. Willis, S. Kininmonth, S. C. Baker, S. Banks, N. S. Barrett, M. A. Becerro, A. T. F. Bernard, J. Berkhout, C. D. Buxton, S. J. Campbell, A. T. Cooper, M. Davey, S. C. Edgar, G. Forsterra, D. E. Galvan, A. J. Irigoyen, D. J. Kushner, R. Moura, P. E. Parnell, N. T. Shears, G. Soler, E. M. A. Strain, and R. J. Thomson (2014). Global conservation outcomes depend on marine protected areas with five key features. *Nature 506*(7487), 216–220.

Ellison, A. M., M. S. Bank, B. D. Clinton, E. A. Colburn, K. Elliott, C. R. Ford, D. R. Foster, B. D. Kloeppel, J. D. Knoepp, and G. M. Lovett (2005). Loss of foundation species: consequences for the structure and dynamics of forested ecosystems. *Frontiers in Ecology and the Environment 3*(9), 479–486.

Elton, C. (1927). *Animal Ecology*. Macmillan Co., New York, USA.

Ernest, S. K. M., B. J. Enquist, J. H. Brown, E. L. Charnov, J. F. Gillooly, V. M. Savage, E. P. White, F. A. Smith, E. A. Hadly, J. P. Haskell, S. K. Lyons, B. A. Maurer, K. J. Niklas, and B. Tiffney (2003). Thermodynamic and metabolic effects on the scaling of production and population energy use. *Ecology Letters 6*, 990–995.

Estes, J., C. H. Peterson, and R. Steneck (2010). Some Effects of Apex Predators in Higher-Latitude Coastal Oceans. In J. Estes and J. Terborgh (Eds.), *Trophic Cascades: Predators, Prey, and the Changing Dynamics of Nature*, pp. 1–18. Island Press, Washington DC, USA.

Estes, J. and J. Terborgh (2010). *Trophic Cascades: Predators, Prey, and the Changing Dynamics of Nature*. Island Press, Washington DC, USA.

Estes, J. A., J. Terborgh, J. S. Brashares, M. E. Power, J. Berger, W. J. Bond, S. R. Carpenter, T. E. Essington, R. D. Holt, J. B. C. Jackson, R. J. Marquis, L. Oksanen, T. Oksanen, R. T. Paine, E. K. Pikitch, W. J. Ripple, S. A. Sandin, M. Scheffer, T. W. Schoener, J. B. Shurin, A. R. E. Sinclair, M. E. Soulé, R. Virtanen, and D. A. Wardle (2011). Trophic Downgrading of Planet Earth. *Science 333*(6040), 301–306.

Fedje, D. W. and R. Mathewes (2011). *Haida Gwaii: Human History and Environment from the Time of Loon to the Time of the Iron People*. University of British Columbia Press.

Fisheries and Oceans Canada (2008). Rockfish Conservation Areas Booklet. http://www.pac.dfo-mpo.gc.ca/fm-gp/maps-cartes/rca-acs/index-eng.html. Date retrieved: May 28, 2014.

Frid, A., B. Connors, A. B. Cooper, and J. Marliave (2013). Size-structured abundance relationships between upper- and mid-trophic level predators on temperate rocky reefs. *Ethology Ecology & Evolution 25*(3), 253–268.

Friedlander, A. and E. E. DeMartini (2002). Contrasts in density, size, and biomass of reef fishes between the northwestern and the main Hawaiian islands: the effects of fishing down apex predators. *Marine Ecology Progress Series 230*, 253–264.

Friedlander, A. and J. Parrish (1998). Habitat characteristics affecting fish assemblages on a Hawaiian coral reef. *Journal of Experimental Marine Biology and Ecology 224*(1), 1–30.

Galván, D., C. Sweeting, and W. Reid (2010). Power of stable isotope techniques to detect size-based feeding in marine fishes. *Marine Ecology Progress Series 407*, 271–278.

Galván, D. E., F. Botto, A. M. Parma, L. Bandieri, N. Mohamed, and O. O. Iribarne (2009). Food partitioning and spatial subsidy in shelter-limited fishes inhabiting patchy reefs of Patagonia. *Journal of Fish Biology 75*(10), 2585–2605.

Gasol, J., P. A. DelGiorgio, and C. M. Duarte (1997). Biomass distribution in marine planktonic communities. *Limnology and Oceanography 42*, 1353–1363.

Gelman, A. (2006). Prior distributions on variance parameters in hierarchical models. *Bayesian Analysis 1*(3), 515–533.

Gelman, A. (2008). Scaling regression inputs by dividing by two standard deviations. *Statistics in Medicine 27*(15), 2865–2873.

Gelman, A., J. B. Carlin, H. S. Stern, D. B. Dunson, A. Vehtari, and D. B. Rubin (2014). *Bayesian Data Analysis*. Chapman & Hall.

Gibson, J. (1988). The maritime trade of the north pacific coast. In W. Washburn (Ed.), *History of Indian–White Relations*, pp. 375–390. Smithsonian Institution, Washington, D.C.

Gibson, J. (1992). *Otter skins, Boston ships, and China goods. The maritime fur trade of the Northwest coast 1785-1841*. McGill – Queen's University Press, Montreal, QC and Kingston, ON.

Gilljam, D., A. Thierry, F. Edwards, D. Figueroa, A. Ibbotson, J. Iwan Jones, R. Lauridsen, O. L. Petchey, G. Woodward, and B. Ebenman (2011). Seeing double: size-based and taxonomic views of food web structure. *Advances in Ecological Research 45*, 68–131.

Gislason, H. and J. Rice (1998). Modelling the response of size and diversity spectra of fish assemblages to changes in exploitation. *ICES Journal of Marine Science 55*(3), 362–370.

Graham, M. H. (2004). Effects of Local Deforestation on the Diversity and Structure of Southern California Giant Kelp Forest Food Webs. *Ecosystems 7*(4), 341–357.

Graham, N., N. K. Dulvy, S. Jennings, and N. Polunin (2005). Size-spectra as indicators of the effects of fishing on coral reef fish assemblages. *Coral Reefs 24*(1), 118–124.

Graham, N. A. J. and K. L. Nash (2012). The importance of structural complexity in coral reef ecosystems. *Coral Reefs 32*(2), 315–326.

Greenstreet, S., A. Bryant, N. Broekhuizen, S. Hall, and M. Heath (1997). Seasonal variation in the consumption of food by fish in the North Sea and implications for food web dynamics. *ICES Journal of Marine Science 54*, 243–266.

Grueber, C. E., S. Nakagawa, R. J. Laws, and I. G. Jamieson (2011). Multimodel inference in ecology and evolution: challenges and solutions. *Journal of Evolutionary Biology 24*(4), 699–711.

Haggarty, D. (2014). Rockfish conservation areas in B.C.: Our current state of knowledge. The David Suzuki Foundation, Vancouver.

Halpern, B. S., S. E. Lester, and K. L. McLeod (2010). Placing marine protected areas onto the ecosystem-based management seascape. *Proceedings of the National Academy of Sciences of the United States of America 107*(43), 18312–18317.

Hamner, W., M. Jones, J. Carleton, I. Hauri, and D. Williams (1988). Zooplankton, planktivorous fish, and water currents on a windward reef face: Great Barrier Reef, Australia. *Bulletin of Marine Science 42*(3), 459–479.

Harding, J. N., J. M. S. Harding, and J. D. Reynolds (2014). Movers and shakers: nutrient subsidies and benthic disturbance predict biofilm biomass and stable isotope signatures in coastal streams. *Freshwater Biology 59*, 1361–1377.

Hixon, M. A. and J. P. Beets (1993). Predation, prey refuges, and the structure of coral-reef fish assemblages. *Ecological Monographs 63*(1), 77–101.

Hocking, M. D., N. K. Dulvy, J. D. Reynolds, R. A. Ring, and T. E. Reimchen (2013). Salmon subsidize an escape from a size spectrum. *Proceedings of the Royal Society of London B Biological Sciences 280*, 20122433.

Holbrook, S. J. and R. J. Schmitt (1988). The combined effects of predation risk and food reward on patch selection. *Ecology*, 125–134.

Holbrook, S. J., R. J. Schmitt, and R. F. Ambrose (1990). Biogenic habitat structure and characteristics of temperate reef fish assemblages. *Austral Ecology 15*(4), 489–503.

Hughes, T., D. Bellwood, C. Folke, R. Steneck, and J. Wilson (2005). New paradigms for supporting the resilience of marine ecosystems. *Trends in Ecology & Evolution 20*(7), 380–386.

Hussey, N. E., M. A. MacNeil, B. C. McMeans, J. A. Olin, S. F. J. Dudley, G. Cliff, S. P. Wintner, S. T. Fennessy, and A. T. Fisk (2014). Rescaling the trophic structure of marine food webs. *Ecology Letters 17*(2), 239–250.

Ings, T., T. C. Ings, J. M. Montoya, J. Bascompte, N. Bluthgen, L. Brown, C. F. Dormann, F. Edwards, D. Figueroa, U. Jacob, J. I. Jones, R. B. Lauridsen, M. E. Ledger, H. M. Lewis, J. M. Olesen, F. F. van Veen, P. H. Warren, and G. Woodward (2008). Ecological networks-foodwebs and beyond. *Journal of Animal Ecology 78*, 253–269.

Irigoyen, A. J., D. E. Galvan, L. A. Venerus, and A. M. Parma (2013). Variability in Abundance of Temperate Reef Fishes Estimated by Visual Census. *PLoS One 8*(4), e61072.

Jackson, J. (2001). What was natural in the coastal oceans? *Proceedings of the National Academy of Sciences of the United States of America 98*, 5411–5418.

Jackson, J. B. and E. Sala (2001). Unnatural oceans. *Scientia Marina 65*(S2), 273–281.

Jackson, J. B. C. (1997). Reefs since Columbus. *Coral Reefs 16*(5), 23–32.

Jennings, S. (2005). Size-based analyses of aquatic food webs. In A. Belgrano, R. E. Ulanowicz, J. Dunne, and U. M. Scharler (Eds.), *Aquatic food webs: an ecosystem approach*, pp. 86–97. Oxford University Press, Oxford, UK.

Jennings, S., C. Barnes, C. Sweeting, and N. Polunin (2008). Application of nitrogen stable isotope analysis in size-based marine food web and macroecological research. *Rapid Communications in Mass Spectrometry 22*(11), 1673–1680.

Jennings, S. and J. L. Blanchard (2004). Fish abundance with no fishing: predictions based on macroecological theory. *Ecology 73*, 632–642.

Jennings, S., J. De Oliveira, and K. J. Warr (2007). Measurement of body size and abundance in tests of macroecological and food web theory. *Ecology 76*, 72–82.

Jennings, S. and N. K. Dulvy (2005). Reference points and reference directions for size-based indicators of community structure. *ICES Journal of Marine Science 62*(3), 397–404.

Jennings, S., S. Greenstreet, and J. Reynolds (1999). Structural change in an exploited fish community: a consequence of differential fishing effects on species with contrasting life histories. *Journal of Animal Ecology 68*(3), 617–627.

Jennings, S. and M. J. Kaiser (1998). The effects of fishing on marine ecosystems. *Advances in Marine Biology 34*, 201–352.

Jennings, S. and S. Mackinson (2003). Abundance-body mass relationships in size-structured food webs. *Ecology Letters 6*, 971–974.

Jennings, S., J. Pinnegar, N. Polunin, and T. Boon (2001). Weak cross-species relationships between body size and trophic level belie powerful size-based trophic structuring in fish communities. *Journal of Animal Ecology 70*(6), 934–944.

Jennings, S. and K. Warr (2003). Smaller predator-prey body size ratios in longer food chains. *Proceedings of the Royal Society of London B Biological Sciences 270*(1522), 1413–1417.

Jennings, S., K. J. Warr, and S. Mackinson (2002). Use of size-based production and stable isotope analyses to predict trophic transfer efficiencies and predator-prey body mass ratios in food webs. *Marine Ecology Progress Series 240*, 11–20.

Jones, G. P. (1988). Ecology of rocky reef fish of north–eastern New Zealand: A review. *New Zealand Journal of Marine and Freshwater Research 22*(3), 445–462.

Keeling, B. E. (2013). Quantifying the Magnitude and Mechanisms Driving Pacific Herring (*Clupea pallasi*) Egg Loss on the Central Coast of British Columbia, Canada. Master's thesis, Simon Fraser University.

Kenyon, K. W. (1969). *The Sea otter in the Eastern Pacific ocean*. U.S. Government Printing Office, Washington, D.C.

Kerr, S. R. and L. M. Dickie (2001). *The Biomass Spectrum: A predator-prey theory of aquatic production*. Columbia University Press, New York, USA.

Kleiber, M. (1932). Body size and metabolism. *Hilgardia 6*, 315–332.

Krebs, C. J. (2009). *Ecology: The Experimental Analysis of Distribution and Abundance*. Pearson Benjamin Cummings, San Francisco, USA.

Krumhansl, K. A. and R. E. Scheibling (2012). Production and fate of kelp detritus. *Marine Ecology Progress Series 467*, 281–302.

Larson, R. J. and E. E. DeMartini (1984). Abundance and vertical distribution of fishes in a cobble-bottom kelp forest off San Onofre, California. *Fishery Bulletin 82*(1), 37–53.

Law, R., M. J. Plank, A. James, and J. L. Blanchard (2009). Size-spectra dynamics from stochastic predation and growth of individuals. *Ecology 90*(3), 802–811.

Leaman, B. M. (1980). The Ecology of Fishes in British Columbia Kelp Beds. Technical Report 22, Marine Resources Branch.

Levin, P. S. and M. E. Hay. Fish-seaweed association on temperate reefs: do small-scale experiments predict large-scale patterns? *Marine Ecology Progress Series 232*, 239–246.

Levin, P. S. and M. E. Hay (1996). Responses of temperate reef fishes to alterations in algal structure and species composition. *Marine Ecology Progress Series 134*, 34–47.

Levin, S. A. (1992). The Problem of Pattern and Scale in Ecology: The Robert H. MacArthur Award Lecture. *Ecology 73*(6), 1943–1967.

Levin, S. A. and S. Carpenter (2009). *The Princeton Guide to Ecology*. Princeton University Press, Princeton, USA.

Lindeman, R. L. (1942). The trophic-dynamic aspect of ecology. *Ecology 23*(4), 399–417.

Ling, S. D. and C. R. Johnson (2012). Marine reserves reduce risk of climate-driven phase shift by reinstating size- and habitat-specific trophic interactions. *Ecological Applications 22*(4), 1232–1245.

Love, M. S., M. H. Carr, and L. J. Haldorson (2002). The ecology of substrate-associated juveniles of the genus *Sebastes*. *Environmental Biology of Fishes 30*(1-2), 225–243.

MacArthur, R. H. and J. W. MacArthur (1961). On bird species diversity. *Ecology 42*(3), 594–598.

Madin, E. and S. Gaines (2010). Field evidence for pervasive indirect effects of fishing on prey foraging behavior. *Ecology 91*(12), 3563–3571.

Madin, E. M. P., S. D. Gaines, J. S. Madin, and R. R. Warner (2010). Fishing Indirectly Structures Macroalgal Assemblages by Altering Herbivore Behavior. *American Naturalist 176*(6), 785–801.

Marliave, J. and W. Challenger (2009). Monitoring and evaluating rockfish conservation areas in British Columbia. *Canadian Journal of Fisheries and Aquatic Sciences 66*(6), 995–1006.

Marquet, P. A. (2005). Scaling and power-laws in ecological systems. *Journal of Experimental Biology 208*(9), 1749–1769.

Matthews, K. R. (1990). An experimental study of the habitat preferences and movement patterns of copper, quillback, and brown rockfishes (*Sebastes* spp.). *Environmental Biology of Fishes 29*(3), 161–178.

Maury, O., B. Faugeras, Y.-J. Shin, J.-C. Poggiale, T. Ben Ari, and F. Marsac (2007). Modeling environmental effects on the size-structured energy flow through marine ecosystems. Part 1: The model. *Progress in Oceanography 74*(4), 479–499.

McCann, K., J. Rasmussen, and J. Umbanhowar (2005). The dynamics of spatially coupled food webs. *Ecology Letters 8*(5), 513–523.

McCauley, D. J., P. A. Desalles, H. S. Young, R. B. Dunbar, R. Dirzo, M. M. Mills, and F. Micheli (2012). From wing to wing: the persistence of long ecological interaction chains in less-disturbed ecosystems. *Scientific Reports 2*, 409.

McCauley, D. J., K. A. MCLEAN, J. Bauer, H. S. Young, and F. Micheli (2012). Evaluating the performance of methods for estimating the abundance of rapidly declining coastal shark populations. *Ecological Applications 22*(2), 385–392.

McCauley, D. J., F. Micheli, H. S. Young, D. P. Tittensor, D. R. Brumbaugh, E. M. P. Madin, K. E. Holmes, J. E. Smith, H. K. Lotze, P. A. Desalles, S. N. Arnold, and B. Worm (2010). Acute effects of removing large fish from a near-pristine coral reef. *Marine Biology 157*(12), 2739–2750.

McCauley, D. J., H. S. Young, R. B. Dunbar, J. A. Estes, B. X. Semmens, and F. Micheli (2012). Assessing the effects of large mobile predators on ecosystem connectivity. *Ecological Applications 22*(6), 1711–1717.

Mcclanahan, T. R. (2000). Recovery of a coral reef keystone predator, *Balistapus undulatus*, in East African marine parks. *Biological Conservation 94*(2), 191–198.

McClanahan, T. R. and N. A. Muthiga (1988). Changes in Kenyan coral reef community structure and function due to exploitation. *Hydrobiologia 166*(3), 269–276.

McClenachan, L., F. Ferretti, and J. K. Baum (2012). From archives to conservation: why historical data are needed to set baselines for marine animals and ecosystems. *Conservation Letters 5*(5), 349–359.

Meehan, T. D. (2006). Energy use and animal abundance in litter and soil communities. *Ecology 87*(7), 1650–1658.

Merino, G., M. Barange, J. L. Blanchard, J. Harle, R. Holmes, I. Allen, E. H. Allison, M. C. Badjeck, N. K. Dulvy, J. Holt, S. Jennings, C. Mullon, and L. D. Rodwell (2012). Can marine fisheries and aquaculture meet fish demand from a growing human population in a changing climate? *22*(4), 795–806.

Minagawa, M. and E. Wada (1984). Stepwise enrichment of ^{15}N along food chains: Further evidence and the relation between δ^{15}N and animal age. *Geochimica et Cosmochimica Acta 48*(5), 1135–1140.

Mora, C. (2006). Coral Reefs and the Global Network of Marine Protected Areas. *Science 312*(5781), 1750–1751.

Mora, C. (2014). *The ecology of fishes on coral reefs*. University of Hawaii Press, In press.

Murie, D. J. (1995). Comparative feeding ecology of two sympatric rockfish congeners, *Sebastes caurinus* (copper rockfish) and *S. maliger* (quillback rockfish). *Marine Biology 124*(3), 341–353.

Myers, R. and B. Worm (2005). Extinction, survival or recovery of large predatory fishes. *Philosophical Transactions of the Royal Society of London B Biological Sciences 360*(1453), 13–20.

Nadon, M. O., J. K. Baum, I. D. WIlliams, J. M. McPherson, B. J. Zgliczynski, B. L. Richards, R. E. Schroeder, and R. E. Brainard (2012). Re-creating missing population baselines for Pacific reef sharks. *26*(3), 493–503.

Naiman, R. J., R. E. Bilby, D. E. Schindler, and J. M. Helfield (2002). Pacific Salmon, Nutrients, and the Dynamics of Freshwater and Riparian Ecosystems. *Ecosystems 5*(4), 399–417.

Nakagawa, S. and H. Schielzeth (2012). A general and simple method for obtaining R2from generalized linear mixed-effects models. *Methods in Ecology and Evolution 4*(2), 133–142.

Nash, K. L., N. A. J. Graham, S. K. Wilson, and D. R. Bellwood (2012). Cross-scale Habitat Structure Drives Fish Body Size Distributions on Coral Reefs. *Ecosystems 16*(3), 478–490.

Nee, S., A. Read, and J. Greenwood (1991). The relationship between abundance and body size in British birds. *Nature 351*, 312–313.

Newton, K., I. Côté, G. Pilling, S. Jennings, and N. Dulvy (2007). Current and future sustainability of island coral reef fisheries. *Current Biology 17*(7), 655–658.

Odum, E. (1959). *Foundations of Ecology*. Saunders, Philadelphia, Pennsylvania, USA.

Odum, H. and E. Odum (1955). Trophic structure and productivity of a windward coral reef community on Eniwetok Atoll. *Ecological Monographs 25*(3), 291–320.

Oh, C.-O., R. Ditton, and J. Stoll (2008). The Economic Value of Scuba-Diving Use of Natural and Artificial Reef Habitats. *21*(6), 455–468.

O'Neill, R. V. and D. L. DeAngelis (1981). *Comparative Productivity and Biomass Relations of Forest Ecosystems*. Dynamic properties of forest ecosystems. Cambridge University Press, Cambridge, UK.

Pandolfi, J., J. Jackson, N. Baron, H. Guzman, T. Hughes, C. Kappel, F. Micheli, J. Ogden, and H. Possingham (2005). ECOLOGY: Enhanced: Are US Coral Reefs on the Slippery Slope to Slime? *Science 307*(5716), 1725–1726.

Pandolfi, J. M., R. H. Bradbury, E. Sala, T. P. Hughes, K. A. Bjorndal, R. G. Cooke, D. McArdle, L. McClenachan, M. J. H. Newman, G. Paredes, R. R. Warner, and J. B. C. Jackson (2003). Global trajectories of the long-term decline of coral reef ecosystems. *Science 301*(5635), 955–958.

Parker, S. J., S. A. Berkeley, J. T. Golden, D. R. Gunderson, J. Heifetz, M. A. Hixon, R. Larson, B. M. Leaman, M. S. Love, J. A. Musick, V. M. O'Connell, S. Ralston, H. J. Weeks, and M. M. Yoklavich (2000). Management of Pacific rockfish. *Fisheries 25*(3), 22–30.

Parnell, P., E. Miller, C. Lennert-Cody, and P. Dayton (2010). The response of giant kelp (*Macrocystis pyrifera*) in southern California to low-frequency climate forcing. *Limnology and Oceanography 55*(6), 2686–2702.

Pauly, D. (1995). Anecdotes and the shifting baseline syndrome of fisheries. *Trends in Ecology & Evolution 10*(10), 430.

Pauly, D. and V. Christensen (1995). Primary production required to sustain global fisheries. *Nature 374*(6519), 255–257.

Petchey, O. L. and A. Belgrano (2010). Body-size distributions and size-spectra: universal indicators of ecological status? *Biology Letters 6*(4), 434–437.

Peters, R. (1983). *The Ecological Implications of Body Size* . Cambridge Studies in Ecology. Cambridge University Press, Cambridge, UK.

Pinnegar, J. K. and N. Polunin (1999). Differential fractionation of δ13C and δ15N among fish tissues: implications for the study of trophic interactions. *Functional Ecology 13*(2), 225–231.

Plummer, M. (2003). JAGS: A program for analysis of Bayesian graphical models using Gibbs sampling. In *Proceedings of the 3rd International Workshop on Distributed Statistical Computing (DSC 2003)*. Version 3.4.0.

Polis, G. A., W. B. Anderson, and R. D. Holt (1997). Toward an integration of landscape and food web ecology: the dynamics of spatially subsidized food webs. *Annual Review of Ecology, Evolution, & Systematics 28*, 289–316.

Polunin, N. and C. M. Roberts (1993). Greater biomass and value of target coral-reef fishes in two small Caribbean marine reserves. *Marine Ecology Progress Series 100*, 167–167.

Polunin, N. V. C. (1996). *Trophodynamics of reef fisheries productivity*, pp. 113–135. Chapman and Hall, New York.

Pope, J. G., J. G. Shepherd, J. Webb, A. Stebbing, and M. Mangel (1994). Successful surf-riding on size spectra: the secret of survival in the sea. *Philosophical Transactions of the Royal Society of London B Biological Sciences 343*(1303), 41–49.

Post, D. (2002). Using stable isotopes to estimate trophic position: models, methods, and assumptions. *Ecology 83*(3), 703–718.

R Core Team (2013). *R: A Language and Environment for Statistical Computing*. R Foundation for Statistical Computing, Vienna, Austria.

Reaka-Kulda, M. L. (1997). The global biodiversity of coral reefs. In M. L. Reaka-Kulda, D. E. Wilson, and E. O. Wilson (Eds.), *Biodiversity II: Understanding and protecting our biological resources*, pp. 83–108. Joseph Henry Press, Washington DC.

Reisewitz, S., J. Estes, and C. Simenstad (2006). Indirect food web interactions: sea otters and kelp forest fishes in the Aleutian archipelago. *Oecologia 146*(4), 623–631.

Reuman, D., C. Mulder, C. Banasek-Richter, M. Cattin Blandenier, A. Breure, H. Hollander, J. Kneitel, D. Raffaelli, G. Woodward, and J. Cohen (2009). Allometry of body size and abundance in 166 food webs. *Advances in Ecological Research 41*, 1–44.

Reuman, D., C. Mulder, and D. Raffaelli (2008). Three allometric relations of population density to body mass: theoretical integration and empirical tests in 149 food webs. *Ecology Letters 11*, 1216–1228.

Reynolds, J., D. NK, and J. S (2001). *Life histories of fishes and population responses to exploitation*. Conservation of exploited species, Conservation Biology 6. Cambridge University Press, Cambridge.

Richards, L. J. (1987). Copper rockfish (*Sebastes caurinus*) and quillback rockfish (*Sebastes maliger*) habitat in the Strait of Georgia, British Columbia. *Canadian Journal of Zoology 65*(12), 3188–3191.

Risk, M. J. (1972). Fish diversity on a coral reef in the virgin islands. *Atoll Research Bulletin 193*, 1–6.

Roberts, C., C. McClean, J. Veron, J. Hawkins, G. Allen, D. McAllister, C. Mittermeier, F. Schueler, M. Spalding, and F. Wells (2002). Marine biodiversity hotspots and conservation priorities for tropical reefs. *Science 295*(5558), 1280–1284.

Rochet, M.-J. and E. Benoît (2011). Fishing destabilizes the biomass flow in the marine size spectrum. *Proceedings of the Royal Society of London B Biological Sciences 279*(1727), 284–292.

Rochet, M. J. and V. M. Trenkel (2003). Which community indicators can measure the impact of fishing? A review and proposals. *Canadian Journal of Fisheries and Aquatic Sciences 60*(1), 86–99.

Roff, G., T. R. Clark, C. E. Reymond, J. x. Zhao, Y. Feng, L. J. Mccook, T. J. Done, and J. M. Pandolfi (2012). Palaeoecological evidence of a historical collapse of corals at Pelorus Island, inshore Great Barrier Reef, following European settlement. *Proceedings of the Royal Society of London B Biological Sciences 280*(1750), 20122100–20122100.

Rogers, A., J. L. Blanchard, and P. J. Mumby (2014). Vulnerability of Coral Reef Fisheries to a Loss of Structural Complexity. *Current Biology 24*, 1000–5.

Rooney, N., K. McCann, G. Gellner, and J. Moore (2006). Structural asymmetry and the stability of diverse food webs. *Nature 442*(7100), 265–269.

Rooper, C. N. and L. J. Haldorson (2000). Consumption of Pacific herring (*Clupea pallasi*) eggs by greenling (Hexagrammidae) in Prince William Sound, Alaska. *Fishery Bulletin 98*(3), 655–659.

Ryther, J. H. (1969). Photosynthesis and fish production in the sea. *Science 166*, 72–76.

Sala, E., E. Ballesteros, P. Dendrinos, A. Di Franco, F. Ferretti, D. Foley, S. Fraschetti, A. Friedlander, J. Garrabou, H. Güçlüsoy, P. Guidetti, B. S. Halpern, B. Hereu, A. A. Karamanlidis, Z. Kizilkaya, E. Macpherson, L. Mangialajo, S. Mariani, F. Micheli, A. Pais, K. Riser, A. A. Rosenberg, M. Sales, K. A. Selkoe, R. Starr, F. Tomas, and M. Zabala (2012). The structure of Mediterranean rocky reef ecosystems across environmental and human gradients, and conservation implications. *PLoS One 7*(2), e32742.

Salomon, A., N. Shears, T. Langlois, and R. Babcock (2008). Cascading effects of fishing can alter carbon flow through a temperate coastal ecosystem. *Ecological Applications 18*(8), 1874–1887.

Salomon, A. K., S. K. Gaichas, N. T. Shears, J. E. Smith, E. M. P. Madin, and S. D. Gaines (2010). Key Features and Context-Dependence of Fishery-Induced Trophic Cascades. *24*(2), 1523–1739.

Sandin, S. A., J. E. Smith, E. E. DeMartini, E. A. Dinsdale, S. D. Donner, A. M. Friedlander, T. Konotchick, M. Malay, J. E. Maragos, D. Obura, O. Pantos, G. Paulay, M. Richie, F. Rohwer, R. E. SCHROEDER, S. Walsh, J. B. C. Jackson, N. Knowlton, and E. Sala (2008). Baselines and degradation of coral reefs in the northern Line Islands. *PLoS One 3*(2), e1548.

Scharf, F. S., F. Juanes, and R. A. Rountree (2000). Predator size - prey size relationships of marine fish predators: interspecific variation and effects of ontogeny and body size on trophic-niche breadth. *Marine Ecology Progress Series 208*, 229–248.

Schielzeth, H. (2010). Simple means to improve the interpretability of regression coefficients. *Methods in Ecology and Evolution 1*(2), 103–113.

Shears, N. and R. Babcock (2002). Marine reserves demonstrate top-down control of community structure on temperate reefs. *Oecologia 132*(1), 131–142.

Sheldon, R., A. Prakash, and W. Sutcliffe, Jr (1972). The size distribution of particles in the ocean. *Limnology and Oceanography 17*(3), 327–340.

Shin, Y., M. Rochet, S. Jennings, J. Field, and H. Gislason (2005). Using size-based indicators to evaluate the ecosystem effects of fishing. *ICES Journal of Marine Science 62*(3), 384–396.

Shulman, M. J. (1984). Resource limitation and recruitment patterns in a coral reef fish assemblage. *Journal of Experimental Marine Biology and Ecology 74*(1), 85–109.

Siddon, E. C., C. E. Siddon, and M. S. Stekoll (2008). Community level effects of *Nereocystis luetkeana* in southeastern Alaska. *Journal of Experimental Marine Biology and Ecology 361*(1), 8–15.

Silverman, B. W. (1986). *Density Estimation for Statistics and Data Analysis*. Monographs on applied probability and statistics. Chapman and Hall.

Silvert, W. and T. Platt (1978). Energy flux in the pelagic ecosystem: a time-dependent equation. *Limnology and Oceanography 23*(4), 813–816.

Smale, D. A., M. T. Burrows, P. Moore, N. O'Connor, and S. J. Hawkins (2013). Threats and knowledge gaps for ecosystem services provided by kelp forests: a northeast Atlantic perspective. *3*(11), 4016–4038.

Smith, A. D. M., C. J. Brown, C. M. Bulman, E. A. Fulton, P. Johnson, I. C. Kaplan, H. Lozano-Montes, S. Mackinson, M. Marzloff, L. J. Shannon, Y. J. Shin, and J. Tam (2011). Impacts of Fishing Low-Trophic Level Species on Marine Ecosystems. *Science 333*(6046), 1147–1150.

Spalding, M., H. Fox, G. Allen, N. Davidson, Z. Ferdana, M. Finlayson, B. Halpern, M. Jorge, A. Lombana, S. Lourie, K. D. Martin, E. Mcmanus, J. Molnar, C. A. Recchia, and J. Robertson (2007). Marine ecoregions of the world: a bioregionalization of coastal and shelf areas. *Bioscience 57*(7), 573–583.

Springer, Y., C. Hays, M. Carr, M. Mackey, and J. Bloeser (2006). Ecology and management of the bull kelp, *Nereocystis luetkeana*: A synthesis with recommendations for future research. *Lenfest Ocean Program at The Pew Charitable Trusts*.

Steneck, R., M. Graham, D. Corbett, J. Erlandson, J. Estes, and M. Tegner (2002). Kelp forest ecosystems: biodiversity, stability, resilience and future. *Environmental Conservation 29*(04), 436–459.

Steneck, R. S. and C. R. Johnson (2014). Kelp Forests: Dynamic patterns, processes and feedbacks. In M. Bertness, B. Silliman, and J. Stachowicz (Eds.), *Marine Community Ecology and Conservation*. Sinauer Associates, Sunderland, Massachusetts.

Steneck, R. S., J. Vavrinec, and A. V. Leland (2004). Accelerating Trophic-level Dysfunction in Kelp Forest Ecosystems of the Western North Atlantic. *Ecosystems 7*(4), 323–332.

Stewart, K. R., R. L. Lewison, D. C. Dunn, R. H. Bjorkland, S. Kelez, P. N. Halpin, and L. B. Crowder (2010). Characterizing Fishing Effort and Spatial Extent of Coastal Fisheries. *PLoS One 5*(12), e14451.

Stuart-Smith, R. D., A. E. Bates, J. S. Lefcheck, J. E. Duffy, S. C. Baker, R. J. Thomson, J. F. Stuart-Smith, N. A. Hill, S. J. Kininmonth, L. Airoldi, M. A. Becerro, S. J. Campbell, T. P. Dawson, S. A. Navarrete, G. A. Soler, E. M. A. Strain, T. J. Willis, and G. J. Edgar (2013). Integrating abundance and functional traits reveals new global hotspots of fish diversity. *Nature 501*(7468), 539–542.

Sweeting, C., J. Barry, C. Barnes, N. Polunin, and S. Jennings (2007). Effects of body size and environment on diet-tissue δ^{15}N fractionation in fishes. *Journal of Experimental Marine Biology and Ecology 340*(1), 1–10.

Talley, D. M. (2008). Spatial Subsidy. In S. E. Jorgensen and B. Fath (Eds.), *Encyclopedia of Ecology*, pp. 3325–3331. Elsevier Science, Oxford, UK.

Tegner, M. J. and P. K. Dayton (2000). Ecosystem effects of fishing in kelp forest communities. *ICES Journal of Marine Science 57*(3), 579–589.

Tews, J., U. Brose, V. Grimm, K. Tielbörger, M. C. Wichmann, M. Schwager, and F. Jeltsch (2004). Animal species diversity driven by habitat heterogeneity/diversity: the importance of keystone structures. *Journal of Biogeography 31*(1), 79–92.

Thibault, K. M., E. P. White, A. H. Hurlbert, and S. K. Ernest (2010). Multimodality in the individual size distributions of bird communities. *Global Ecology and Biogeography 20*(1), 145–153.

Thompson, R. M., M. Hemberg, B. M. Starzomski, and J. B. Shurin (2007). Trophic levels and trophic tangles: the prevalence of omnivory in real food webs. *Ecology 88*(3), 612–617.

Tolimieri, N., K. Andrews, G. Williams, S. Katz, and P. S. Levin (2009). Home range size and patterns of space use by lingcod, copper rockfish and quillback rockfish in relation to diel and tidal cycles. *Marine Ecology Progress Series 380*, 229–243.

Trebilco, R., J. K. Baum, A. K. Salomon, and N. K. Dulvy (2013). Ecosystem ecology: size-based constraints on the pyramids of life. *Trends in Ecology & Evolution 28*(7), 423–431.

Trebilco, R., K. W. Demes, L. C. Lee, B. E. Keeling, N. A. Sloan, H. L. Stewart, and A. K. Salomon (2014). Summary of Baseline Kelp Forest Surveys Within and Adjacent to Gwaii Haanas National Park Reserve, National Marine Conservation Area Reserve and Haida Heritage Site, Haida Gwaii, British Columbia, Canada. *Canadian Data Report of Fisheries and Aquatic Sciences 1252*.

Tyberghein, L., H. Verbruggen, K. Pauly, C. Troupin, F. Mineur, and O. De Clerck (2011). Bio-ORACLE: a global environmental dataset for marine species distribution modelling. *Global Ecology and Biogeography 21*(2), 272–281.

Wang, H., W. Morrison, and A. Singh (2009). Modeling inverted biomass pyramids and refuges in ecosystems. *Ecological Modelling 220*, 1376–1382.

Ward-Paige, C., J. M. Flemming, and H. K. Lotze (2010). Overestimating Fish Counts by Non-Instantaneous Visual Censuses: Consequences for Population and Community Descriptions. *PLoS One 5*(7), e11722.

Ware, D. M. (2000). *Fisheries Oceanography: an Integrative Approach to Fisheries Ecology and Management*. Blackwell Science, Oxford, UK.

Watson, J. and J. Estes (2011). Stability, resilience, and phase shifts in rocky subtidal communities along the west coast of Vancouver Island, Canada. *Ecological Monographs 81*(2), 215–239.

Watson, R. A., G. M. Carlos, and M. A. Samoilys (1995). Bias introduced by the non-random movement of fish in visual transect surveys. *Ecological Modelling 77*(2), 205–214.

Watson, R. A. and T. J. Quinn, II (1997). Performance of transect and point count underwater visual census methods. *Ecological Modelling 104*(1), 103–112.

Webb, T. J., N. K. Dulvy, S. Jennings, and N. V. C. Polunin (2011). The birds and the seas: body size reconciles differences in the abundance–occupancy relationship across marine and terrestrial vertebrates. *Oikos 120*(4), 537–549.

White, E., S. Ernest, and A. Kerkhoff (2007). Relationships between body size and abundance in ecology. *Trends in Ecology & Evolution 22*(6), 323–330.

Williams, E. C. (1941). *An ecological study of the floor fauna of the Panama rain forest*, Volume 6. The Academy.

Willis, T. J. and M. J. Anderson (2003). Structure of cryptic reef fish assemblages: relationships with habitat characteristics and predator density. *Marine Ecology Progress Series 257*, 209–221.

Wilson, S. K., F. R, M. S. Pratchett, N. A. J. Graham, N. K. Dulvy, R. A. Turner, A. Cakacaka, and N. Polunin (2010). Habitat degradation and fishing effects on the size structure of coral reef fish communities. *Ecological Applications 20*(2), 442–451.

Wyatt, A., A. Waite, and S. Humphries (2010). Variability in Isotope Discrimination Factors in Coral Reef Fishes: Implications for Diet and Food Web Reconstruction. *PLoS One 5*, e13682.

Wyatt, A. S. J., A. M. Waite, and S. Humphries (2012). Stable isotope analysis reveals community-level variation in fish trophodynamics across a fringing coral reef. *Coral Reefs 31*(4), 1029–1044.

Yamanaka, K. L. and G. Logan (2010). Developing British Columbia's Inshore Rockfish Conservation Strategy. *Marine and Coastal Fisheries: Dynamics, Management, and Ecosystem Science 2*(1), 28–46.

Yang, L. H., J. L. Bastow, K. O. Spence, and A. N. Wright (2008). What can we learn from resource pulses? *Ecology 89*(3), 621–634.

Yvon-Durocher, G., J. M. Montoya, M. Trimmer, and G. Woodward (2011). Warming alters the size spectrum and shifts the distribution of biomass in freshwater ecosystems. *Global Change Biology 17*(4), 1681–1694.

Yvon-Durocher, G., J. Reiss, J. Blanchard, B. Ebenman, D. M. Perkins, D. C. Reuman, A. Thierry, G. Woodward, and O. L. Petchey (2011). Across ecosystem comparisons of size structure: methods, approaches and prospects. *Oikos 120*(4), 550–563.

Appendix A

Supplementary materials for Chapter 3

A.1 Supplementary tables

Table A.1: Species surveyed on transects and sampled for stable isotope analysis, with visually assessed stomach contents

species	n surveyed	n sampled	mass range surveyed (g)	mass range sampled (g)	prey items (no. of sampled fish for which item present in gut)			
					fish	crabs	other reef invertebrates	pelagic zooplankton
Black rockfish (*Sebastes melanops*)	1452	34	36–1923	10–1563	16	0	8	6
Brown Irish lord (*Hemilepidotus spinosus*)	1		441–441					
Buffalo sculpin (*Enophrys bison*)	1		639–639					
Cabezon (*Scorpaenichthys marmoratus*)	4	2	1248–1862	1450–7500	0	1	1	0
Canary rockfish (*Sebastes pinniger*)	4	12	110–951	240–1450	0	0	0	1
China rockfish (*Sebastes nebulosus*)	128	26	39–1050	4–884	3	15	9	1
Copper rockfish (*Sebastes caurinus*)	245	42	38–1297	14–2400	11	15	13	9
Kelp greenling (*Hexagrammos decagrammus*)	476	23	34–1950	80–1075	6	10	8	7
Kelp perch (*Brachyistius frenatus*)	1		94–94					
Lingcod (*Ophiodon elongatus*)	26	27	208–1381	478–17900	12	0	1	1
Painted greenling (*Oxylebius pictus*)	32	1	43–216	40–40	0	0	1	0
Puget Sound rockfish (*Sebastes emphaeus*)	106		85–119					
Quillback rockfish (*Sebastes maliger*)	195	33	40–1273	9–1180	9	8	8	8
Red Irish lord (*Hemilepidotus hemilepidotus*)	3	4	49–226	90–170	1	1	2	0
Rock greenling (*Hexagrammos lagocephalus*)	3		355–355					
Striped perch (*Embiotoca lateralis*)	13		129–678					
Tiger rockfish (*Sebastes nigrocinctus*)	1		97–97					
Vermilion rockfish (*Sebastes miniatus*)	9	1	262–883	800–800	0	0	0	0
Yellowtail rockfish (*Sebastes flavidus*)	1837	20	33–495	3–1300	3	0	0	0

A.2 Supplementary figures

.

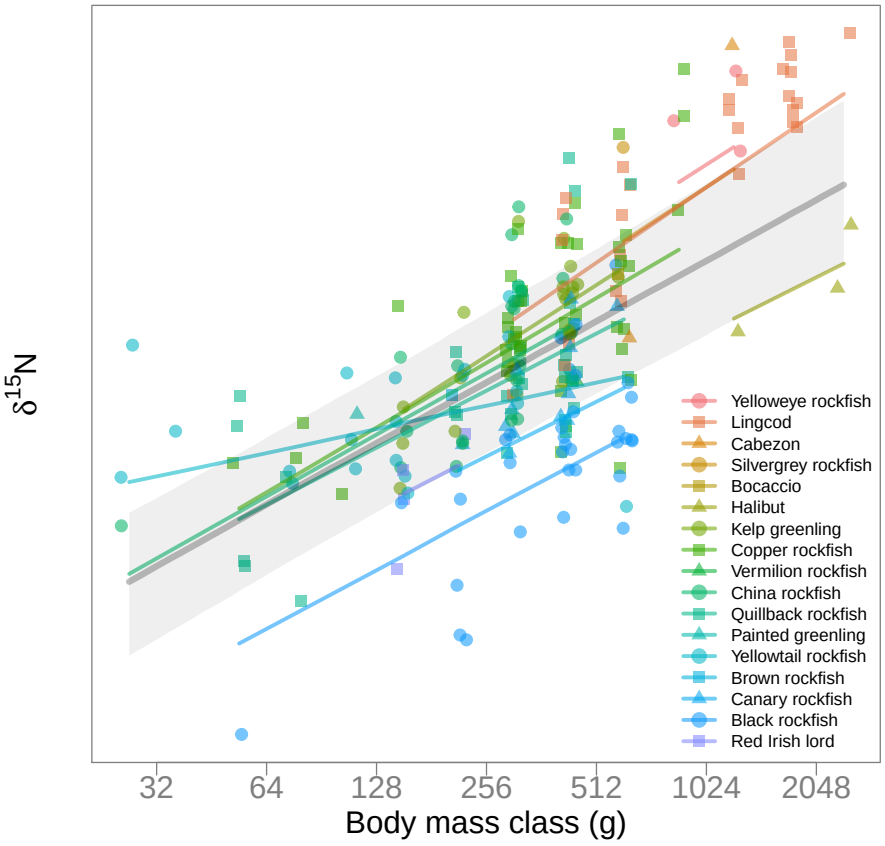

Figure A.1: The relationship between δ^{15}N, a proxy for trophic position, and body-size for the kelp forest reef fishes on Haida Gwaii, British Columbia, Canada. Gray line and shaded band indicate the global fit and 95% confidence intervals. Colored lines indicate the mean fits for individual fish species.

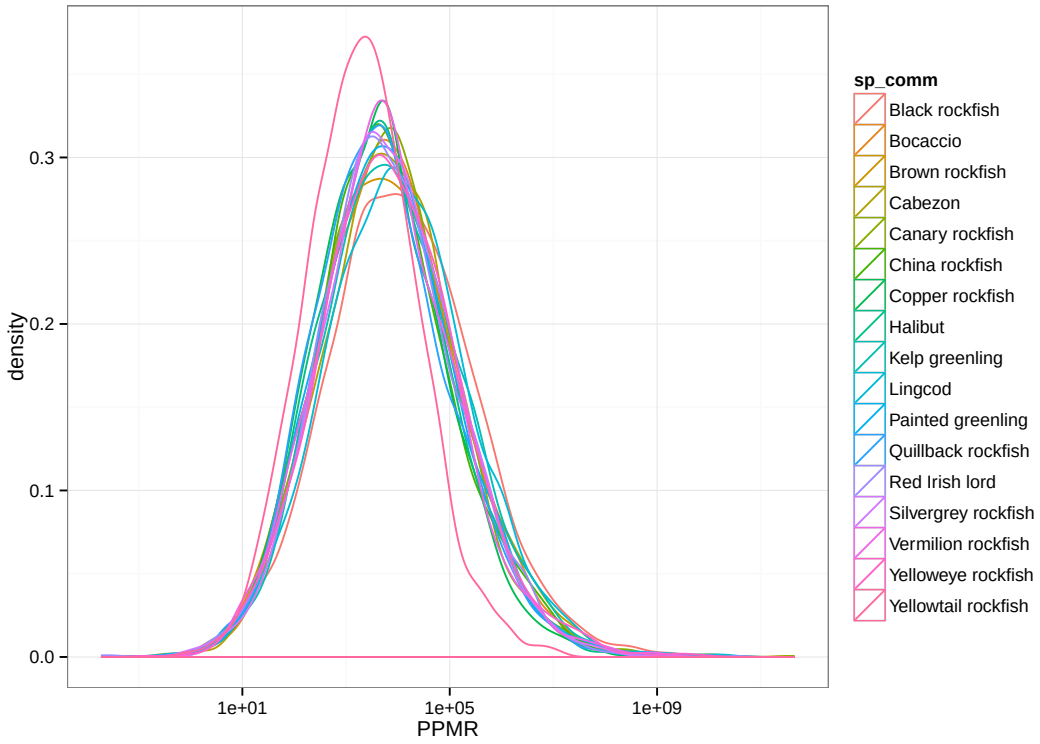

Figure A.2: Results of jackknife analysis showing the distribution of PPMR estimates obtained, excluding one species at a time from the model. Colour coding indicates the individual species excluded in each iteration.

Figure A.3: Species-level slope estimates from weighted hierarchical linear model fit with `lmer` vs. the non-weighted hierarchical Bayesian model fit using `JAGS` that incorporates measurement errors. The global slope estimates are shown as coloured vertical lines and are nearly the same. Area of dots is proportional to the weights for `lmer` model points and held constant for `JAGS` model points. Confidence intervals are +/- 1.96 random effect standard errors for `lmer` and 2.5 and 97.5 quantiles for `JAGS`. Estimates are ordered by decreasing `JAGS` estimate from top to bottom.

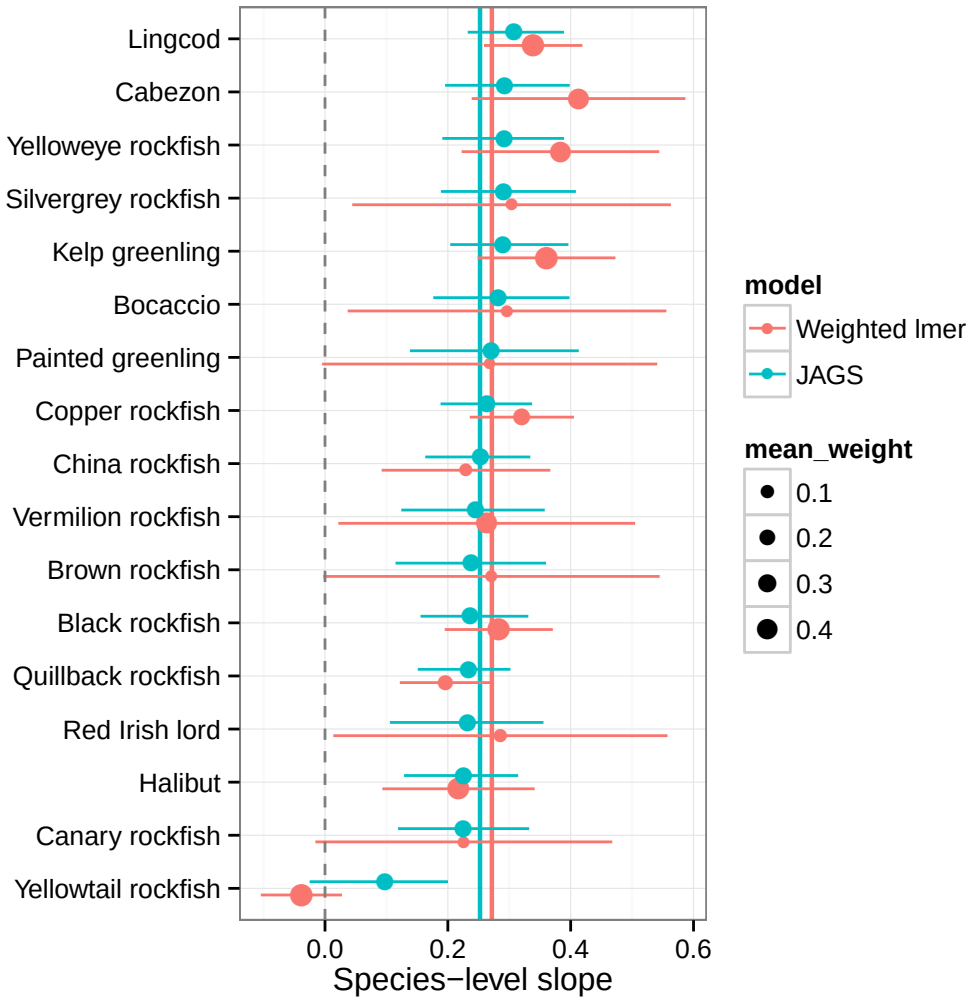

A.3 JAGS code for Bayesian hierarchical model

```
model {
  # Priors
  b0 ~ dnorm(0, 1.0E-6) # intercept
  b1 ~ dnorm(0, 1.0E-6) # slope
  sigma_res ~ dunif(0, 100) # residual SD

  # weakly informative priors (Gelman 2006)
  # half-Cauchy with scale parameter of 10
  sp_b0_sd ~ dt(0, 1/(10*10), 1) T(0, ) # species intercept multilevel SD
  sp_b1_sd ~ dt(0, 1/(10*10), 1) T(0, ) # species slope multilevel SD
  ar_b0_sd ~ dt(0, 1/(10*10), 1) T(0, ) # area intercept multilevel SD

  # Transformations from variance to precision
  tau_res <- pow(sigma_res, -2)
  frac_tau <- pow(frac_sd, -2)
  sp_b0_tau <- pow(sp_b0_sd, -2)
  sp_b1_tau <- pow(sp_b1_sd, -2)
  ar_b0_tau <- pow(ar_b0_sd, -2)
  d15N_tau <- pow(d15N_sd, -2)

  # Multilevel effects for species
  for (j in 1:N_sp) {
    sp_b0[j] ~ dnorm(0, sp_b0_tau) # intercepts
    sp_b1[j] ~ dnorm(0, sp_b1_tau) # slopes
  }

  # Multilevel effects for area
  for (k in 1:N_ar) {
    ar_b0[k] ~ dnorm(0, ar_b0_tau) # intercepts
  }

  # Likelihood data model
  for (i in 1:N) {
    y_hat[i] <- b0 + sp_b0[sp[i]] + ar_b0[area[i]] +
      (b1 + sp_b1[sp[i]]) * log_m[i] # predicted delta 15 N
    obs_delta[i] ~ dnorm(delta[i], d15N_tau) # measurement error on d15N
    delta[i] ~ dnorm(y_hat[i], tau_res) # likelihood model
  }

  # Derived values
  frac ~ dnorm(frac_mu, frac_tau) # fractionation rate with error
  ppmr_exponent <- frac / b1 # exponent in PPMR equation

  # Predictions at area random effect of zero
  for (i in 1:N) {
    y_hat2[i] <- b0 + sp_b0[sp[i]] +
```

```
      (b1 + sp_b1[sp[i]]) * log_m[i] # predicted delta 15 N
  }

  # Fixed effect predictions at smoothed set of log_m
  for (h in 1:N_pred) {
    y_hat3[h] <- b0 + b1 * log_m_pred[h] # predicted delta 15 N at smoothed log_m
  }
}
```

Appendix B

Supplementary materials for Chapter 4

B.1 Supplementary tables

Table B.1: Table of saturated models. In biomass spectrum models, M is the midpoint of each log_2 body mass class.
blah

Response	*Nereocystis* covariate	Model specification
total biomass ($\sum$(B))	canopy score	$log_2(\sum(\text{B})) \sim \text{rugosity} * \text{canopy score} + \text{depth stratum} + (1\|\text{site}) + (1\|\text{year})$
total biomass ($\sum$(B))	stipe density	$log_2(\sum(\text{B})) \sim \text{rugosity} * \text{stipe density} + \text{depth stratum} + (1\|\text{site}) + (1\|\text{year})$
mean individual body mass ($\overline{\text{M}}$)	canopy score	$\overline{\text{M}} \sim \text{rugosity} * \text{canopy score} + \text{depth stratum} + (1\|\text{site}) + (1\|\text{year})$
mean individual body mass ($\overline{\text{M}}$)	stipe density	$\overline{\text{M}} \sim \text{rugosity} * \text{stipe density} + \text{depth stratum} + (1\|\text{site}) + (1\|\text{year})$
biomass spectrum	canopy score	$log_2(\text{biomass}) \sim \text{M} * \text{rugosity} * \text{canopy score} + \text{M} * \text{depth stratum} + (1 + \text{M}\|\text{site}) + (1\|\text{year})$
biomass spectrum	stipe density	$log_2(\text{biomass}) \sim \text{M} * \text{rugosity} * \text{canopy score} + (1 + \text{M}\|\text{site}) + (1\|\text{year})$

Table B.2: Species surveyed on transects

Species	n surveyed
Yellowtail rockfish (*Sebastes flavidus*)	1837
Black rockfish (*Sebastes melanops*)	1452
Kelp greenling (*Hexagrammos decagrammus*)	476
Copper rockfish (*Sebastes caurinus*)	245
Quillback rockfish (*Sebastes maliger*)	195
China rockfish (*Sebastes nebulosus*)	128
Puget Sound rockfish (*Sebastes emphaeus*)	106
Painted greenling (*Oxylebius pictus*)	32
Lingcod (*Ophiodon elongatus*)	26
Striped perch (*Embiotoca lateralis*)	13
Vermilion rockfish (*Sebastes miniatus*)	9
Canary rockfish (*Sebastes pinniger*)	4
Cabezon (*Scorpaenichthys marmoratus*)	4
Rock greenling (*Hexagrammos lagocephalus*)	3
Red Irish lord (*Hemilepidotus hemilepidotus*)	3
Tiger rockfish (*Sebastes nigrocinctus*)	1
Kelp perch (*Brachyistius frenatus*)	1
Buffalo sculpin (*Enophrys bison*)	1
Brown Irish lord (*Hemilepidotus spinosus*)	1

Table B.3: Summary of strength of support for models in the averaged set ($\Delta_i < 2$) for the effects of biophysical predictors on total biomass ($\sum$(B)) and mean individual body mass ($\overline{\text{M}}$). Models are compared via differences in Aikaike's Information Criterion (corrected for small sample size, AIC_c), likelihood of the model given the data ($log(\mathcal{L})$), and normalized Akaike's weight (W_i), indicating the weight of evidence in favour of model i.

Response	*Nereocystis* predictor	Predictors	df	$log(\mathcal{L})$	AIC_c	Δ_i	W_i
$\sum$(B)	canopy score	depth stratum	5.00	-136.29	283.46	0.00	0.51
$\sum$(B)	canopy score	depth stratum, rugosity	6.00	-135.72	284.70	1.24	0.28
$\sum$(B)	canopy score	depth stratum, canopy score	6.00	-135.99	285.24	1.77	0.21
$\sum$(B)	stipe density	stipe density	5.00	-89.47	190.31	0.00	0.46
$\sum$(B)	stipe density	depth stratum, stipe density	6.00	-88.69	191.33	1.02	0.28
$\sum$(B)	stipe density	depth stratum, stipe density, rugosity	7.00	-87.40	191.46	1.15	0.26
$\overline{\text{M}}$	canopy score	depth stratum, rugosity	6.00	-471.73	956.72	0.00	0.42
$\overline{\text{M}}$	canopy score	depth stratum	5.00	-472.94	956.77	0.05	0.41
$\overline{\text{M}}$	canopy score	rugosity	5.00	-473.84	958.57	1.84	0.17
$\overline{\text{M}}$	stipe density	depth stratum, stipe density, rugosity, stipe density*rugosity	8.00	-315.12	649.75	0.00	0.67
$\overline{\text{M}}$	stipe density	depth stratum, stipe density	6.00	-318.61	651.17	1.42	0.33

Table B.4: Summary of strength of support for models in the averaged set ($\Delta_i < 2$) for the effects of biophysical predictors on the slope and intercept of site-scale biomass spectra. Models are compared via differences in Aikaike's Information Criterion (corrected for small sample size, AIC_c), likelihood of the model given the data ($log(\mathcal{L})$), and normalized Akaike's weight (W_i), indicating the weight of evidence in favour of model i. Predictors listed under slope and intercept are included with 2-way interactions with body mass, and predictors listed under intercept only are included without interactions.

Nereocystis covariate	df	$log(\mathcal{L})$	\$AIC$_c$	Δ_i	W_i	Intercept only	Slope and intercept
canopy score	11.00	-635.10	1293.04	0.00	0.72	depth strat, nereo	rugosity
canopy score	12.00	-634.95	1294.91	1.87	0.28	nereo	rugosity, depth strat
stipe density	12.00	-447.73	920.92	0.00	0.08	nereo, depth strat, nereo*rugosity	rugosity
stipe density	7.00	-453.30	921.11	0.19	0.07	body mass only, no covariates	
stipe density	8.00	-452.27	921.20	0.28	0.07	nereo	–
stipe density	11.00	-449.00	921.22	0.30	0.07	nereo, nereo*rugosity	rugosity
stipe density	10.00	-450.12	921.24	0.33	0.06	depth strat	rugosity
stipe density	11.00	-449.02	921.26	0.34	0.06	nereo, depth strat	rugosity
stipe density	10.00	-450.24	921.50	0.58	0.06	rugosity, nereo, depth strat	–
stipe density	9.00	-451.45	921.72	0.80	0.05	–	rugosity
stipe density	9.00	-451.49	921.80	0.88	0.05	rugosity, depth strat	–
stipe density	11.00	-449.35	921.92	1.00	0.05	rugosity, nereo, depth strat, nereo*rugosity	–
stipe density	10.00	-450.46	921.94	1.02	0.05	nereo	rugosity
stipe density	11.00	-449.53	922.29	1.37	0.04	rugosity, nereo	depth strat
stipe density	8.00	-452.84	922.35	1.43	0.04	depth strat	–
stipe density	9.00	-451.81	922.44	1.52	0.04	nereo, depth strat	–
stipe density	12.00	-448.51	922.47	1.55	0.04	rugosity, nereo, nereo*rugosity	depth strat
stipe density	9.00	-451.82	922.47	1.55	0.04	rugosity, nereo	–
stipe density	10.00	-450.75	922.52	1.60	0.03	rugosity	depth strat
stipe density	10.00	-450.76	922.54	1.62	0.03	rugosity, nereo, nereo*rugosity	–
stipe density	8.00	-452.94	922.54	1.63	0.03	rugosity	–
stipe density	13.00	-447.54	922.78	1.87	0.03	nereo, nereo*rugosity	rugosity, depth strat
stipe density	9.00	-452.01	922.85	1.93	0.03	–	depth strat

B.2 Supplementary figures

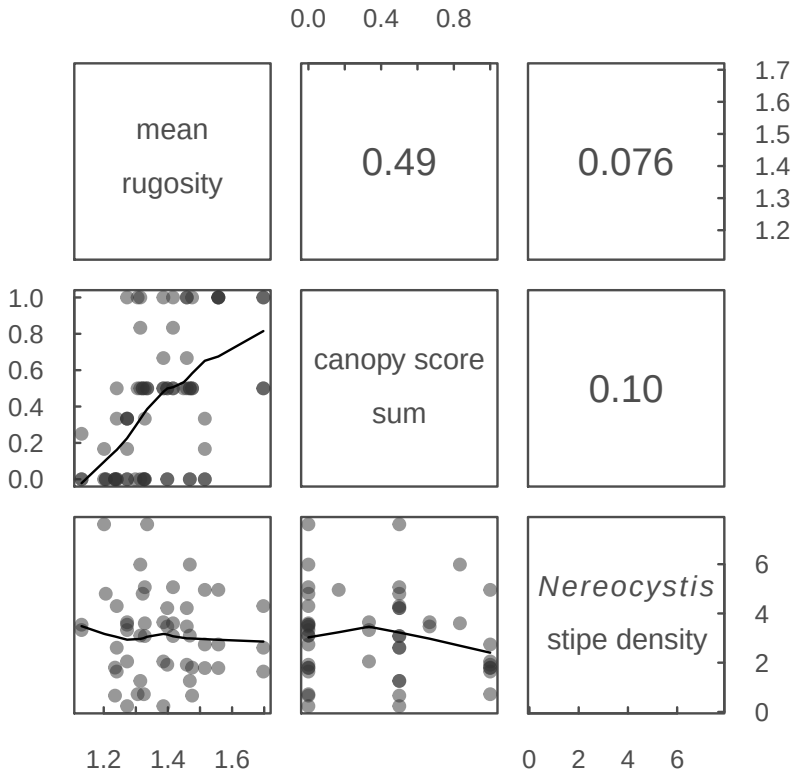

Figure B.1: Correlations (top panes are pairwise correlation coefficients) between habitat complexity covariates included in models. Lines are LOWESS smoothers.

Appendix C

Supplementary materials for Chapter 5

C.1 Methods

C.1.1 Fish survey methods

Fish communities were surveyed with paired 50 x 5 m belt transects in shallow reef habitats, using the standard Reef Life Survey (RLS) methods (full details are provided in an online methods manual at `http://reeflifesurvey.com/files/2008/09/NEW-Methods-Manual_15042013.pdf`, and see Stuart-Smith et al. 2013). These include estimation of the abundance and size of all fishes observed along transects. Individual fish or schools were partitioned into the following size classes, in mm: 25, 50, 75, 100, 125, 150, 200, 250, 300, 350, 400, 500, and 625, with lengths of fish larger than this individually estimated to the nearest 125 mm. The dataset used consisted of 4,970 transects at 1,982 sites, in 74 of the world's marine ecoregions, with a mean of 2.4 transects per site, at a mean depth of 7.6 m (Stuart-Smith et al., 2013).

A large proportion of the RLS surveys were conducted by skilled volunteer SCUBA divers trained to scientific data collection standards. Volunteers undertake surveys with professional researchers using a consistent methodology that has been evaluated and proven effective for broad-scale studies (Edgar et al., 2009; Edgar and Stuart-Smith, 2009). Rigorous measures were applied to ensure consistency and quality of data, with all divers involved having either substantial prior experience or detailed one-on-one training, and extensive data-checking was applied post-dive and before addition to the database (Stuart-Smith et al., 2013). During training, fish size estimates by divers were calibrated with objects of known size or markings on an underwater slate, and with scientific trainers experienced in the methods. More detail relating to Reef Life Survey activities, training of divers and of the processes from observation to collation and curation of the data is provided in the supplementary information of (Stuart-Smith et al., 2013).

C.1.2 Analysis

Fish abundance counts and size estimates were converted to biomass estimates using length–wet mass relationships available for each species (in some cases genus and family) in FishBase (www.fishbase.org). Bias in divers' perception of fish size underwater was additionally corrected using relationships from (Edgar et al., 2004). Given known biases in visual census methods, biomass estimates in this study should be considered in a relative sense, rather than as providing accurate values of absolute fish biomass at sites. Individual fish were then assigned to log_2 body mass bins.

Small fishes are subject to poor detectability by divers using visual census methods (Ackerman, 2000). Similarly, very large fishes are rarely observed in most reef fish communities, and are susceptible to over-counting when present (Ward-Paige et al., 2010). Therefore, we restricted our analysis to fishes in the body mass range from 32 g to 65.5 kg. The lower cutoff was selected as it represented the modal body-size for the dataset, following (Ackerman et al., 2004). The upper cutoff was selected as it resulted in 95% of sites having the maximum observed body-size being encompassed.

Biomass spectra models

Biomass spectra were fit as linear mixed-effects models using the R package `lme4` (Bates et al., 2013). There are several alternative methods for describing size spectra (e.g. log-linear regression, cumulative distribution fitting, maximum-likelihood estimation of probability distribution fits, White et al. 2007). We chose the linear mixed-effects modeling approach as it provides a parsimonious way of accounting for the spatially nested structure of the data, and for modeling the effects of covariates. All biomass within each body-mass bin was summed to the mid-point (M) of the bin, and divided by the total area surveyed to give biomass-per-unit-area (B). Models were then fit linear regressionas with $log_2(\mathrm{B})$ as the predictor and $log_2(\mathrm{M})$ as the response. The spatially nested structure of the data was accounted for by including site within ecoregion as a random effect in models. We defined ecoregions following the Marine Ecoregions of the World (MEOW; Spalding et al. 2007). Body mass class (M) was centered about zero for model fitting in order to remove correlations between the slope and intercept (Daan et al., 2005).

In order to evaluate the effects of human population pressures on the scaling of biomass with body mass, while controlling for biophysical conditions, we added covariates for human coastal population, the number of key MPA conservation features (NEOLI features as per Edgar et al. 2014) and temperature (mean and variability), depth and species richness to the models described above (Figures C.5 – C.8, Table C.1, Edgar et al. 2014). The effects of covariates on

the slopes of biomass spectra were modeled by including 2–way interaction terms between each covariate and M. The non-interactive effect of each covariate gives the effect each covariate on biomass spectra intercepts (or 'height', as M was centered around 0).

Models with all covariates and their 2–way interactions with M were constructed using restricted error maximum likelihood (REML) fitting. For ease of interpretation, effect sizes are presented in standardized units, where a 1 unit change in a predictor implies that a change of 1 SD of that predictor would result in a change of 2SD in the response (Schielzeth, 2010). Predictions were made using models fit with all covariates in their original units.

We also conducted all–combinations model selection and model averaging based on AICc on the saturated models using the function `dredge` in the package `MuMIn` (Bartoń, 2013). There was no appreciable difference in inference or predictions using averaged models, so the results from the full model rather than the averaged model are presented here for simplicity.

C.2 Supplementary tables

Table C.1: Sources and derivations for covariates included in models

Covariate	Description and units	Scale	Source and/or reference
Mean T	Temporal mean from monthly climatologies 2002-2007	5 arcmin (9.2 km)	http://www.oracle.ugent.be Tyberghein et al. 2011
Temperature variability	Temporal mean from monthly climatologies 2002-2007	5 arcmin (9.2 km)	http://www.oracle.ugent.be Tyberghein et al. 2011
Depth	Depth of transect in m, as recorded in survey	Transect (50m)	RLS surveys
Species richness	Number of species recorded on transects	Transect (50m)	RLS surveys

Continued on next page

Table C.1 – *Continued from previous page*

Covariate (abbreviation)	**Description and units**	**Scale**	**Source, ref**
Human coastal population	Index of population pressure calculated by fitting a smoothly tapered surface to each settlement point on a year 2000 world population density grid (CIESIN and CIAT 2005) using a quadratic kernel function (Silverman 1986). Populations were screened for a density greater than 1000 people per 0.04 degree cell, and the search radius was set at 3.959 degrees.	Site	Derived
NEOLI score	Number of key MPA conservation features	Site	Edgar et al. 2014

Table C.2: Average biomass depletion of within the 73 Ecoregions surveyed

Ecoregion	% Depletion		Latitude zone
	All fish	**fish >1 kg**	
Malvinas/Falklands	-97.08	-98.04	Temperate
Celtic Seas	-96.43	-97.88	Temperate
Sea of Japan/East Sea	-96.04	-97.49	Temperate
Oyashio Current	-95.39	-97.39	Temperate
North Sea	-94.55	-97.38	Temperate
Gulf of Maine/Bay of Fundy	-92.56	-96.08	Temperate
East African Coral Coast	-87.85	-95.68	Tropical
Northern California	-85.05	-94.02	Temperate
Western Mediterranean	-84.74	-93.18	Temperate
Bassian	-83.08	-92.84	Temperate
Puget Trough/Georgia Basin	-81.56	-95.7	Temperate
Lesser Sunda	-81.53	-92.88	Tropical
Chiloense	-81.27	-96.76	Temperate
Solomon Archipelago	-81.22	-97.75	Tropical
Central Kuroshio Current	-80.95	-92.79	Temperate
South Kuroshio	-75.68	-95.89	Tropical
Vanuatu	-74.86	-94.88	Tropical
Western Bassian	-74.64	-80.9	Temperate
Rapa-Pitcairn	-72.96	-77.12	Tropical
Hawaii	-71.3	-93.12	Tropical
Seychelles	-70.61	-93.65	Tropical
Southern Caribbean	-70.49	-92.54	Tropical
Guayaquil	-65.19	-91.48	Tropical
Maldives	-65.19	-89.13	Tropical
Three Kings-North Cape	-64.9	-94.17	Temperate
Northern and Central Red Sea	-62.85	-91.5	Tropical
South Australian Gulfs	-62.38	-86.96	Temperate
Gulf of Thailand	-58.69	-92.19	Tropical

Continued on next page

Table C.2 – *Continued from previous page*

Ecoregion	% Depletion		Latitude zone
	All fish	**fish >1kg**	
Torres Strait Northern Great Barrier Reef	-58.48	-91.94	Tropical
Bight of Sofala/Swamp Coast	-58.24	-91.63	Tropical
Cocos-Keeling/Christmas Island	-57.98	-95.1	Tropical
Tonga Islands	-57.67	-93.65	Tropical
Coral Sea	-57.37	-75.55	Tropical
Western Sumatra	-55.23	-94.41	Tropical
Southern California Bight	-51.15	-92.78	Temperate
Shark Bay	-50.78	-90.17	Temperate
Azores Canaries Madeira	-49.57	-79.75	Temperate
Southern Cook/Austral Islands	-49.22	-91.59	Tropical
Bismarck Sea	-48.85	-93.87	Tropical
Easter Island	-47.85	-86.44	Tropical
Adriatic Sea	-44.45	-93.68	Temperate
Society Islands	-44.08	-83.02	Tropical
Bonaparte Coast	-39.86	-70.55	Tropical
Agulhas Bank	-39.16	-94.11	Temperate
North Patagonian Gulfs	-38.61	-90.58	Temperate
Central and Southern Great Barrier Reef	-36.99	-81.12	Tropical
Greater Antilles	-34.84	-64.8	Tropical
Northeastern New Zealand	-33.35	-88.01	Temperate
Samoa Islands	-32.41	-90.99	Tropical
Leeuwin	-32	-79.22	Temperate
Fiji Islands	-28.32	-89.08	Tropical
Ningaloo	-19	-81.82	Tropical
Houtman	-14.33	-74.84	Temperate
Southwestern Caribbean	-12.92	-85.57	Tropical
Chiapas-Nicaragua	-8.93	-88.22	Tropical
Phoenix/Tokelau/Northern Cook Islands	-7.87	-65.54	Tropical
Tuamotus	-5.4	-55	Tropical
Eastern Brazil	-3.87	-83.01	Tropical

Continued on next page

Table C.2 – *Continued from previous page*

Ecoregion	**% Depletion**		**Latitude zone**
	All fish	**fish >1kg**	
Cape Howe	-0.01	-85.5	Temperate
Lord Howe and Norfolk Islands	4.2	-56.6	Tropical
Manning-Hawkesbury	11.19	-84.04	Temperate
Tweed-Moreton	17.86	-61.3	Temperate
Exmouth to Broome	35.55	-66.94	Tropical
Marquesas	56.74	-73.99	Tropical
Arnhem Coast to Gulf of Carpenteria	58.1	-27.73	Tropical
Floridian	105.43	-69.35	Tropical
Nicoya	125.14	109.82	Tropical
Northern Galapagos Islands	134.23	42.29	Tropical
Panama Bight	144.09	-33.23	Tropical
Kermadec Island	201.62	37.53	Temperate
Western Galapagos Islands	222.69	-59.01	Tropical
Cocos Islands	224.15	54.74	Tropical
Eastern Galapagos Islands	322.76	-24.22	Tropical

C.3 Supplementary figures

.

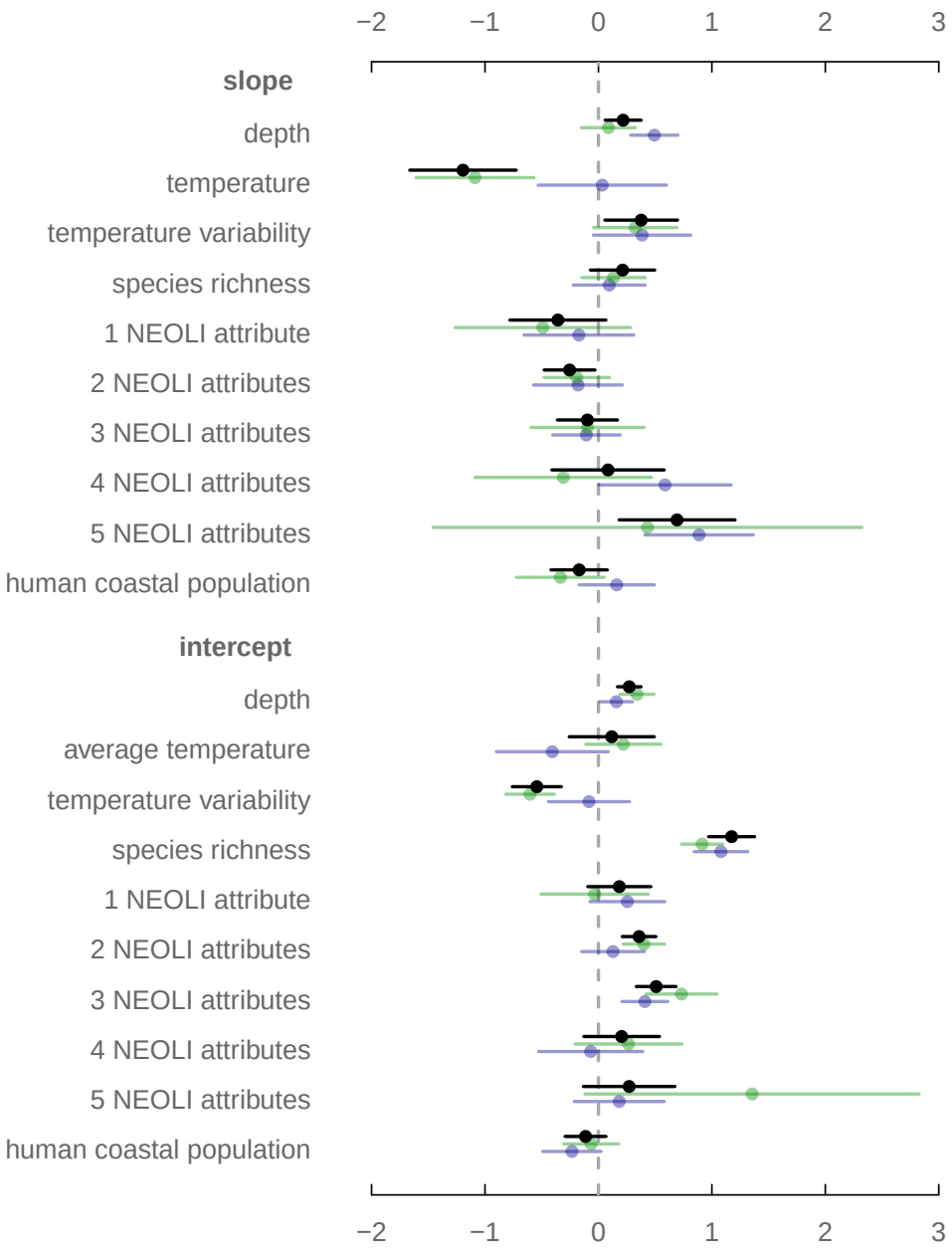

Figure C.1: Points and lines indicate the standardized coefficient estimates and 95% confidence intervals for effects on the slope (top) and intercept (bottom) of the biomass spectra. Black points represent estimates from models that include temperate and tropical sites together, while colored points represent estimates from separate tropical (blue) and temperate (green) models. Standardized estimates are in standard deviation units, obtained by subtracting the mean and dividing by two standard deviations.

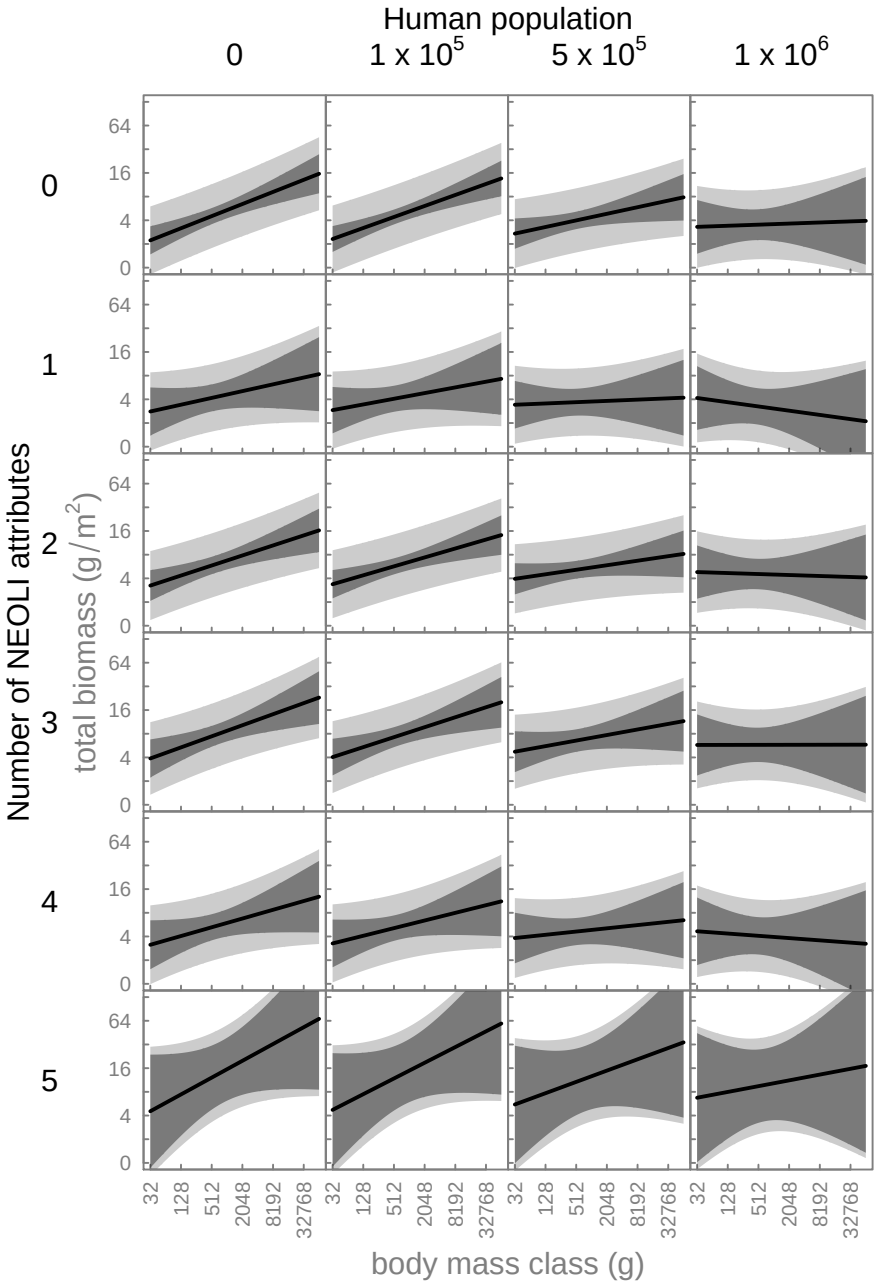

Figure C.2: Model predictions for varying strength of MPA protection and human coastal population density for temperate sites only.

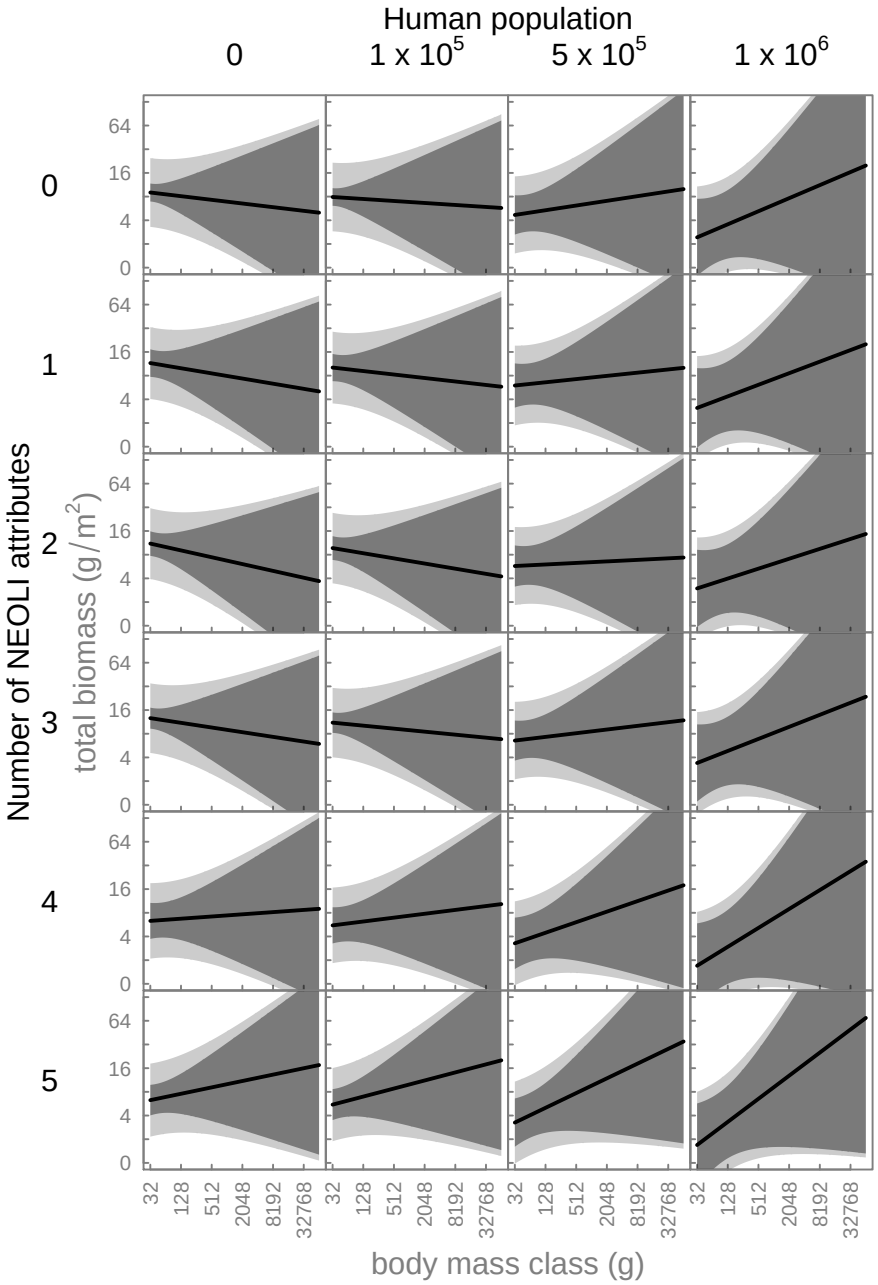

Figure C.3: Model predictions for varying strength of MPA protection and human coastal population density for tropical sites only.

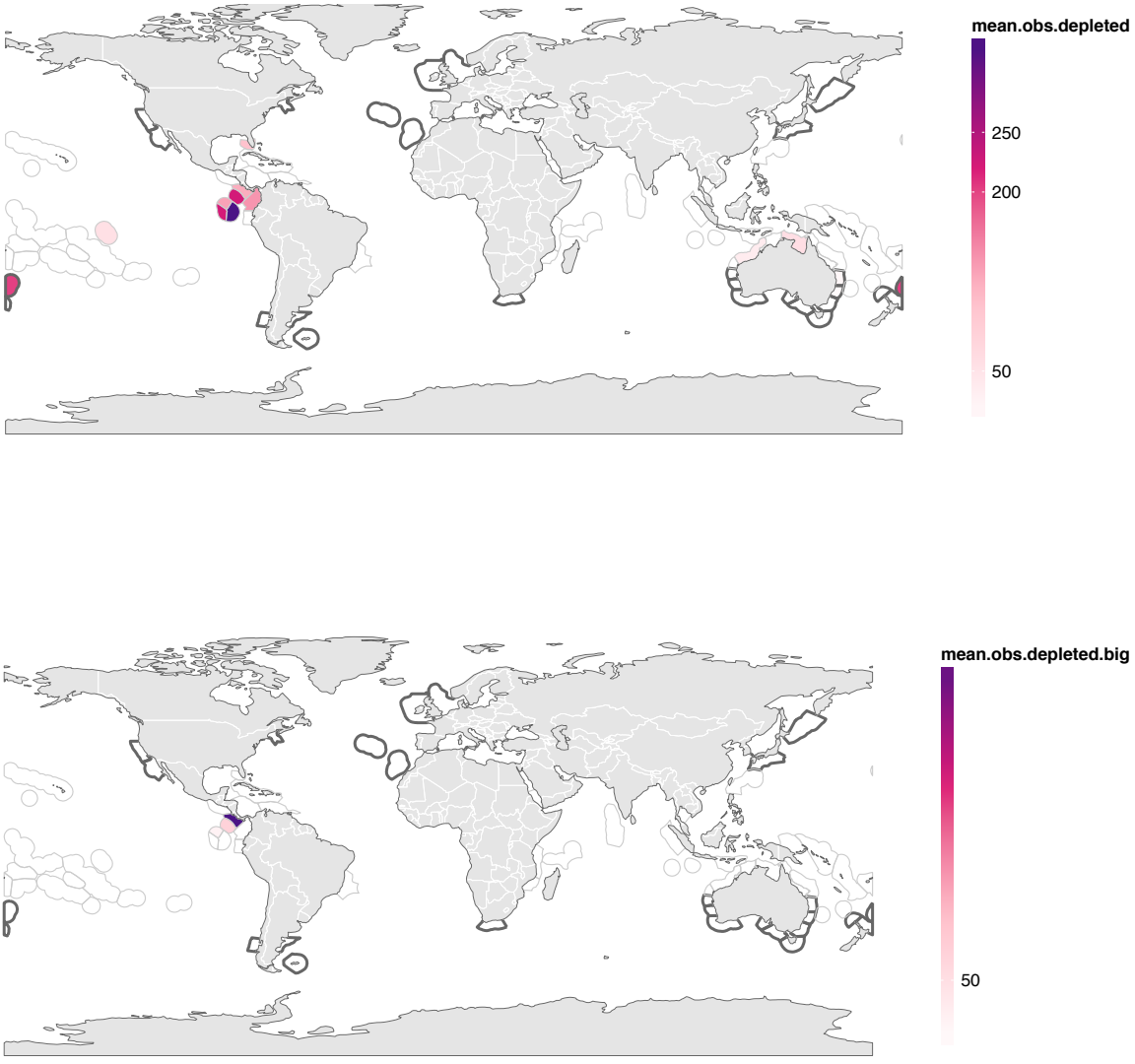

Figure C.4: Average percentage by which observed biomass exceeded the baseline estimate for sites where observed biomass exceeded the baseline estimate for (a) all fishes and (b) fishes >1kg.

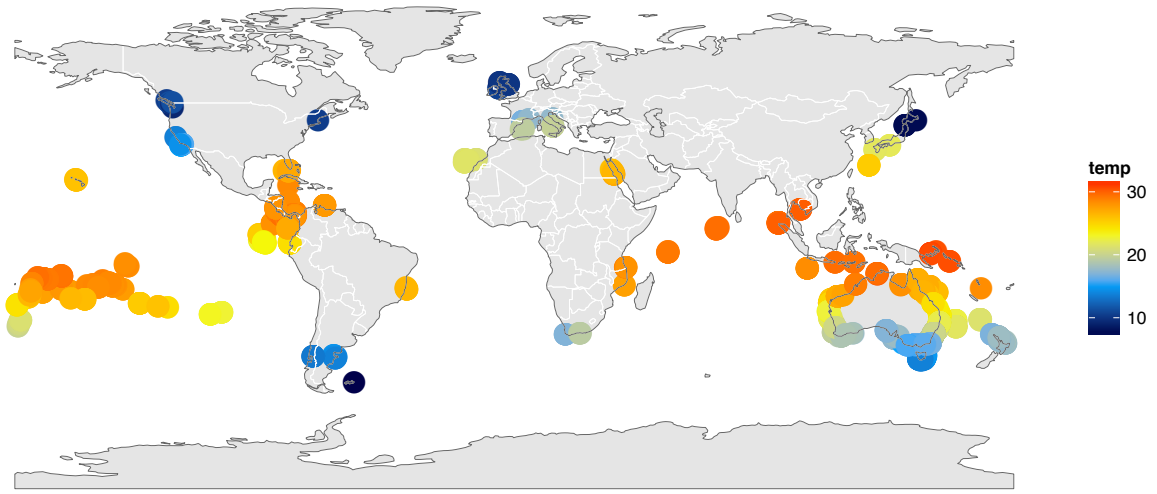

Figure C.5: Mean temperature. See table C.1 for source and derivation.

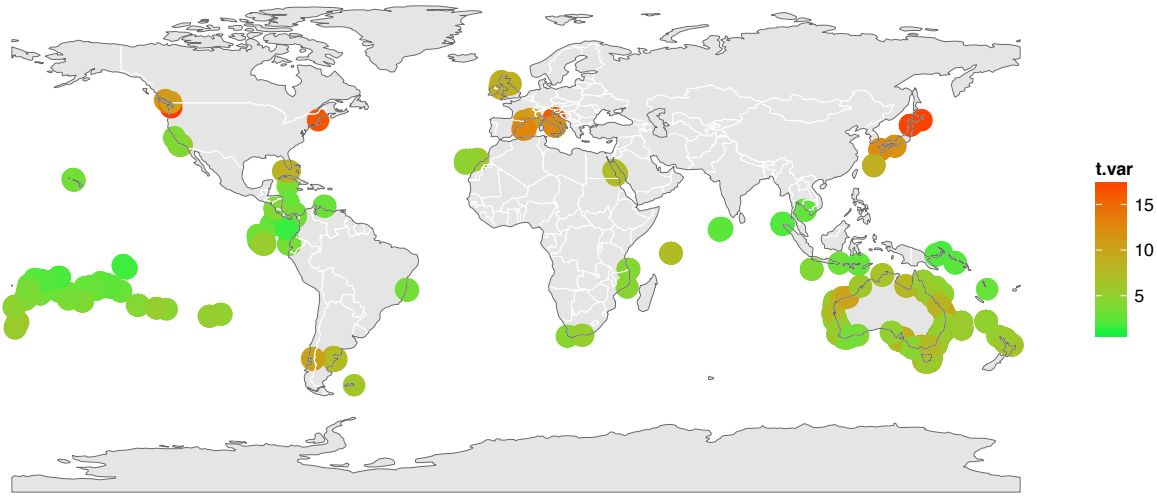

Figure C.6: Temperature variability. See table C.1 for source and derivation.

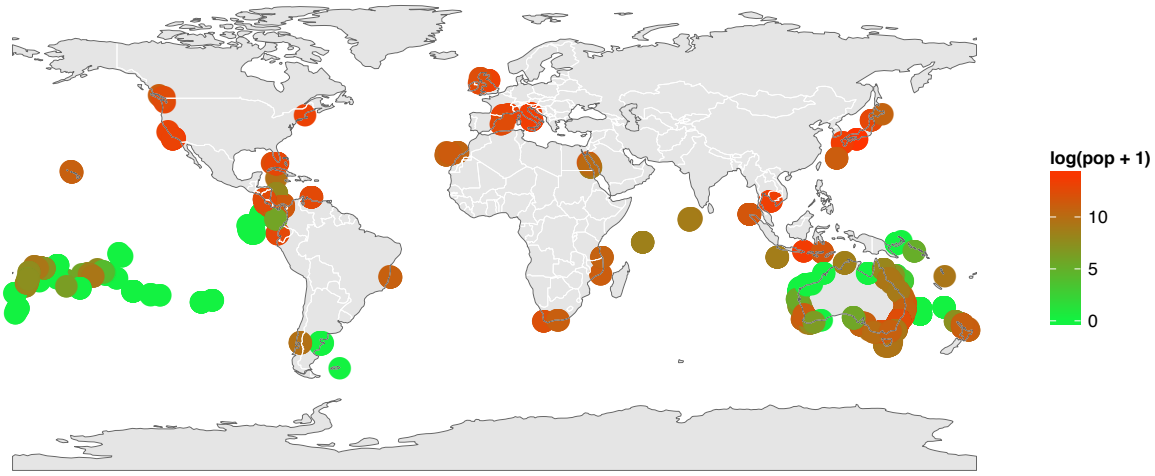

Figure C.7: Human coastal population density. See table C.1 for source and derivation.

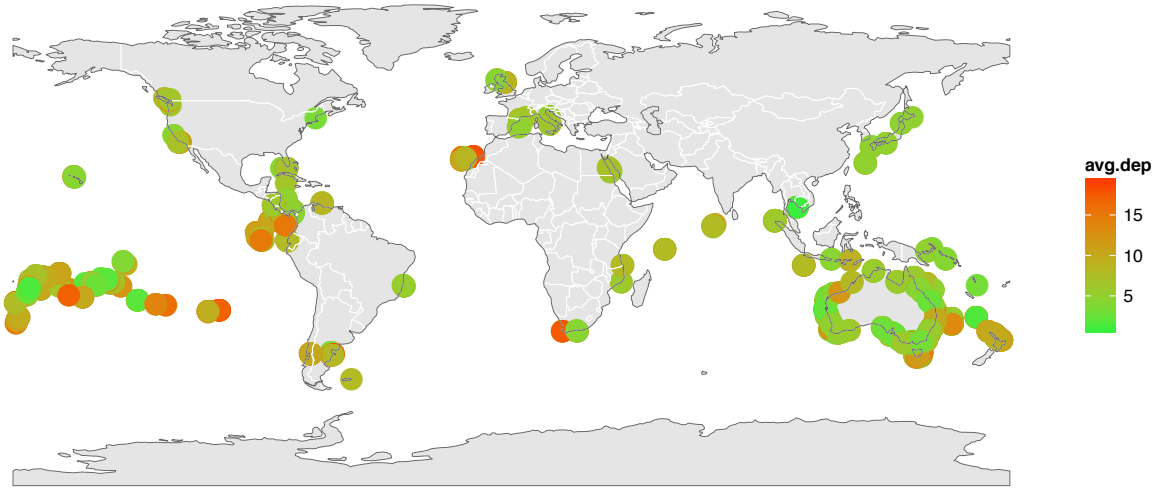

Figure C.8: Average depth of surveys at sites.